ESD-TR-65-13

TECHNIQUES FOR OBJECTIVE

HEMISPHERIC ANALYSIS AND PREDICTION

OF THE JET STREAM

David B. Spiegler
John T. Ball
et al.

September 1965

433L SYSTEM PROGRAM OFFICE
ELECTRONICS SYSTEMS DIVISION
AIR FORCE SYSTEMS COMMAND
UNITED STATES AIR FORCE
L. G. Hanscom Field, Bedford, Mass.

ESSW

AD0622711

Qualified users may obtain copies of this report from the Defense Documentation Center.

When U.S. Government drawings, specifications, or other data are used for any purpose other than a definitely related Government procurement operation, the Government thereby incurs no responsibility nor any obligation whatsoever, and the fact that the Government may have formulated, furnished, or in any way supplied the said drawings, specifications, or other data, is not to be regarded by implication or otherwise, or in any manner licensing the holder or any other person or corporation, or conveying any rights or permission to manufacture, use, or sell any patented invention that may in any way be related thereto.

TECHNIQUES FOR OBJECTIVE HEMISPHERIC ANALYSIS
AND PREDICTION OF THE JET STREAM

Electronics Systems Division
Air Force Systems Command
United States Air Force
ESD-TR-65-13

David B. Spiegler
John T. Ball, et al.

ERRATA

With reference to Part II, Section V (Pg. 107—144) of the report, the following background information is useful to the reader before noting the corrections presented here.

Because the five-day sample of constant pressure prognoses and analyses supplied to us by 3rd Weather Wing (3rd WW) was in a grid array on magnetic tape, the grid arrays had to be read and printed at United Aircraft Research Laboratories (UARL) using a procedure for 3rd WW grids that has frequently been used in the past. For some undetermined reason, these values on tape were read and printed by the computer in an order directly opposite to what the real order was supposed to be. This was true for the analyses, the prognoses, and the error fields. Thus, it has no effect whatsoever on the evaluation of the diagnostic LMW prediction technique described; this fact cannot be overemphasized. The only effect it does have on the results presented in Section V is that the hemispheric geography is flipped relative to the analysis, prognostic, and error isopleths (e.g., North America should be where central Asia is and vice-versa). The prognoses, analyses, and error fields do not change.

The incorrect reading and printing of the grids (Figures 5 through 12, Part II, Section V) went unnoticed because raw data had not been available from 3rd WW to check observed station values against the analyses (due to security classification in force at the time for these data tapes). Recent acquisition of the station radiosonde observations resulted in the discovery of the incorrect orientation of the grids.

Because of this incorrect orientation, the following changes are necessary to the report.

Location	Error	Correction
P. 108 § 8, ¶2, lines 3 and 4	but over central and eastern Asia and the western Pacific	but over North America and the western Atlantic
P. 109, second full ¶, line 4	forecasts occurred over central and eastern Asia	forecasts occurred over North America
P. 109, second full ¶, line 5	and over an area near Hawaii	and over north-eastern Africa
P. 109, second full ¶, line 7	Over the North Atlantic Ocean	Over eastern Asia and the western Pacific
P. 111-144, Figures 5—12	The base map should be rotated 180° (e.g., what is now 100°E longitude should be 80°W longitude).	

ESD-TR-65-13

TECHNIQUES FOR OBJECTIVE
HEMISPHERIC ANALYSIS AND PREDICTION
OF THE JET STREAM

David B. Spiegler
John T. Ball
et al.

September 1965

FOREWORD

ABSTRACT

This report comprises two parts: Part I documents an objective <u>analysis</u> technique for level of maximum wind (LMW) parameters, and Part II presents two LMW <u>prediction</u> techniques.

The objective hemispheric <u>analysis</u> technique incorporates information from data areas into LMW analyses for no-data areas. This is done in a quantitative, objective, and consistent manner by using LMW regression equations that specify the initial-guess fields for the analysis. The analysis technique locates jet cores between grid points, and generates observations along these cores by using horizontal jet profiles. This technique produces high-quality analyses that compare favorably with subjective analyses, and that are generally consistent with one another.

The first <u>prediction</u> technique is based on a procedure wherein potential predictors are obtained from a network grid oriented with respect to the LMW wind direction at the predictand point. Prediction equations are obtained by applying the screening regression technique to predictors selected from initial-state LMW parameters (and their 12-hr change) and wind speed values at constant pressure surfaces. Tests on independent data showed that these equations produce prognoses that are better than persistence for all polar and subtropical jet-stream categories.

The second prediction technique applies diagnostic LMW regression equations (originally derived to produce the initial-guess fields in the LMW analysis) to constant-pressure-surface numerical prognoses. A five-day data sample of numerical prognoses was used to test the technique. Evaluation of the resulting LMW prognoses indicated that the 12- and 24-hr prognoses were generally good representations of the observed LMW fields, and that the 36- and 48-hr prognoses were occasionally good over some areas of the hemisphere.

REVIEW AND APPROVAL

Publication of this technical report does not constitute Air Force approval of the report's findings or conclusions. It is published only for the exchange and stimulation of ideas.

Robert L. Houghten
Lt. Colonel, USAF
Acting System Program Director

TABLE OF CONTENTS

PART I

LIST OF ILLUSTRATIONS

LIST OF TABLES

TABLE OF CONTENTS

PART II

LIST OF ILLUSTRATIONS

LIST OF TABLES

xi

PART I

A TECHNIQUE for ANALYSIS of
LEVEL of MAXIMUM WIND PARAMETERS

by

David B. Spiegler

SECTION I

INTRODUCTION

The National Meteorological Center (NMC) presently sends hand-analyzed level-
of-maximum wind (LMW) analyses for the United States and immediate areas outside
its borders to users via the national facsimile network. These analyses are for the
maximum wind speed, the level of maximum wind, and an averaged vertical shear below
and above the LMW.

The work described here represents an attempt to develop an objective (computer)
technique for the analysis of five LMW parameters for the Northern Hemisphere. These
parameters are:

        (a) the wind direction at the LMW $[W_d(L)]$,

        (b) the wind speed at the LMW $[W_s(L)]$,

        (c) the height of the LMW $[Z(L)]$,

        (d) the shear below the LMW (S_b), and

        (e) the shear above the LMW (S_a).

The objective technique was developed in direct support of a 3rd Weather Wing
requirement for a program dealing with an improved method for analyzing and fore-
casting clear-air turbulence.

Because the analyses are for the Northern Hemisphere—an area that has widely-
variable data density—the initial-guess fields are of prime importance. Thus, the analy-
sis technique uses an established relationship[1] between the LMW parameters and the
information routinely available from constant-pressure-surface analysis of height,
temperature, and wind. The initial guesses are corrected by using station observations
of the LMW parameters (from a preprocessed data tape) and the successive approxima-
tion analysis technique (SAT) [1].

For the wind-speed analysis at the LMW the jet cores are located, and "observa-
tions" are "generated" at the jet core by using models of horizontal jet profiles.

Verifications of the analyses are determined by the areal-mean-error method [6].

---

[1]The relationship is established by means of regression equations, for each of the
LMW parameters, that are a function of the type of jet and its strength (e.g., strong-
polar jet, weak-moderate subtropical jet, etc.).

SECTION II

LMW SCREENING REGRESSION EXPERIMENTS

Three data preprocessor programs were necessary for the derivation of regression equations that are used, with constant-pressure-surface analysis, to generate initial-guess fields for the LMW parameters. Descriptions of the functions of the three programs follow:

(a) Jet Stream Preprocessor I (JSP-I)—combines the wind data from the constant-pressure radiosonde observations with the rawinsonde data. It also determines the height of LMW and the wind speed at the LMW, and computes the vertical wind shear above and below the LMW for each of the observation stations. If there are wind speeds in the sounding that are within three knots of $W_s(L)$, the wind profile is considered to contain a multiple maximum. In these cases, $Z(L)$ is determined by averaging the $Z(L)$ reports within one grid interval of the "problem" station; the calculated $Z(L)$ at that station is the height that is closest to the average of the $Z(L)$'s from the nearby stations.

(b) Jet Stream Preprocessor II (JSP-II)—produces a tape with a total of 58 parameters that are obtained directly, or computed, from information available at constant pressure surfaces and which are considered as predictors for LMW fields. These 58 parameters, including four LMW parameters [$W_d(L)$ is excluded], are:

(i)

$Z(7)$	$Z(5)$	$Z(4)$	$Z(3)$	$Z(2)$	$Z(1)$
$T(7)$	$T(5)$	$T(4)$	$T(3)$	$T(2)$	$T(1)$
$W_d(7)$	$W_d(5)$	$W_d(4)$	$W_d(3)$	$W_d(2)$	$W_d(1)$
$W_s(7)$	$W_s(5)$	$W_s(4)$	$W_s(3)$	$W_s(2)$	$W_s(1)$

where: Z = height; T = temperature; W_d = wind direction; W_s = wind speed; and 7, 5, 4, 3, 2, and 1 represent the 700-, 500-, 400-, 300-, 200-, and 100-mb levels [e.g., $Z(7)$ is the height of the 700-mb level].

(ii)

$h(7-5)$	$\Delta T(7-5)$	$\Delta W_s(7-5)$	$\Delta T/\Delta n(7-5)$	$(\partial h^*/\partial n \sin \alpha)\,(5)$
$h(5-4)$	$\Delta T(5-4)$	$\Delta W_s(5-4)$	$\Delta T/\Delta n(5-4)$	$(\partial h^*/\partial n \sin \alpha)\,(4)$
$h(5-3)$	$\Delta T(5-3)$	$\Delta W_s(5-3)$	$\Delta T/\Delta n(5-3)$	$(\partial h^*/\partial n \sin \alpha)\,(3)$
$h(4-3)$	$\Delta T(4-3)$	$\Delta W_s(4-3)$	$\Delta T/\Delta n(4-3)$	$(\partial h^*/\partial n \sin \alpha)\,(2)$
$h(3-2)$	$\Delta T(3-2)$	$\Delta W_s(3-2)$	$\Delta T/\Delta n(3-2)$	$(\partial h^*/\partial n \sin \alpha)\,(1)$
$h(2-1)$	$\Delta T(2-1)$	$\Delta W_s(2-1)$	$\Delta T/\Delta n(2-1)$	

where: h = thickness of a layer bounded by two mandatory constant pressure surfaces; ΔT = difference in temperature between two mandatory constant pressure surfaces; ΔW_s = difference in magnitude of the wind speed between constant pressure surfaces; $\Delta T/\Delta n$ = the horizontal temperature gradient in the middle of a layer between constant pressure surfaces; and $\partial h^*/\partial n \sin \alpha$ = the temperature gradients at a constant pressure surface where h* is a pseudo-thickness and $\sin \alpha$ denotes the direction of the gradient (α = the angle between the thermal and actual wind).

(iii) r_2 $Z(L)$ $W_s(L)$ S_a S_b

where r_2 = the radius of curvature at 200 mb. The purpose of this program is to have the data in a form that can be used with a screening regression program to generate equations for specifying the four LMW parameters [$W_d(L)$ is specified separately by a procedure described in Section III].

(c) Jet Stream Categories (JSC)—stratifies the station data on the basis of wind speeds at 200 and 300 mb, the latitude of the station, and a combination of both wind speeds and latitude. The purpose of this program is to have the screening regression derive different equations for jets of various strength and type. The exact specification of the categories (see Table I) was determined by examining several months of LMW data.

Three months of a winter upper-air data sample from the National Meteorological Center were run through the three preprocessor programs. Screening regression experiments for obtaining equations for the initial guesses of LMW parameters were designed. The main purpose of the experiments was to obtain the most practical set of equations from an operational standpoint, while keeping the errors within acceptable limits. Selective "addition" and "subtraction" of possible predictors [listed in (b) above] for several different screening runs gave the information necessary to decide which equations were the most useful.

A program that derives multiple linear-regression equations by using a screening procedure has been written and was used in the study. The screening procedure selects, from a set of possible predictors, a subset that contributes significantly and independently to reducing the variance of the predictand. The predictor having the highest linear

3

TABLE I

JET STREAM CATEGORIES AND THEIR DEFINITIONS

Jet-stream category	Description	Latitude	Definition				
			$W_s(3)$		$W_s(2)$	$W_s(2) - W_s(3)$	$W_s(3) - W_s(2)$
1	No Jet	—	< 50	and	< 50	—	—
2	Weak—Moderate Subtropical Jet	0—30°N	50—99*	or	50—99*	—	—
		30—45°N	50—99*	or	50—99*	> 10	—
3	Strong Subtropical Jet	0—30°N	≥ 100†	or	≥ 100†	—	—
		30—45°N	≥ 100†	or	≥ 100†	> 15	—
4	Weak—Moderate Subtropical—Polar Jet	30—45°N	50—99*	or	50—99*	< 10 and	< 10
5	Strong Subtropical—Polar Jet	30—45°N	≥ 100†	or	≥ 100†	< 15 and	< 15
6	Weak—Moderate Polar Jet	> 45°N	50—99*	or	50—99*	—	—
		30—45°N	50—99*	or	50—99*	—	> 10
7	Strong Polar Jet	> 45°N	≥ 100†	or	≥ 100†	—	—
		30—45°N	≥ 100†	or	≥ 100†	—	> 15

*When $W_s(3)$ or $W_s(2)$ is required by category definition to be between 50—99 knots, only the following three cases apply:
(a) $W_s(3)$ < 50 knots, $W_s(2)$ = 50—99 knots; (b) $W_s(3)$ = 50—99 knots, $W_s(2)$ < 50 knots; and (c) $W_s(3)$ = 50—99 knots, $W_s(2)$ = 50—99 knots.

†When $W_s(3)$ or $W_s(2)$ are required by category definition to be ≥ 100 knots, only the following three cases apply:
(a) $W_s(3)$ < 100 knots, $W_s(2)$ ≥ 100 knots; (b) $W_s(3)$ ≥ 100 knots, $W_s(2)$ < 100 knots; (c) $W_s(3)$ ≥ 100 knots, $W_s(2)$ ≥ 100 knots.

correlation with the specified predictand is selected from an array of possible pre-
dictors. Next, the partial correlation coefficients between each of the remaining
predictors and the predictand (holding the first predictor constant) are examined, and
the predictor associated with the highest coefficient is then selected as the second
predictor. Additional predictors are selected in a similar manner. This procedure is
repeated until a chosen predictor fails to explain a significant additional percentage of
the remaining variance of the predictand or until a specified number of predictors is
selected. The criterion of significance employed is a modified F-test described by
Miller [3].

To justify the definitions used for the various LMW categories, contingency tables
were computed that relate the category definitions to definitions of jet types gained
by synoptic experience and given by the height of the LMW.

For the purposes of the contingency tables, the definitions of polar and sub-
tropical jets, and jets that are not clearly polar or subtropical (subtropical–polar) are
as follows for winter data:

        (a) Polar [$Z(L) < 34,000$ ft]

        (b) Subtropical [$Z(L) > 37,000$ ft]

        (c) Subtropical–polar [$34,000 \leq Z(L) \leq 37,000$ ft]

The contingency tables [Table II, (a) and (b)] are based on station data from the
developmental data sample (December 1963, and January—February 1964). The defini-
tions based on 300- and 200-mb wind speeds and latitude appear to be satisfactory with
only a small percentage of the cases in the lower left or upper right corners of the
tables.

TABLE II
RELATION OF JET CATEGORY DEFINITIONS TO HEIGHT OF THE LMW

(a) Weak–Moderate Jets

Jet-stream category	Conditions assuming $W_S(3)$ or $W_S(2)$ equal to 50–99	Polar Jet $Z(L) < 34,000$ ft			Subtropical–Polar Jet $34,000 \leq Z(L) \leq 37,000$ ft			Subtropical Jet $Z(L) > 37,000$ ft		
		No. of cases	% of total cases in category	% of total Polar Jet cases	No. of cases	% of total cases in category	% of total Subtropical Polar Jet cases	No. of cases	% of total cases in category	% of total Subtropical jet cases
6	(a) $W_S(3) - W_S(2) > 10$ and latitude $\geq 30°N$ or (b) latitude $> 45°N$	1987	74.7	77.6	355	13.4	35.4	317	12.9	12.8
4	$W_S(2) - W_S(3)| \leq 10$ and $30 \leq$ latitude $\leq 45°N$	463	34.0	18.1	365	26.8	36.4	535	39.2	21.7
2	(a) $W_S(2) - W_S(3) > 10$ and latitude $\leq 45°N$ or (b) latitude $< 30°N$	110	4.5	4.3	284	14.1	28.2	1616	80.4	65.5

6

TABLE II (cont'd)

(b) Strong jets

Jet-stream category	Conditions assuming $W_S(3)$ or $W_S(2) \geq 100$	Polar Jet $Z(L) < 34,000$ ft			Subtropical–Polar Jet $34,000 \leq Z(L) \leq 37,000$ ft			Subtropical Jet $Z(L) > 37,000$ ft		
		No. of cases	% of total cases in category	% of total Polar Jet cases	No. of cases	% of total cases in category	% of total Subtropical Polar Jet cases	No. of cases	% of total cases in category	% of total Subtropical jet cases
7	(a) $W_S(3) - W_S(2) > 15$ and latitude $\geq 30°N$ or (b) latitude $> 45°N$	384	80.5	70.3	68	14.3	16.3	25	5.2	2.2
5	(a) $|W_S(2) - W_S(3)| \leq 15$ or (b) $30° \leq$ latitude $\leq 45°N$	106	22.2	19.5	179	37.5	42.9	192	40.3	17.0
3	(a) $W_S(2) - W_S(3) > 15$ and latitude $\leq 45°N$ or (b) latitude $< 30°N$	56	4.9	10.2	170	14.9	40.8	915	80.2	80.8

SECTION III

METHOD OF ANALYSIS AND VERIFICATIONS OF LMW PARAMETERS

Initial-guess fields for all LMW parameters except $W_d(L)$, are generated by the derived regression equations. The analysis program determines which jet-stream category a particular grid point is in, and uses the appropriate regression equations for each of the LMW parameters. The initial guesses are <u>not</u> generated simultaneously, because one (or more) already-analyzed LMW fields are often predictors in the equation(s) for the other field(s). The initial guesses are adjusted by using the preprocessed LMW station data and the successive approximation analysis technique [1]. For the $W_s(L)$ field, the jet core is located, and observations are generated at the core by employing models of horizontal jet-stream profiles. The details for the determination of each of the LMW fields, their order in the analysis procedure, and the verification procedure follow.

1. Wind Direction at the LMW [$W_d(L)$]

The procedure for determining wind direction at the LMW is:

(a) for grid points that are at latitude < 30°N, the wind direction (W_d) at 200 mb [$W_d(2)$] is used as the $W_d(L)$.

(b) for grid points that lie between 30° and 45°N: if the radius of curvature at 200 mb (r_2) is positive, $W_d(3)$ is used as $W_d(L)$; if r_2 is negative or zero, $W_d(2)$ is specified as the $W_d(L)$.

(c) for grid points that are at latitudes > 45°N, $W_d(3)$ is also the $W_d(L)$.

2. Wind Speed at the LMW [$W_s(L)$]

The initial-guess field is generated by the appropriate equations (see the Appendix) that are dependent upon the category in which a particular grid point is located. The initial-guess field of $W_s(L)$ is "corrected" by using station observations of $W_s(L)$ and SAT. The number of passes through the data is an input item, but the maximum number of passes is five, some of which may be made with additional generated observations.

The jet cores are located after a specified number of passes. The first approximation to defining the jet core is obtained by searching among grid points for the maxi-

mum wind speed within a specified area. For the analyses using the winter-data sample the areas are enclosed by those grid points having a wind-speed value greater than or equal to 75 knots.

A systematic search is performed within the area by tagging grid points that are maximums (the search is systematic in the sense that it proceeds independently along the vertical, horizontal, and diagonal lines of grid points). The grid points with the most "tags" are the first approximations to the jet cores. More specific details and a discussion of, and solutions for, the various problems are contained in the specifications for the LMW computer program [5].

The set of consecutive stored grid points, which are the first approximation to a jet core, is then used with a parabola-fitting routine to determine the "exact" location of a jet core between grid points.

After the jet cores have been located, observations are generated at the midpoints of the jet-core segments by using Endlich and McLean's jet-stream model [2] which relates the wind speed at the core to the wind speed at some specified perpendicular distance from the core (see Fig. 1). By using the model, two observations are generated at the same points on the core, i.e., one from the wind on the high-pressure side and the other from the wind on the low-pressure side. The average of these two "generated" observations is used as the final observation for the midpoint of a core segment.

There is an option to make an additional pass for analysis of $W_s(L)$ with the generated data and the actual station data using a relatively-small influence radius. The generated observations may be assigned a weight relative to the actual data for this pass.

3. Verification of $W_s(L)$

The analysis of $W_s(L)$ is verified by the areal-mean/root-mean-square error method [6]. This method approximates an area integral of the error over the analysis area by withholding some percentage of the observations and verifying them against the withheld- and analysis-station observations, which are equally weighted. The withheld-station observations approximate the maximum error points in the analysis field, but the number of withheld stations required by the areal-mean-error method usually does not equal the number of maximum-error points. Therefore, the withheld stations were

9
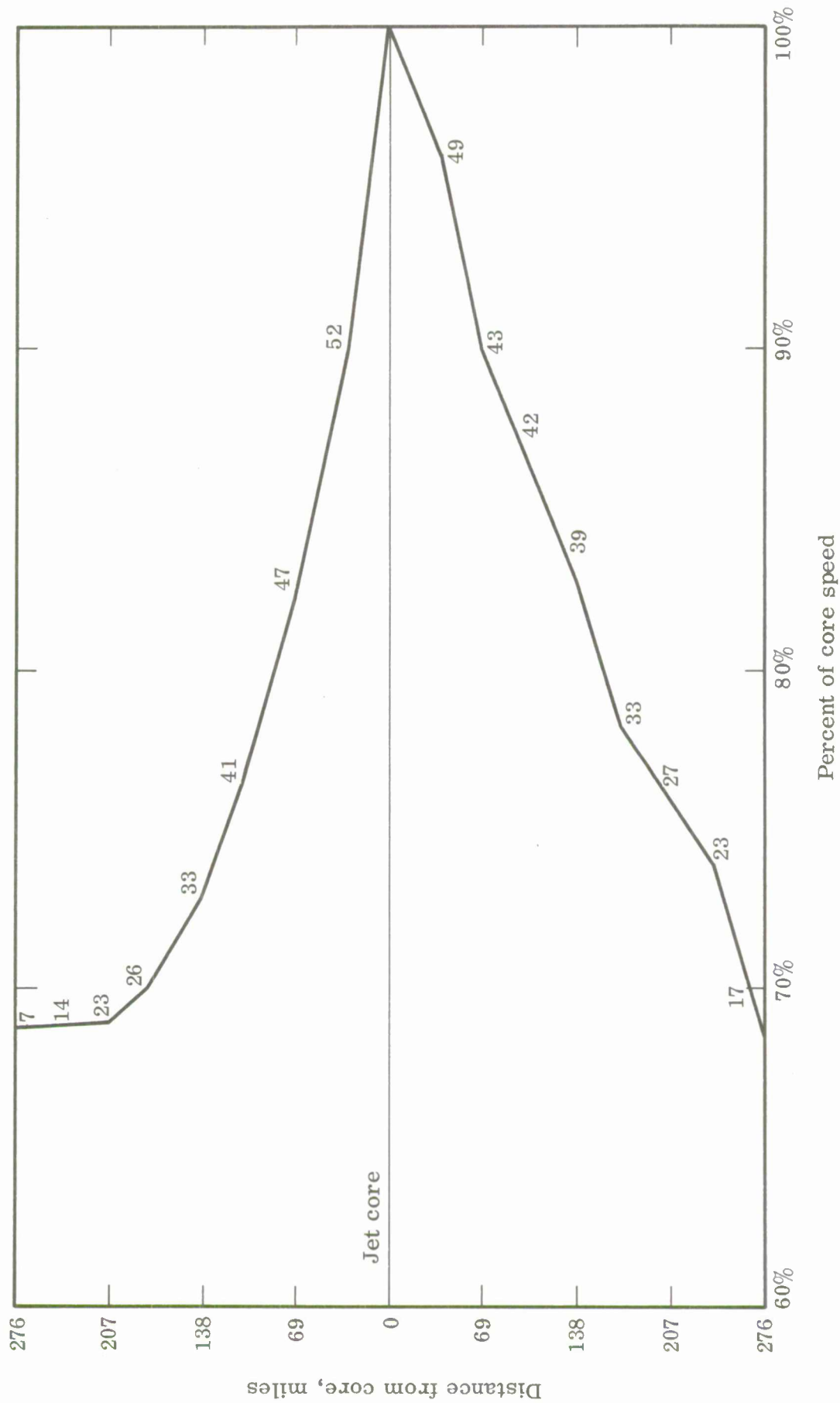
Fig. 1. Average horizontal profile of wind speeds in the jet stream (taken from [2]).

10

selected to represent equally the entire spectrum of maximum errors over the analysis area. The assumption is that the maximum error is inversely proportional to the density of the data. The density of each station is computed prior to the analysis, and withheld stations are selected on the basis of three LMW-wind-speed and three station-density categories (see Table III).

TABLE III
SELECTION OF WITHHELD STATIONS ON THE BASIS OF
STATION DENSITY AND LMW WIND SPEED

| Density (ρ_T) | Category | | |
| | A | B | C |
	No. of stations $W_s(L) > 100$	No. of stations $51 \leq W_s(L) \leq 100$	No. of stations $W_s(L) \leq 50$
Low: 0.11 to 0.32	3	4	3
Med: 0.33 to 0.43	4	3	3
High: $\geq$ 0.44	3	3	4

4. Analysis and Verification of Z(L)

The initial-guess field for Z(L) is generated with the appropriate regression equations after determining which category each grid point is in. The successive approximation analysis technique is then used with the station data for Z(L) to adjust the initial-guess field.

Where the $W_s(L)$ is less than 75 knots, Z(L) at adjacent grid points and/or stations may vary widely; this is a common characteristic of adjacent wind profiles that exhibit relatively weak maximums. For this reason, the analysis is meaningful only over those areas on the Z(L) chart where the $W_s(L)$ is greater than 75 knots.

Verification of Z(L) is done with the areal-mean/root-mean-square error method using the identical set of withheld stations used in the verification of $W_s(L)$.

5. Analysis and Verification of S_b and S_a

Both of these parameters have initial guesses generated by the appropriate regression equations. As may be seen from the equations in the Appendix, $W_s(L)$ and Z(L) are often "predictors" for S_b and S_a.

Once again, SAT is used with the preprocessed station data to adjust the initial-guess fields.

SECTION IV

RESULTS

The evaluation of the quality of the analysis technique was based on the results from two general classes of experiments—the experiments for deriving the initial-guess equations for the LMW analysis fields, and the experiments with the analyses that were generated by the analysis procedure.

6. Results of LMW Regression Experiments

Non-derived predictors (e.g., temperatures and wind speeds) and derived predictors (e.g., thermal winds and shears) are among the possible predictors[2] for the LMW param-eters (see Section I). In the design of the experiments, a minimum of three to a maximum of seven screening runs were specified for each predictand in each category. The dif-ferences between the individual screening runs for a particular predictand were in the variables specified as possible predictors. The objective in having several screening runs was to answer the following questions:

(a) Will the non-derived (simple) predictors alone satisfactorily specify the LMW parameters?

(b) Will the derived (sophisticated) predictors alone give a better result than the non-derived predictors alone?

(c) Will a combination of non-derived and derived predictors yield the best results?

(d) Does the height at the LMW $[Z(L)]$ add more to the specification of the wind speed at the LMW $[W_s(L)]$ than the wind speed adds to the height?

(e) Are the previously analyzed LMW fields important in specifying the shears above and below the LMW?

The answers to these questions are contained in Table IV, which lists the selected predictors for the LMW parameters for each of the LMW categories, and the associated dependent and independent data results. The LMW screening regression equations for each type of jet category are in the Appendix.

---

[2] W_d and Z at constant-pressure surfaces, and all parameters containing 400-mb information, were not included as possible predictors in any of the screening runs.

12

Category	Predictand	Selected predictors	% red.	Number of cases		rms error		Std. dev.		Means		Units
			(dep)	(dep)	(ind)	(dep)	(ind)	(dep)	(ind)	(dep)	(ind)	
1	$Z(L)$	$W_g(1)$, $W_g(7)$, $T(7)$	37	3482	467	9611	9472	12076	12630	34403	33850	ft
	$W_g(L)$	$W_g(2)$, $W_g(1)$, $W_g(5)$	60	3482	467	7.5	9.7	11.9	12.2	42.7	43.9	knot
	S_a	S_b, $W_g(1)$, $W_g(L)$	39	3482	467	0.93	0.95	1.19	1.20	−1.48	−1.87	knot 10^{-3} ft
	S_b	$W_g(L)$, $W_g(2)$, $W_g(5)$, $Z(L)$	41	3482	467	0.79	1.48	1.04	1.48	+1.72	+1.79	knot 10^{-3} ft
2	$Z(L)$	$W_s(1)$, $W_s(3)$, $T(5)$	14	2010	317	4740	3806	5127	4199	40019	40125	ft
	$W_s(L)$	$W_s(2)$	55	2010	317	12.5	8.8	18.6	16.0	83.5	82.6	knot
	S_a	$W_s(L)$, $W_s(1)$, $W_s(2)$	32	2010	317	2.49	1.29	3.01	1.61	−3.14	−2.73	knot 10^{-3} ft
	S_b	$Z(L)$, $W_s(L)$, $W_s(3)$	63	2010	317	2.14	1.18	3.53	1.58	+3.32	+3.01	knot 10^{-3} ft
3	$Z(L)$	$W_g(3)$, $W_g(1)$, $W_g(2)$	06	1141	135	3914	3291	4046	3596	39214	38750	ft
	$W_g(L)$	$W_g(2)$	67	1141	135	12.7	10.0	22.0	24.2	132.7	132.07	knot
	S_a	$W_g(L)$, $W_g(2)$, $Z(L)$, $W_g(1)$	39	1141	135	2.98	1.83	3.83	2.75	−4.96	−4.95	knot 10^{-3} ft
	S_a	$W_g(L)$, $W_g(2)$, $Z(L)$, $W_g(1)$, S_b	43	1141	135	2.88	1.72	3.83	2.75	−4.96	−4.95	knot 10^{-3} ft
	S_b	$Z(L)$, $W_g(3)$, $W_g(L)$	81	1141	135	1.24	1.13	2.84	2.38	+4.57	+4.28	knot 10^{-3} ft
4	$Z(L)$	$W_g(1)$, $T(7)$, $W_g(5)$, $W_g(3)$, $W_g(2)$	23	1363	211	5767	5512	6587	6898	35659	37584	ft
	$W_g(L)$	$W_g(2)$	54	1363	211	12.7	8.9	18.6	15.9	80.5	81.8	knot
	S_a	$W_g(L)$, $W_g(3)$, $W_g(1)$	36	1363	211	2.34	1.33	2.94	1.34	−2.63	−2.32	knot 10^{-3} ft
	S_b	$W_g(L)$, $Z(L)$, $W_g(3)$, $W_g(5)$	49	1363	211	2.50	1.14	3.48	1.39	+2.55	+2.24	knot 10^{-3} ft
5	$Z(L)$	$T(7)$, $W_g(1)$, $W_g(3)$, $W_g(2)$	19	477	70	4736	4668	5251	5061	36339	35494	ft
	$W_g(L)$	$W_g(3)$, $W_g(2)$	71	477	70	11.2	10.2	21.0	22.6	132.2	126.84	knot
	S_a	$Z(L)$, S_b, $W_g(1)$	50	477	70	1.87	2.04	2.66	2.25	−3.74	−3.22	knot 10^{-3} ft
	S_a	$Z(L)$, S_b, $W_g(1)$, $W_g(L)$, $W_g(2)$	58	477	70	1.73	1.80	2.66	2.25	−3.74	−3.22	knot 10^{-3} ft
	S_b	$Z(L)$, $W_g(L)$, $W_g(3)$	69	477	70	1.59	1.42	2.87	2.66	+3.57	+3.57	knot 10^{-3} ft
6	$Z(L)$	$W_g(5)$, $W_g(2)$, $W_g(3)$	27	2543	319	4991	6440	5830	7396	30998	33459	ft
	$W_g(L)$	$W_g(3)$, $W_g(2)$	68	2543	319	8.7	11.3	15.4	16.8	77.4	80.8	knot
	S_a	$W_g(L)$, $W_g(2)$, $Z(L)$, $W_g(1)$	56	2543	319	1.09	1.46	1.65	2.06	−3.06	−3.07	knot 10^{-3} ft
	S_b	$W_g(L)$, $W_g(5)$, $Z(L)$, $W_g(3)$	67	2543	319	0.93	0.91	1.61	1.63	+2.97	+2.97	knot 10^{-3} ft
7	$Z(L)$	$T(5)$, $W_g(2)$, $W_s(3)$	26	477	56	3407	4429	3958	4909	30884	31701	ft
	$W_g(L)$	$W_g(3)$, $W_g(2)$	64	477	56	11.6	12.3	19.4	22.5	126.5	130.4	knot
	S_a	$W_g(L)$, $W_g(2)$, $Z(L)$, $W_g(3)$	67	477	56	1.64	2.00	2.87	2.43	−5.55	−4.90	knot 10^{-3} ft
	S_b	$Z(L)$, $W_g(L)$, $W_g(5)$	62	477	56	1.68	1.90	2.73	2.30	+5.16	+5.14	knot 10^{-3} ft
	S_b	$Z(L)$, $W_g(L)$, $W_g(5)$, $W_g(3)$	67	477	56	1.57	1.72	2.73	2.30	+5.16	+5.14	knot 10^{-3} ft

The outcome of the experiments, with respect to the selected predictors, is interesting. Percent reduction of variance (% red.) and rms errors were the criteria used for choosing the equations. It is evident from Table IV that the derived predictors failed to add significantly to the non-derived predictors. It is also evident that the derived predictors alone did not yield results as good as those from the non-derived predictors. Table V indicates the superiority of the non-derived predictors for each predictand and each category.

For jet-stream categories 2 through 7, the screening runs using non-derived predictors, from which the equations were selected, are compared with screening runs that use derived predictors (it is implicit that if LMW predictors were used in the experiment for the simple predictors, the same LMW predictors were used in the experiment with the sophisticated predictors).

A smaller number of experiments were run for Category 1 than for Categories 2 through 7. Table V contains all the experiments for the seven categories. There is no direct comparison of predictors in Category 1, but results indicated that non-derived predictors were more highly correlated with the LMW parameters than were the derived predictors.

The following conclusions may be drawn from the table:

(a) A higher number of derived predictors is often necessary to attain the same percent reduction as the simple predictors.

(b) For two thirds of the predictands (Categories 2—7), all the derived predictors (plus LMW parameters where indicated) do not result in as high a percent reduction as four or less simple predictors (plus LMW parameters where indicated).

(c) When the number of derived and non-derived predictors is the same, the percent reductions are within 2.5% of each other. In Categories 2—7 this occurs only with Z(L). Although the percent reductions are approximately the same for these six cases, it is easier to use non-derived fields in an operational system.

The results for the LMW equations on independent data (Table IV) indicate that the equations are stable, with independent errors near or lower than the dependent errors.

TABLE V
PERCENT REDUCTION OF VARIANCE ASSOCIATED WITH
DERIVED AND NON-DERIVED PREDICTORS*

(a) Category 1

Predictand	Possible predictors	Selected predictors	% red.	Total % red.
$Z(L)$	ND†	$W_s(1)$	19.6	
		$W_s(7)$	12.1	36.7
		$T(7)$	5.0	
	D + ND	$W_s(1)$	19.6	
		$W_s(7)$	12.1	37.5
		$\Delta W_s(3-2)$	5.8	
$W_s(L)$	ND†	$W_s(2)$	40.0	
		$W_s(1)$	12.7	60.4
		$W_s(5)$	7.7	
	D + ND	$W_s(2)$	40.0	
		$\Delta W_s(2-1)$	12.7	60.4
		$W_s(5)$	7.7	
S_a	ND	$W_s(1)$	3.1	
		$W_s(3)$	4.1	8.5
		$T(3)$	1.3	
	D + ND	$\Delta W_s(2-1)$	3.2	
		$\Delta W_s(3-2)$	4.0	8.3
		$W_s(7)$	1.1	
	D + ND + LMW†	S_b	12.8	
		$W_s(1)$	5.0	38.7
		$W_s(L)$	20.9	
S_b	ND	$W_s(1)$	1.4	
		$T(5)$	1.1	2.5
		$T(1)$	0.0	
	D + ND	$W_s(1)$	1.4	
		$\Delta W_s(5-3)$	0.2	1.6
		$W_s(3)$	0.0	
	D + ND + LMW†	$W_s(L)$	20.2	
		$W_s(2)$	8.1	41.1
		$W_s(5)$	5.9	
		$Z(L)$	6.9	

*D = derived; ND = non-derived.

†Selected for use.

TABLE V (cont'd)

(b) Category 2

Predictand	Possible predictors	Selected predictors	% red.	Total % red.
$Z(L)$	ND†	$W_S(1)$	6.1	14.5
		$W_S(3)$	5.4	
		$T(5)$	3.0	
	D	$W_T(2-1)$	7.2	14.8
		$\Delta W_S(3-2)$	4.2	
		$\Delta T(3-2)$	1.1	
		$\Delta W_S(2-1)$	1.7	
		$W_T(5-3)$	0.6	
$W_S(L)$	ND†	$W_S(2)$	55.1	55.1
	D	ALL	28.9	28.9
S_a	ND + LMW†	$W_S(L)$	21.3	31.8
		$W_S(1)$	7.5	
		$W_S(2)$	3.0	
	D + LMW	$W_S(L)$	21.3	33.3
		S_b	4.5	
		$Z(L)$	4.6	
		$\Delta W_S(2-1)$	2.9	
S_b	ND + LMW†	$Z(L)$	28.6	63.5
		$W_S(L)$	15.2	
		$W_S(3)$	19.7	
	D + LMW	ALL	58.5	58.5

TABLE V (cont'd)

(c) Category 3

Predictand	Possible predictors	Selected predictors	% red.	Total % red.
$Z(L)$	ND†	$W_s(3)$	2.1	
		$W_s(1)$	3.1	6.4
		$W_s(2)$	1.2	
	D	$\Delta W_s(3-2)$	4.4	
		$W_T(2-1)$	2.9	8.3
		$h(7-5)$	1.0	
$W_s(L)$	ND†	$W_s(2)$	66.5	66.5
	D	ALL	49.5	49.5
S_a	ND + LMW†	$W_s(L)$	14.3	
		$W_s(2)$	11.4	39.2
		$Z(L)$	6.5	
		$W_s(1)$	7.0	
	D + LMW	$W_s(L)$	6.0	
		$Z(L)$	12.7	
		S_b	3.8	40.3
		$\Delta W_s(3-2)$	3.5	
		$\Delta W_s(2-1)$	14.3	
S_b	ND + LMW†	$Z(L)$	25.8	
		$W_s(3)$	11.6	81.0
		$W_s(L)$	43.6	
	D + LMW	ALL	71.3	71.3

TABLE V (cont'd)

(d) Category 4

Predictand	Possible predictors	Selected predictors	% red.	Total % red.
Z(L)	ND†	$W_S(1)$	4.8	23.3
		T(7)	5.2	
		$W_S(5)$	4.6	
		$W_S(3)$	1.4	
		$W_S(2)$	7.3	
	D	$\Delta W_S(3-2)$	13.8	25.1
		$W_T(2-1)$	3.4	
		$W_T(5-3)$	3.4	
		$\Delta h(7-5)$	3.9	
		$\Delta T(2-1)$	0.6	
$W_S(L)$	ND†	$W_S(2)$	53.6	53.6
	D	ALL	28.9	28.9
S_a	ND + LMW†	$W_S(L)$	22.5	36.5
		$W_S(3)$	10.9	
		$W_S(1)$	3.1	
	D + LMW	ALL	34.5	34.5
S_b	ND + LMW†	$W_S(L)$	17.9	48.6
		Z(L)	14.7	
		$W_S(3)$	11.9	
		$W_S(2)$	4.1	
	D + LMW	ALL	40.0	40.0

18

TABLE V (cont'd)

(e) Category 5

Predictand	Possible predictors	Selected predictors	% red.	Total % red.
$Z(L)$	ND†	$T(7)$	4.0	18.6
		$W_s(1)$	2.7	
		$W_s(3)$	3.8	
		$W_s(2)$	8.1	
	D	$\Delta W_s(3-2)$	13.5	19.4
		$W_T(2-1)$	3.4	
		$\Delta h(5-3)$	1.7	
		r_2	0.8	
$W_s(L)$	ND†	$W_s(3)$	68.2	71.5
		$W_s(2)$	3.3	
	D	ALL	50.6	50.6
S_a	ND + LMW†	$Z(L)$	12.6	57.6
		S_b	29.4	
		$W_s(1)$	8.2	
		$W_s(L)$	2.0	
		$W_s(2)$	5.4	
	D + LMW	ALL	57.2	57.2
S_b	ND + LMW†	$Z(L)$	35.9	69.2
		$W_s(L)$	15.8	
		$W_s(3)$	17.5	
	D + LMW	ALL	63.7	63.7

TABLE V (cont'd)

(f) Category 6

Predictand	Possible predictors	Selected predictors	% red.	Total % red.
Z(L)	ND†	$W_s(5)$	7.5	26.7
		$W_s(2)$	13.6	
		$W_s(3)$	5.6	
	D	$W_T(3-2)$	22.7	29.1
		$W_T(5-3)$	4.0	
		$\Delta T(5-3)$	2.4	
$W_s(L)$	ND†	$W_s(3)$	59.9	68.1
		$W_s(2)$	8.2	
	D	ALL	35.1	35.1
S_a	ND + LMW†	$W_s(L)$	22.1	55.9
		$W_s(2)$	21.2	
		Z(L)	5.4	
		$W_s(1)$	7.2	
	D + LMW	ALL	46.1	46.1
S_b	ND + LMW†	$W_s(L)$	21.2	66.8
		$W_s(5)$	20.1	
		Z(L)	20.6	
		$W_s(3)$	4.9	
	D + LMW	ALL	49.0	49.0

TABLE V (cont'd)

(g) Category 7

Predictand	Possible predictors	Selected predictors	% red.	Total % red.
$Z(L)$	ND†	$T(5)$	14.6	25.9
		$W_s(2)$	5.3	
		$W_s(3)$	6.0	
	D	$W_T(3-2)$	17.9	25.9
		$\Delta h(7-5)$	6.3	
		$\Delta T(3-2)$	1.7	
$W_s(L)$	ND†	$W_s(3)$	57.7	64.6
		$W_s(2)$	6.9	
	D	ALL	48.2	48.2
S_a	ND + LMW†	$W_s(L)$	15.1	67.4
		$W_s(2)$	25.5	
		$Z(L)$	20.6	
		$W_s(3)$	6.2	
	D + LMW	ALL	64.8	64.8
S_b	ND + LMW†	$Z(L)$	16.5	62.3
		$W_s(L)$	16.0	
		$W_s(5)$	29.8	
	D + LMW	ALL	52.6	52.6

The above discussion of the tables answers the first three questions posed earlier in this section. Answers to questions (d) and (e) are found in Table IV under the column headed "Selected predictors".

The height of the LMW is not selected as a significant predictor for $W_s(L)$, and vice versa. Both $Z(L)$ and $W_s(L)$ are often selected as predictors for the shears, and the shear below is selected as a predictor for the shear above in Categories 1, 3, and 5.

7. Verification and Evaluation of LMW Analyses

The analysis procedure described in Section III was used with a winter data sample (for a time period not within the three month sample used to derive the equations). LMW analyses for twelve observation times were generated, verified, and evaluated.

The verification of the analyses was accomplished by using the areal-mean-error method, and the evaluation consisted of: (1) a diagnosis of the meaning of the error statistics, (2) a comparison of the computer analyses with hand-analyzed charts, and (3) a consistency check to determine if the analyses of the LMW parameters for each observation time were consistent with one another.

8. Areal-mean-error-method Statistics

The overall rms errors for four LMW parameters for twelve observation times during January 1963 are presented in Table VI. The column headed "Analysis rms error" shows the root-mean-square error at stations used in the analysis, and the column headed "Withheld rms error" shows the error at the withheld stations.

The total rms error of 15.4 knots (Category A) for $W_s(L)$ at the final pass of the analysis is quite low when one considers that this category comprises stations that are reporting wind speeds in excess of 100 knots. The error of the wind speed for this category is something less than 15%, and is probably closer to 10% because there are frequently observed maximum winds of 150 to 200 knots, especially over Eastern Asia and the Western Pacific Ocean.

It is readily evident in the overall verification statistics for all the LMW parameters that the reduction in the total rms error from the initial guess to the final pass is due almost entirely to the reduction in the rms error at analysis stations (see Analysis-rms-error column of Table VI). In fact, the withheld-station rms error is,

TABLE VI
OVERALL rms ERRORS FOR LMW PARAMETERS FOR
12 OBSERVATION TIMES

Parameter	Verification category	Error (initial guess/final pass)		
		Total rms error	Analysis rms error	Withheld rms error
$W_s(L)$ (knot)	A	21.9 15.4	22.7 7.0	21.1 20.6
	B	12.5 9.7	12.2 3.5	12.8 13.3
	C	10.1 8.7	7.8 2.6	11.9 12.1
$Z(L)$ (ft)	A	4818 3533	4798 1566	4837 4744
	B	7378 5738	6769 2301	7940 7782
	C	9933 7257	10262 3671	9593 9585
S_b (knot 10^{-3} ft)	A	2.11 1.75	1.72 0.46	2.45 2.43
	B	1.61 1.22	1.48 0.37	1.73 1.68
	C	1.05 0.70	1.15 0.31	0.94 0.94
S_a (knot 10^{-3} ft)	A	2.26 1.87	1.86 0.38	2.60 2.62
	B	1.47 1.17	1.38 0.31	1.56 1.62
	C	0.94 0.77	0.77 0.25	1.08 1.05

in a few cases, slightly higher for the final pass than it was for the initial guess. This result is <u>not</u> surprising because:

       (a) The analysis-station rms error essentially indicates how well the analysis technique fits the observations (and these points may be considered as minimum error points over the analysis area).

       (b) The withheld stations, which approximate maximum error points, do not contribute to the analysis, by definition. A station withheld over a sparse data area may be the only station in the area (e.g., a stationary weather ship in the ocean) and the analysis over that area will remain unchanged from the initial guess to the final pass.

       (c) Withheld stations over medium or high data-density areas are not allowed to influence the analysis. The surrounding analysis stations, however, may change the analysis to the extent that the point at which there is a with-held station observation may actually be in less agreement with the final analysis than it was with the initial-guess analysis.

An important point about the verification statistics is that prior to use of SAT for analysis with station data, the overall rms errors for the initial guess of all LMW parameters was approximately equal for both the analysis stations and the withheld stations (approximate minimum- and maximum-error points, respectively). Two inter-pretations of the data in Table VI that may be made here are: (1) a good initial guess is essential to any hemispheric analysis procedure, and (2) the rms-error values for the initial guesses of the LMW parameters indicate high-quality initial guesses.

Figure 2 clearly illustrates, for a series of individual observation times, the lack of bias between the initial-guess Analysis-rms and Withheld-rms errors for Category A of $W_s(L)$. The Withheld-rms error is significantly lower than the Analysis-rms error six times and the converse is true four times; the remaining two instances have insignificant differences.

Figure 3 shows the LMW wind-speed analyses for 8 and 9 January, 1963. The highest initial-guess Withheld-rms error occurred on 8 January and the lowest occurred on 9 January. Withheld station observations are plotted on the analyses. Figures 4 and 5 are the 300- and 200-mb height analyses for 8 and 9 January, 1963, respectively. They
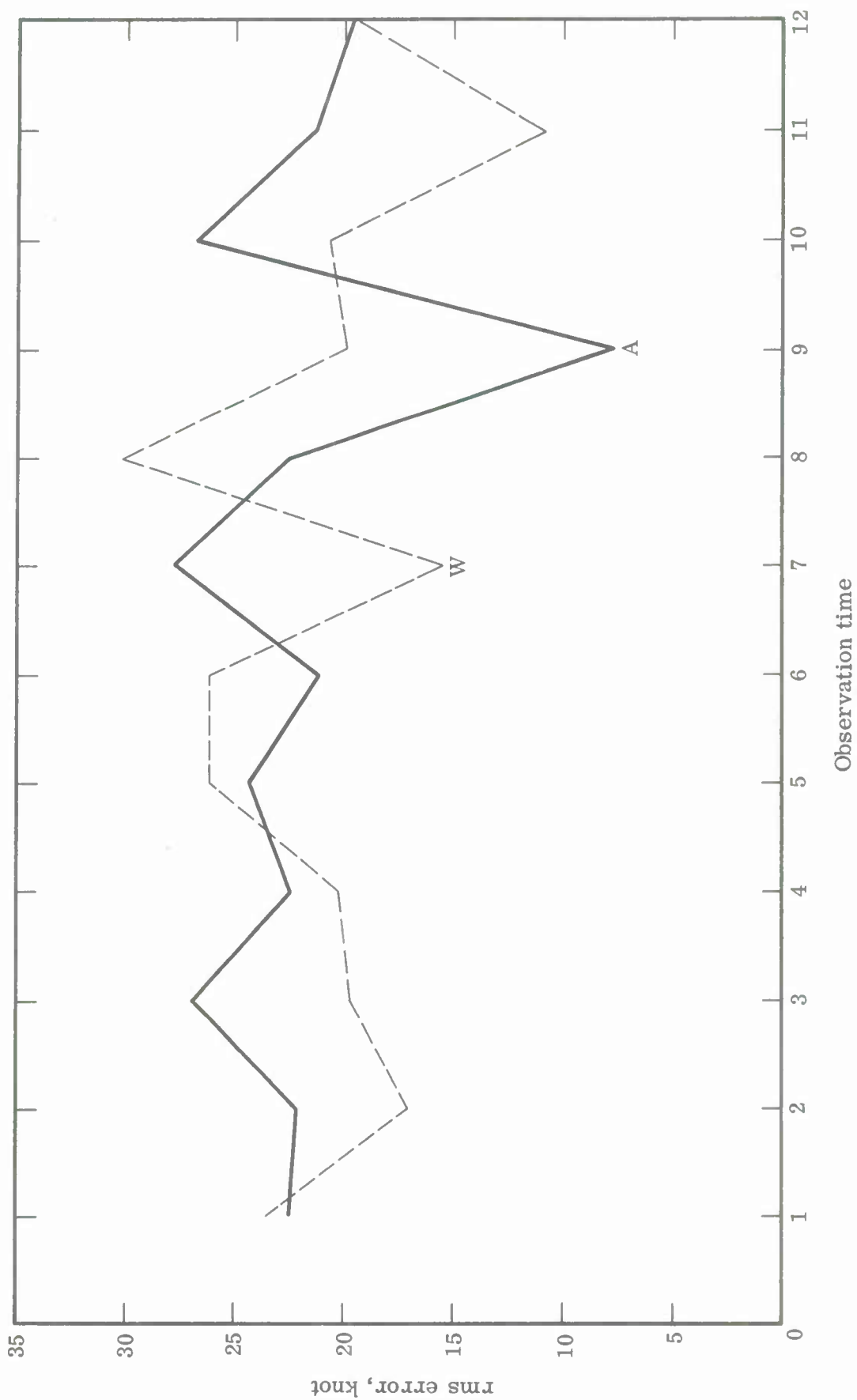
Fig. 2. Initial guess rms errors for LMW wind speed at analysis and withheld stations for 12 observation times (area where W_L >100 knots).

Fig. 3(a). Objective LMW wind speed analysis, 1200Z, January 8, 1963 (knots).
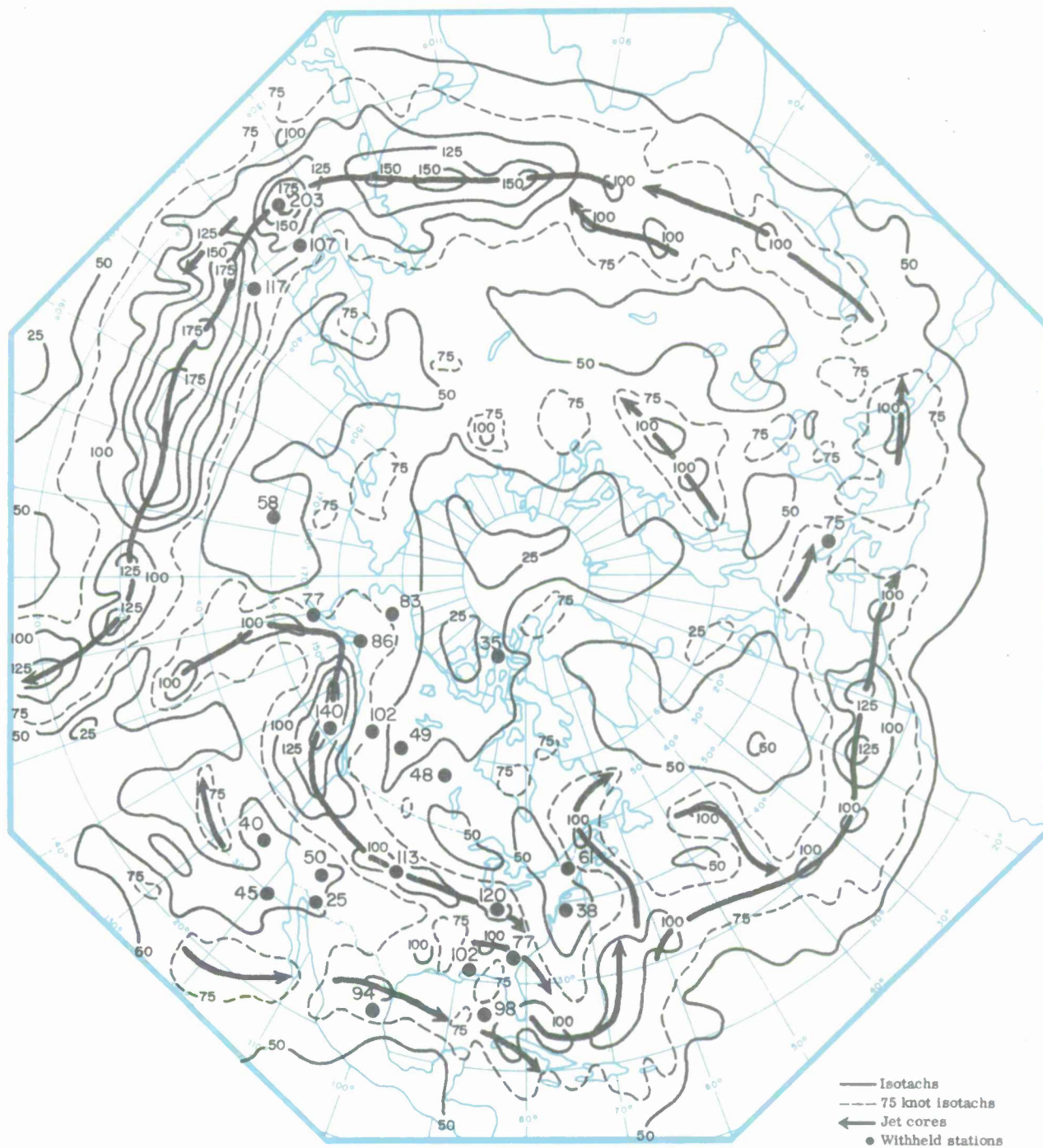
Fig. 3(b). Objective LMW wind speed analysis, 1200Z, January 9, 1963 (knots).
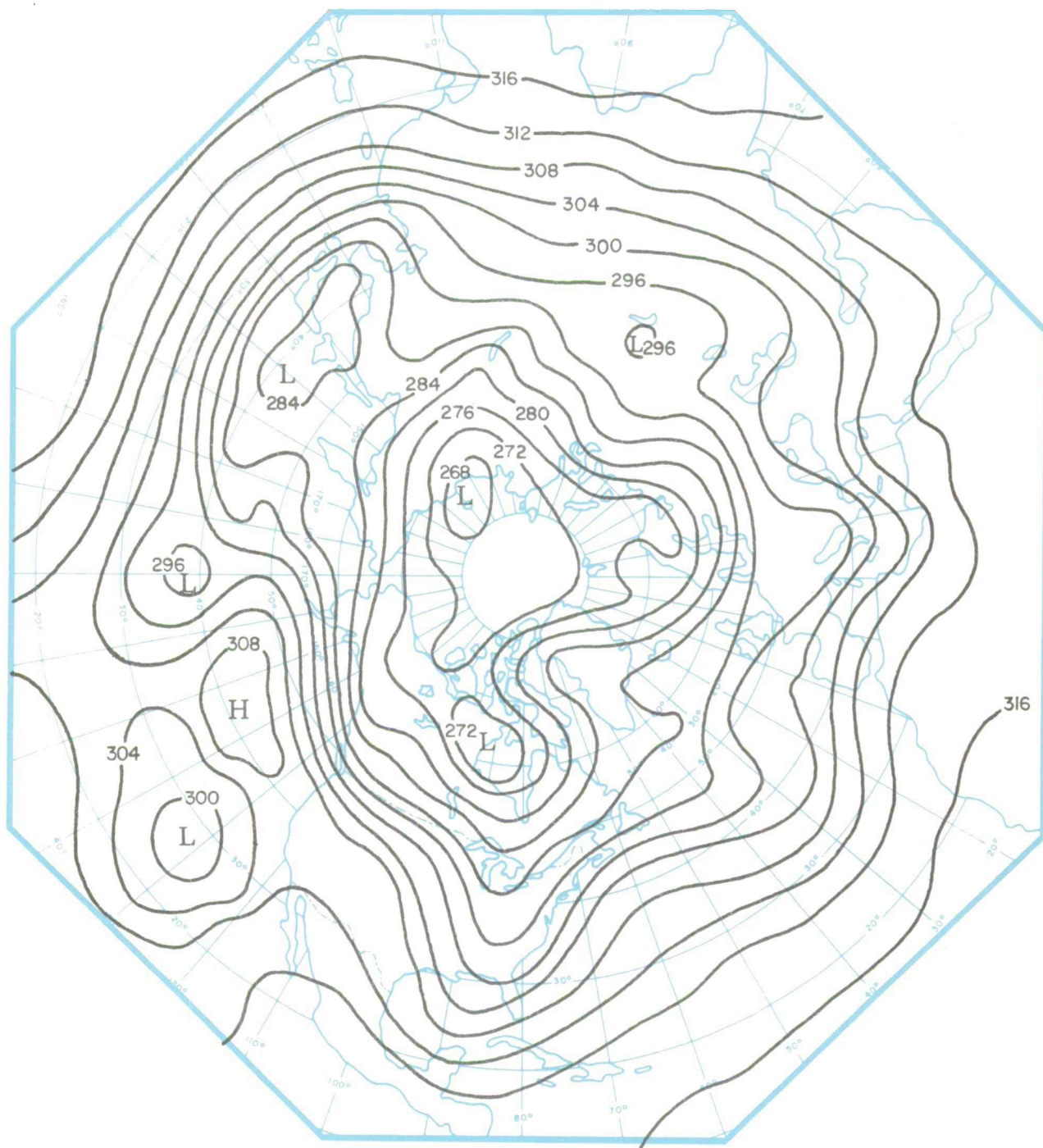
Fig. 4(a). 300-mb analysis, 1200Z, January 8, 1963 (10^2 ft).
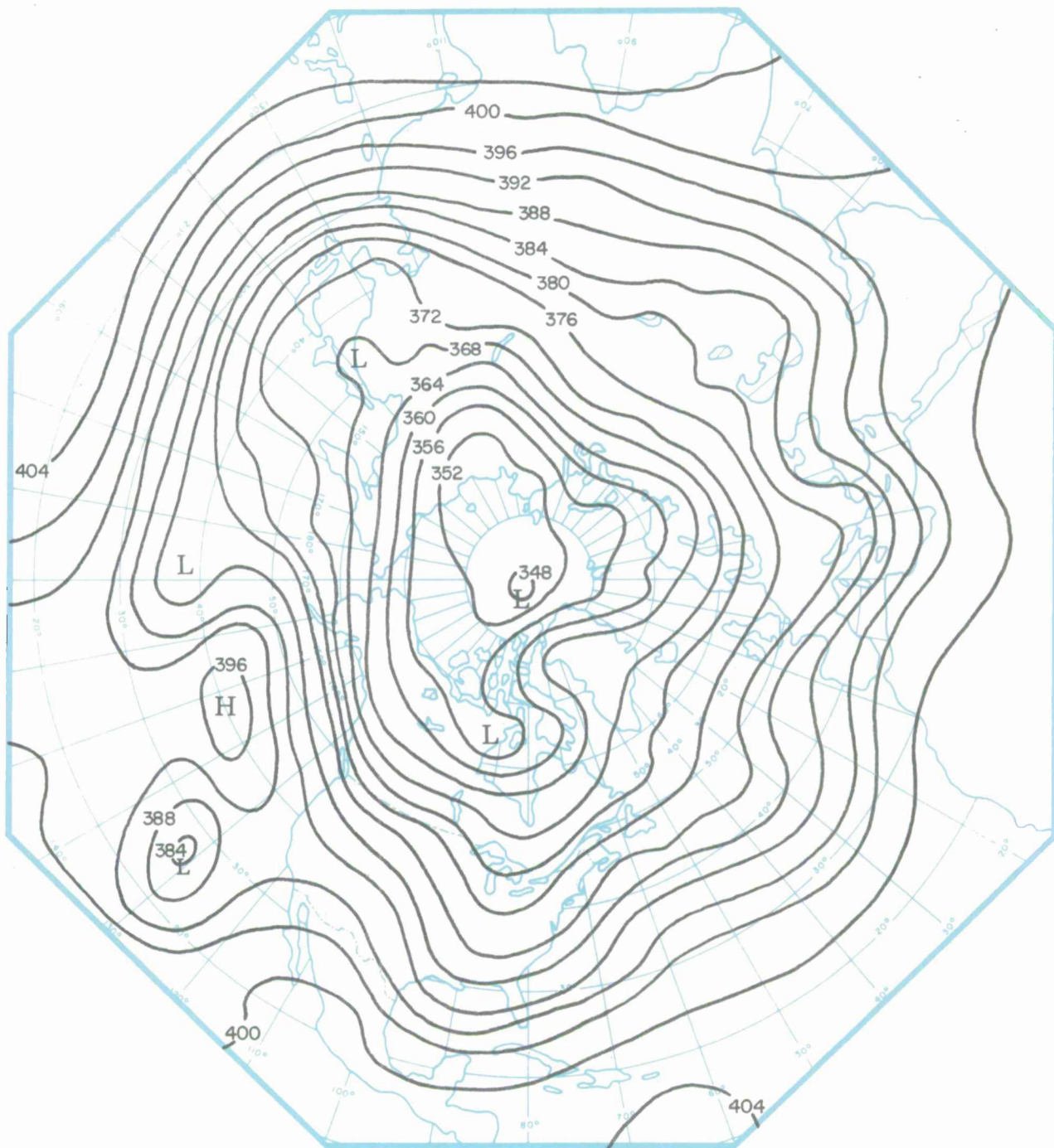
Fig. 4(b). 200-mb analysis, 1200Z, January 8, 1963 (10^2 ft).

29
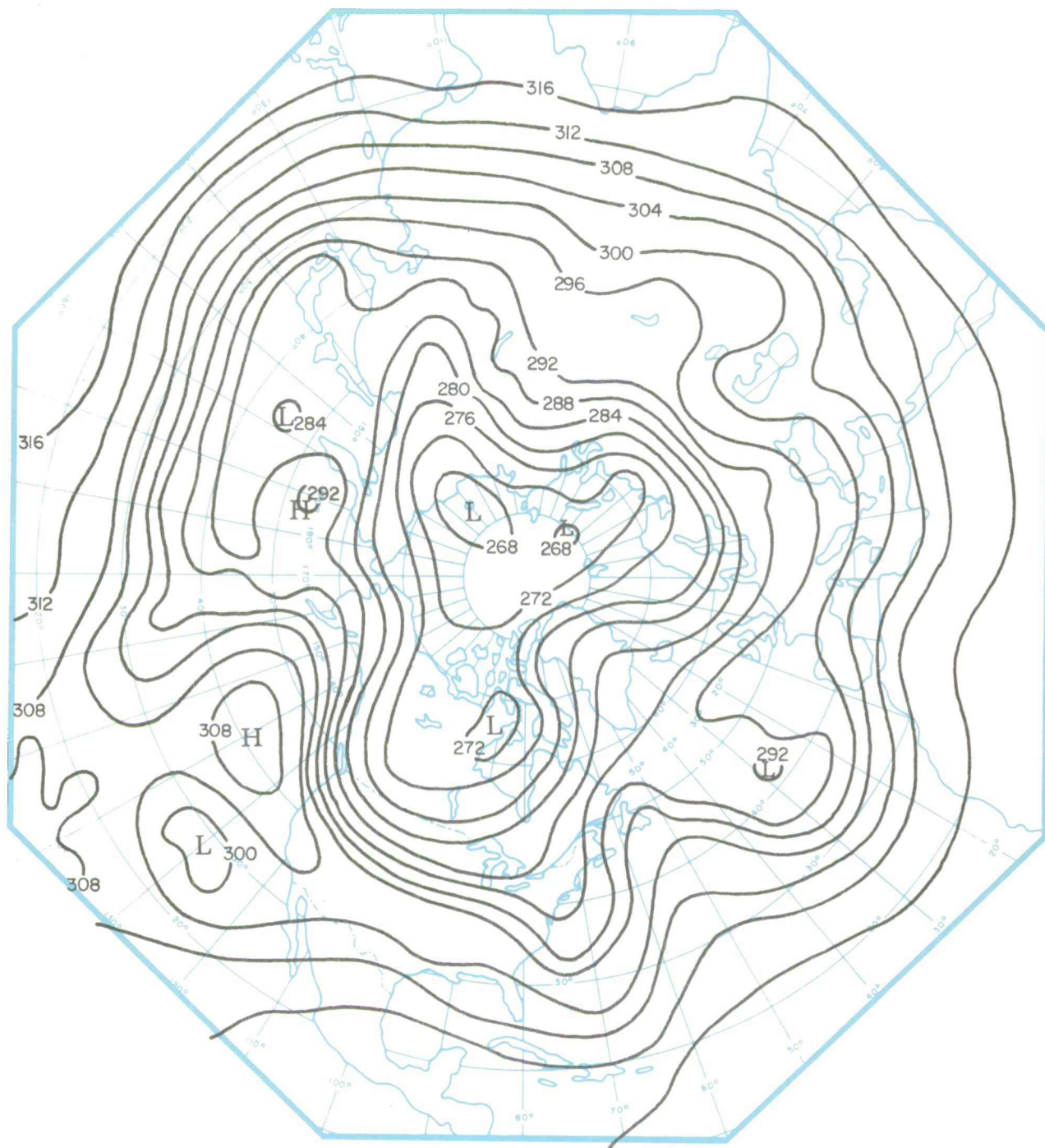
Fig. 5(a). 300-mb analysis, 1200Z, January 9, 1963 (10^2 ft).
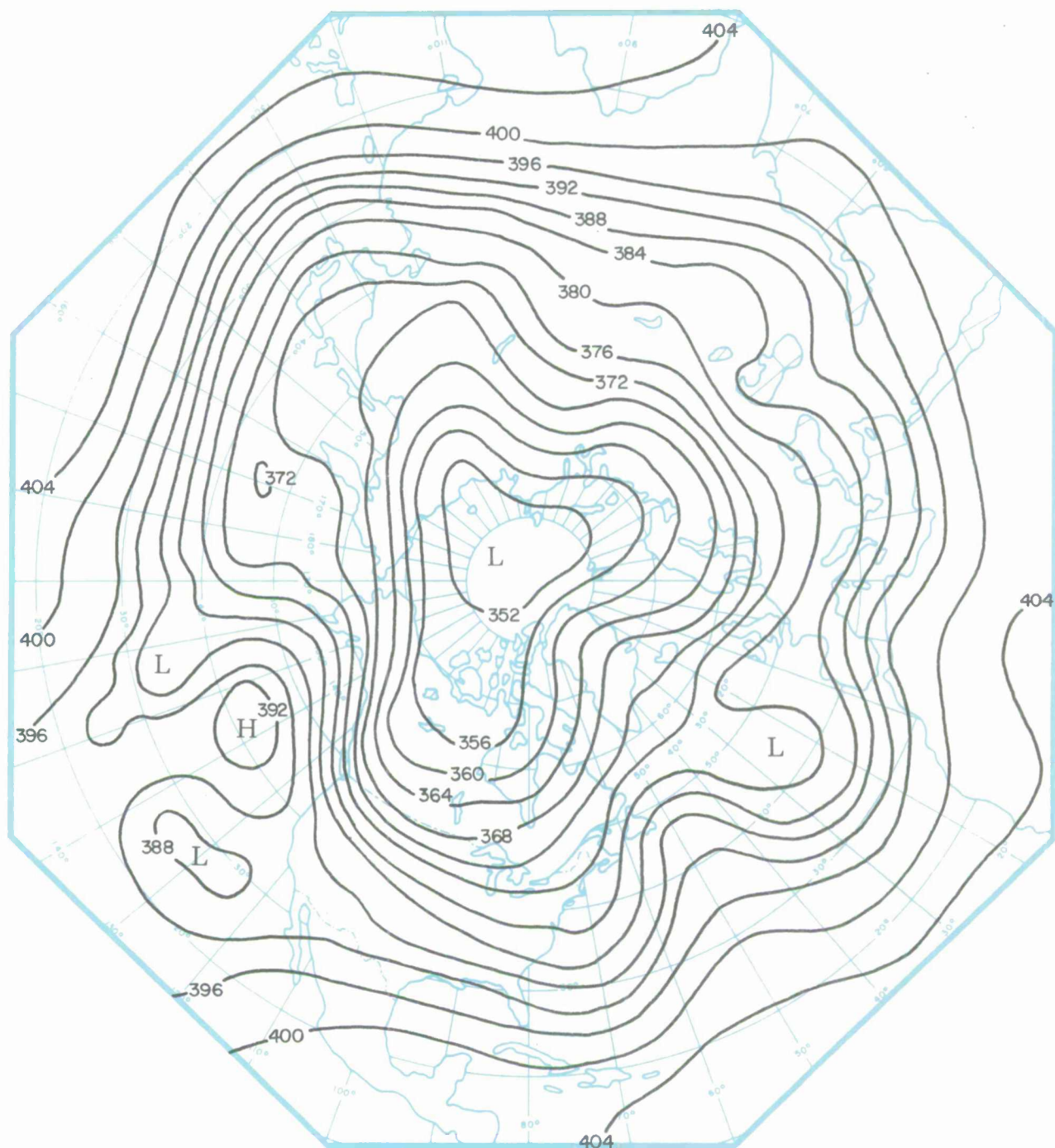
Fig. 5(b). 200-mb analysis, 1200Z, January 9, 1963 (10^2 ft).

are shown because the predictors for $W_s(L)$ for Categories 2—7 are the 300- and/or 200-mb wind speeds (which are derived from the height analyses).

Because vertical wind profiles sometimes indicate high wind speeds over a layer that may be as much as 10,000 feet or more thick, with more than one identical maximum speed within that layer, Z(L) is sometimes difficult to specify. With this in mind, the total rms error for verification Category A [$W_s(L)$ > 100 knots] for 3533 ft is considered to be a reasonably low value.

Where $W_s(L)$ is less than 100 knots and, particularly, less than 50 knots (Categories B and C), the height of the LMW may vary widely at adjacent grid points and/or stations. This is a common characteristic of adjacent wind profiles that exhibit relatively weak maximums. Thus, it is not surprising that the rms errors for Z(L) increase with decreasing maximum wind speed.

Conversely, the rms errors for the shears below and above the LMW decrease with increasing wind speed, but have approximately the same percent error because the values of vertical wind shear are generally greater for the higher than for the lower maximum wind speeds.

The total rms errors for individual observation times for the initial-guess and final pass for each of the four LMW parameters is graphically represented in Figs. 6, 7 and 8.

9. Objective (computer) versus Subjective (man) LMW Analysis Comparison

Although the areal-mean-error method of verification gives useful information about the quality of the analysis technique, the evaluation is not complete unless a comparison is made of the objective computer analysis of the LMW parameters and the subjective analyses performed by a human analyst. Comparisons for each of the LMW parameters are discussed individually below.

Wind Speed at the LMW—Figure 9 illustrates some of the objective—subjective comparisons of the jet cores, the associated maximum isotachs, and the 75-knot isotachs. These and the other objective and subjective analyses of $W_s(L)$ for the twelve observation times reveal that there are only minor differences in the analyses over the dense data areas, while more differences are apparent over the sparser data areas. These differences are attributed primarily to the human analyst drawing to the available

32
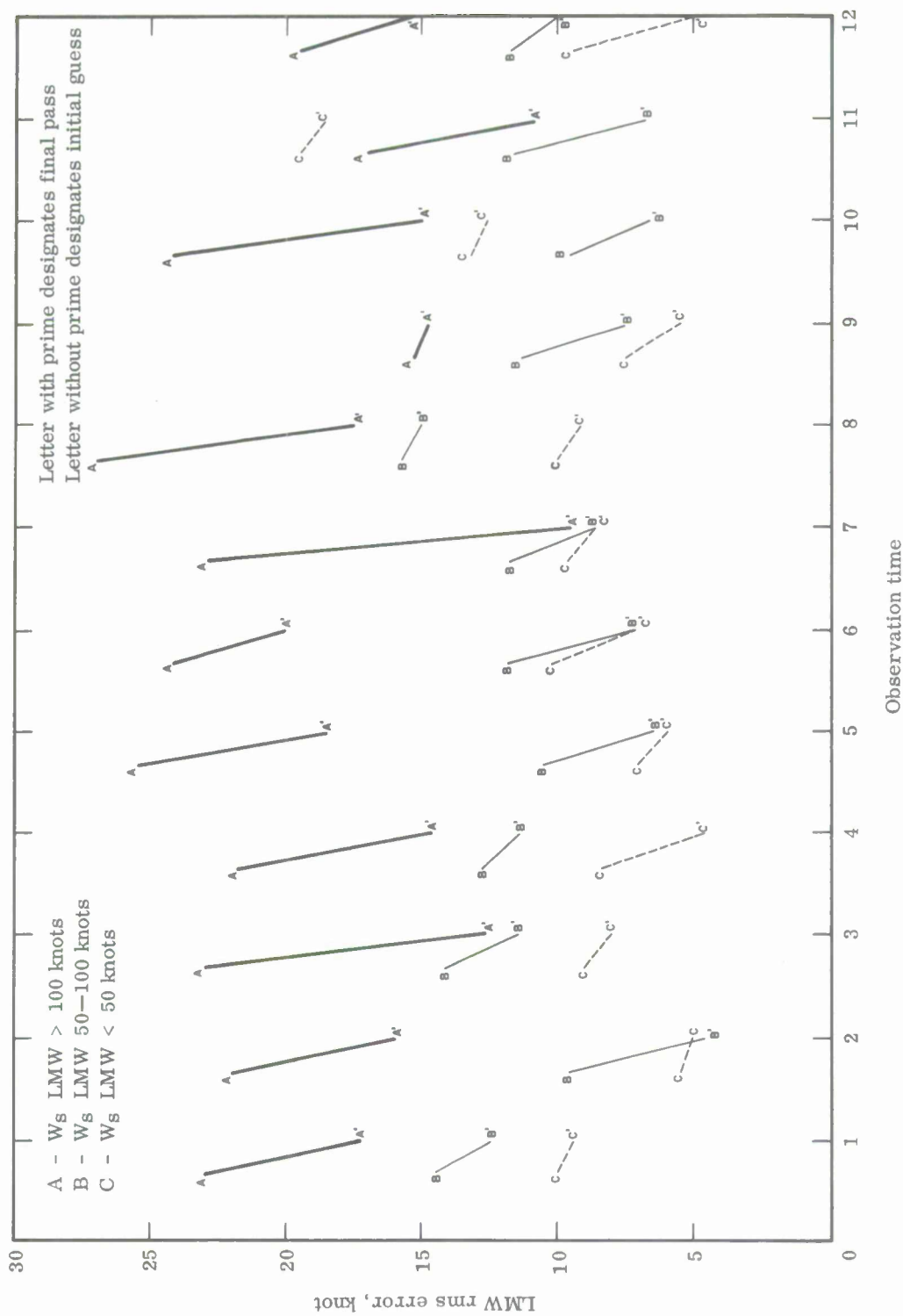
Fig. 6. Rms errors of wind speed at the LMW for three wind-speed categories for 12 observation times.

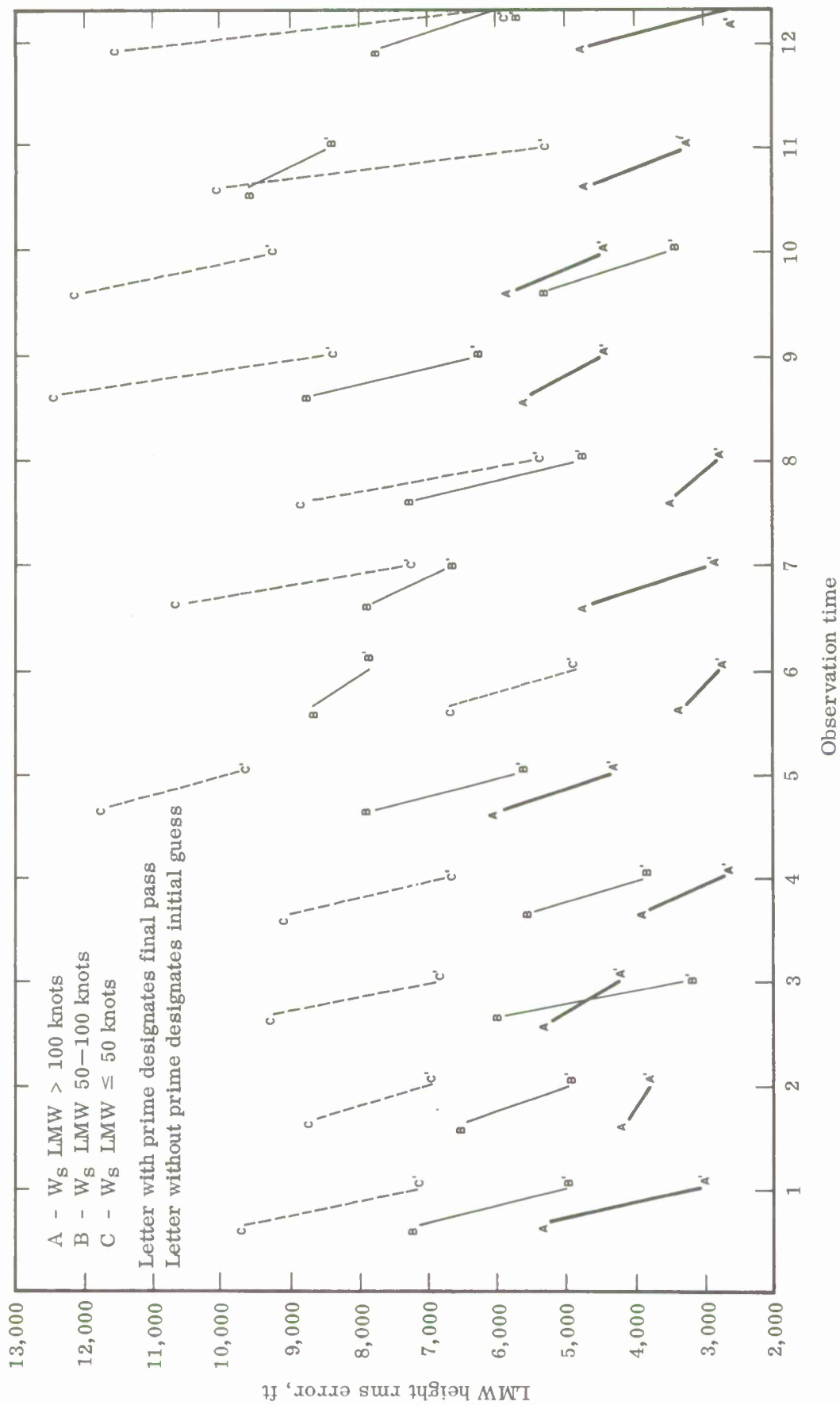Fig. 7. Rms errors of height of the LMW for three wind-speed categories for 12 observation times.
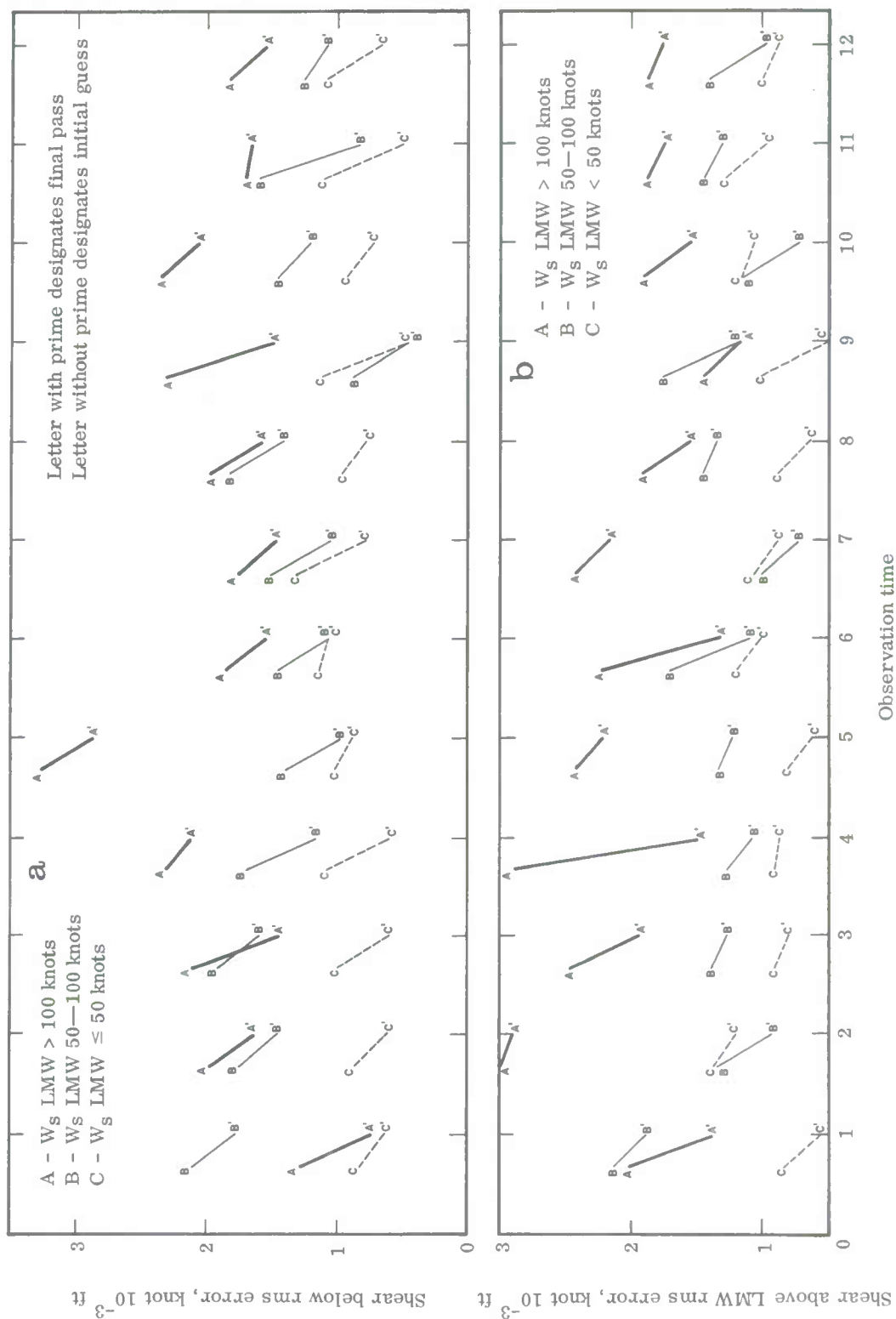
34

Fig. 8. Rms errors of shears below (a) and above (b) the LMW for three wind-speed categories for 12 observation times.

35
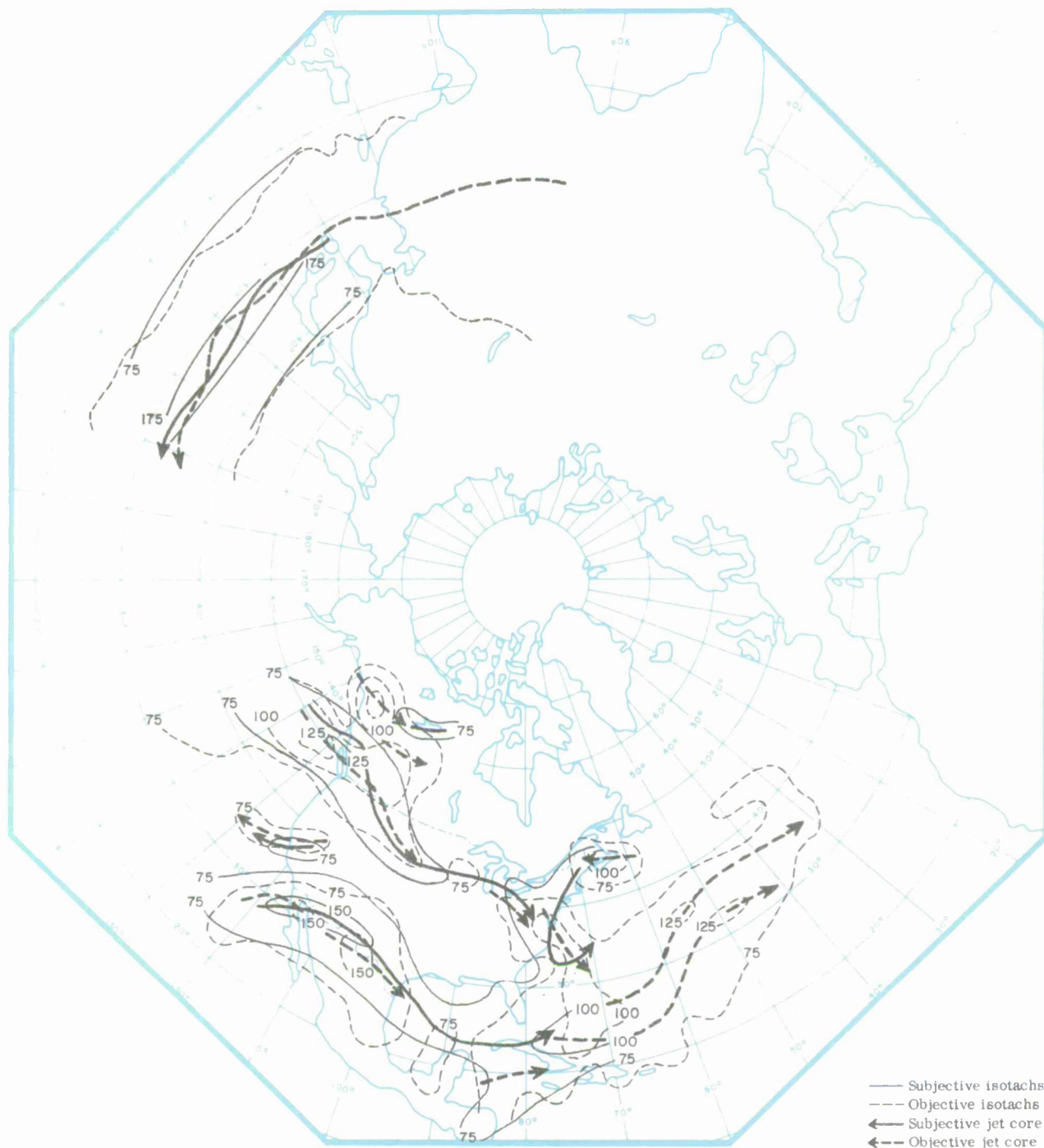
Fig. 9(a). Objective and subjective jet stream analysis comparison, 1200Z, January 1, 1963 (knots).
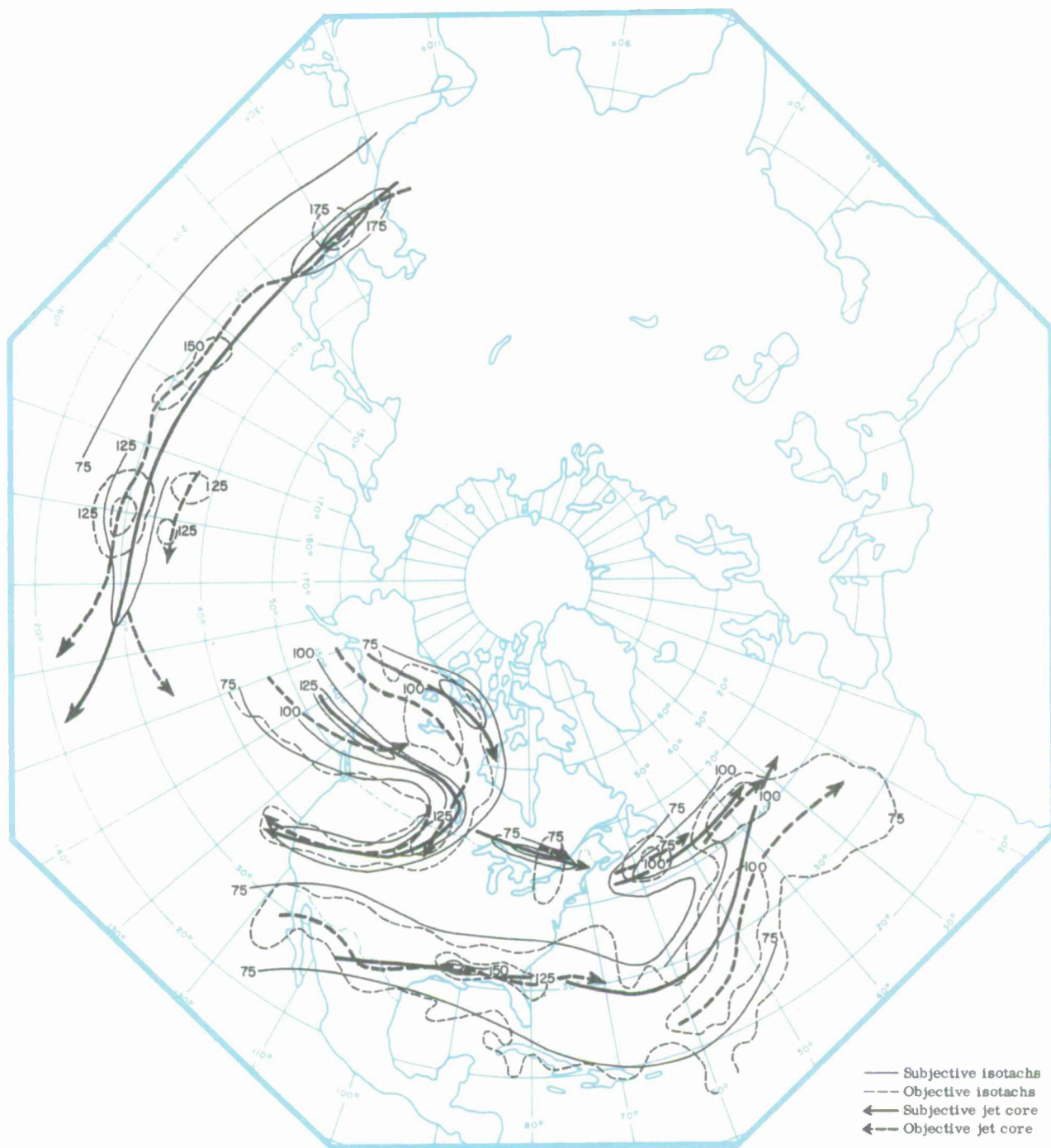
Fig. 9(b). Objective and subjective jet stream analysis comparison, 1200Z, January 5, 1963 (knots).

data, resulting in a tendency for the jet cores to be positioned close to the observing station when, in reality, the maximum wind speeds may be further from the station.

A subjective analysis could not be performed over the no-data areas, but the nature of this computer analysis technique provides for an analysis over the entire grid [e.g., the initial guess of the LMW wind speed uses 200- and/or 300-mb wind speeds as predictors (see Table VI and the Appendix)]. These wind speeds are derived from 200- and 300-mb height analyses by using the gradient-wind equation. The initial guesses to the constant-pressure-surface height analyses are 12-hr dynamic prognoses that verify (terminate) at analysis time. Thus, information from the data areas (for the previous 12 hrs) is incorporated over the no-data and sparse-data areas of the LMW analyses in a quantitative, consistent, and objective manner. For example, the ocean areas off the east coasts of continents are generally no-data areas, but the dynamic prognosis is usually based on the initial conditions over the continent. In this study, the 300- and 200-mb height analyses were not available to the human analyst. Had they been available, the analyst would have incorporated the information in a subjective manner that probably would not be as quantitatively consistent as the objective procedure.

Height of the LMW—As mentioned previously, the analysis of $Z(L)$ is only meaningful over those areas where $W_s(L) > 75$ knots. Examination of the objective and subjective analyses of $Z(L)$ over these areas reveals that they are in general agreement, although the objective technique has a tendency to indicate cells of high and low heights near individual stations.

Figure 10 illustrates the objective versus the subjective $Z(L)$ charts for the same observation times as for the wind speed at the LMW. In some cases there appear to be important differences in the analyzed values over a particular area, but this, primarily, is due to the stations that were withheld from the objective analysis and included in the subjective analysis.

Shears Below and Above the LMW—The objective and subjective analyses of vertical shears of horizontal wind speed below and above the LMW exhibit general patterns that are similar. The detailed patterns appear to differ in some cases, especially near the jet cores where the subjective analyst tended to elongate the maximum shear centers while the objective analysis indicated more circular maximums. The magnitude

Fig. 10(a). Objective and subjective height of LMW analysis comparison, 1200Z, January 1, 1963 (10^3 ft).
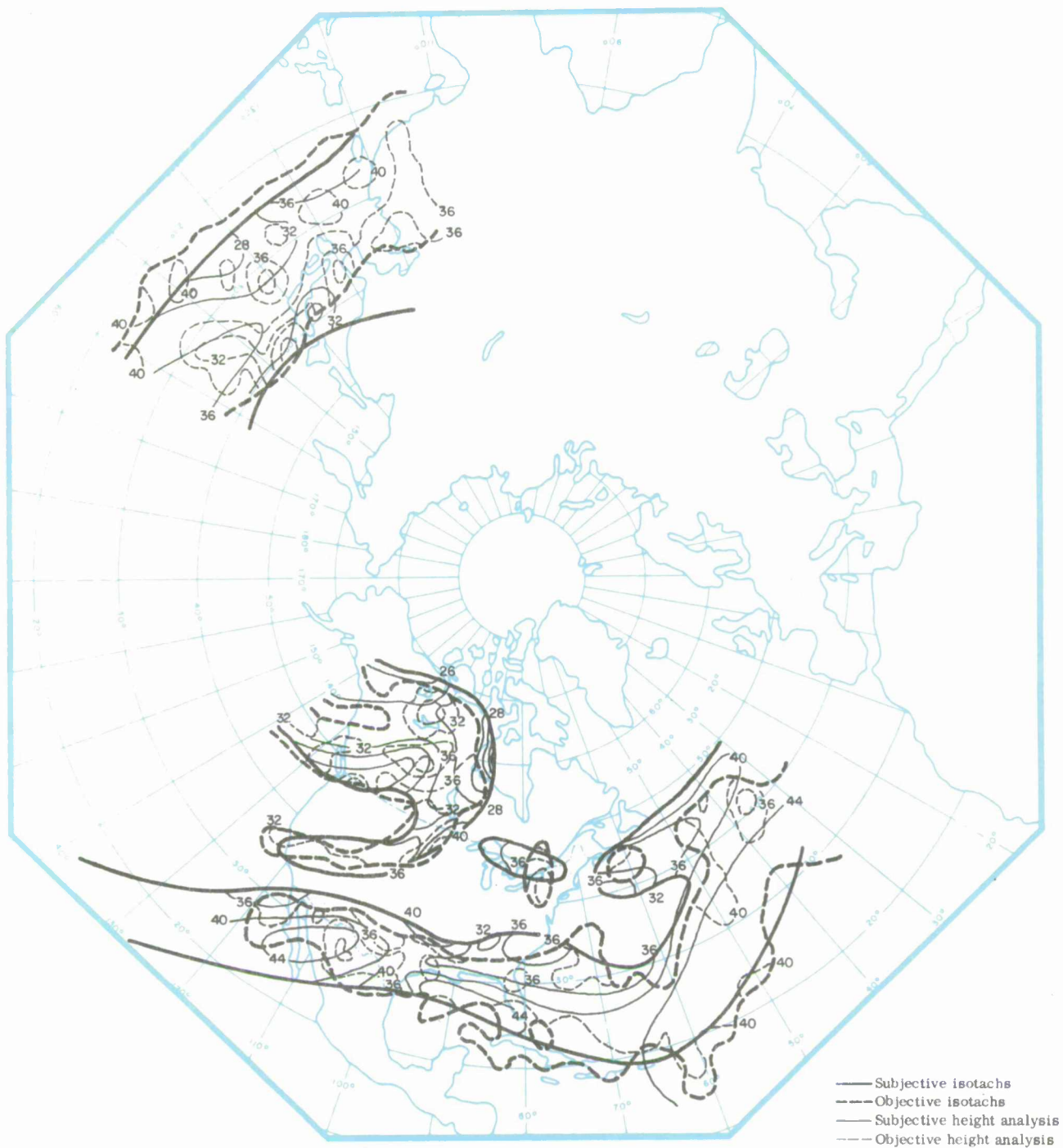
Fig. 10(b). Objective and subjective height of LMW analysis comparison, 1200Z, January 5, 1963 (10^3 ft).

of the shears is similar. Figures 11 and 12 show the analyses of shear below and above the LMW for the same four observation times as for the wind-speed and the wind-height analyses.

10. Consistency Between LMW Parameters

An important phase of the evaluation was to check for consistency between the LMW parameters. A study of the five LMW fields for each of the observation times in the January, 1963 data sample indicated that the analyses, in general, were consistent with one another. The height of the LMW was usually at a higher elevation for jets at lower latitudes (subtropical jets) and at a lower elevation for mid- and higher-latitude jets (polar jets). Where two jets were relatively close to each other in the horizontal, higher elevations of the height of the LMW were found in the jet to the right, when facing in the downstream direction, (i.e., the direction toward which the wind is blowing). This is in agreement with what is known to occur.

The maximum values of vertical shears of the horizontal-wind speed frequently were observed to be in the regions of maximum wind speeds.

Comparisons between Figs. 9 through 12, and between the five parts of Fig. 13, will verify these statements.

The exceptions to the general cases occur in regions where the vertical wind profiles are blunt in the region of maximum wind (i.e., where there is really no clear level of maximum wind and where high wind speeds exist over a relatively thick layer of 8—15 thousand feet or more [4]). Because the analysis technique specifies a level of maximum wind, a particular level is indicated somewhere in the thick layer of high wind speeds, although the level selected in these cases is not meaningful by itself.

The shear below and above the level of maximum wind is averaged for layers that are 10—12 thousand feet thick. In the cases of thick vertical layers of high wind speed, either the shear below, above, or a combination of both may be computed to be a relatively low value, depending on where in the layer the level of maximum wind is specified. Solutions to the problems caused by thick layers of maximum wind speeds are offered in Section V.

The following interesting items should be noted in the five parts of Fig. 13:

　　　　(a) The generated observations along the jet cores tend to elongate the

41
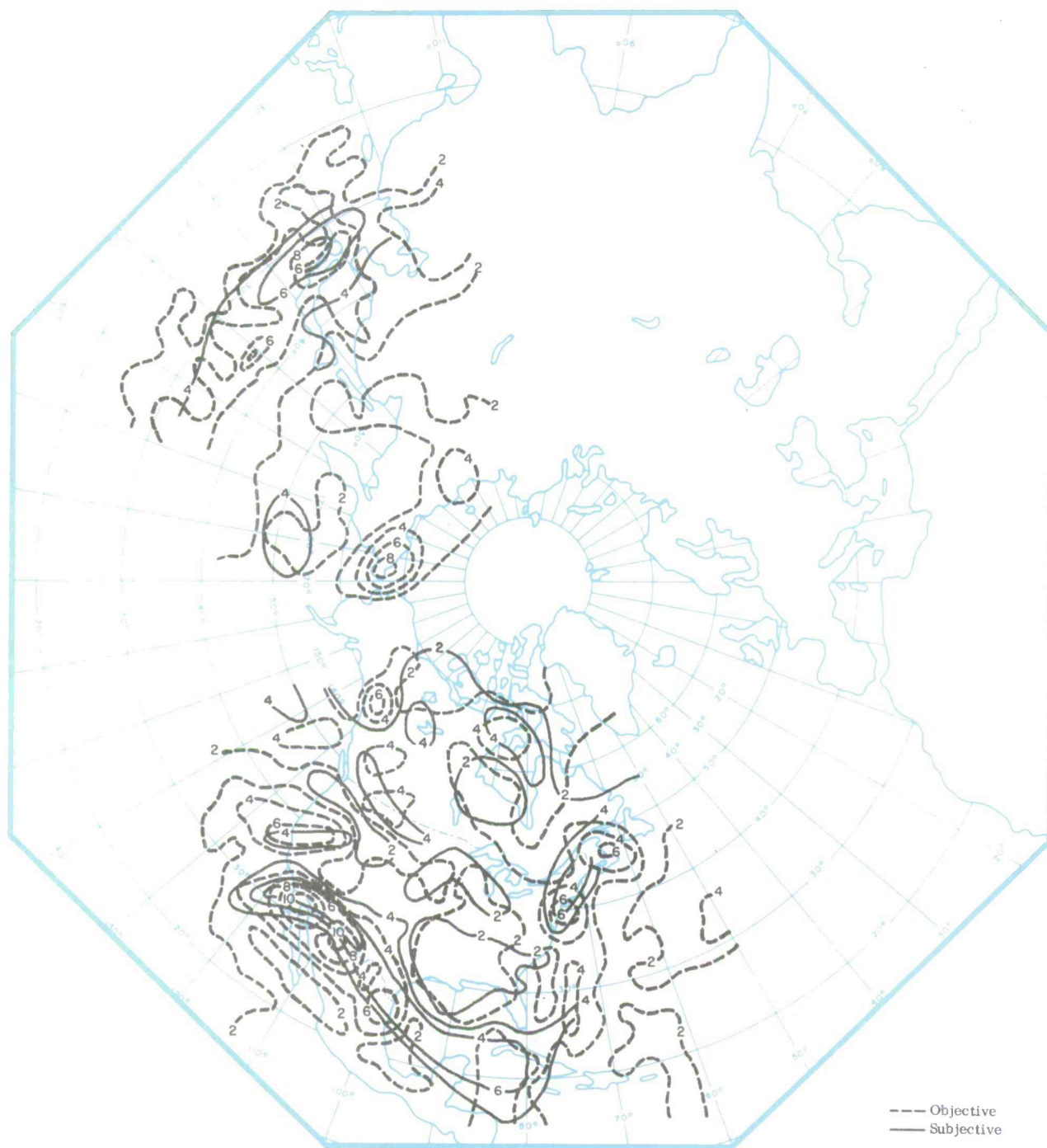
Fig. 11(a). Objective and subjective shear below the LMW analysis comparison, 1200Z, January 1, 1963 (knot 10^{-3} ft).
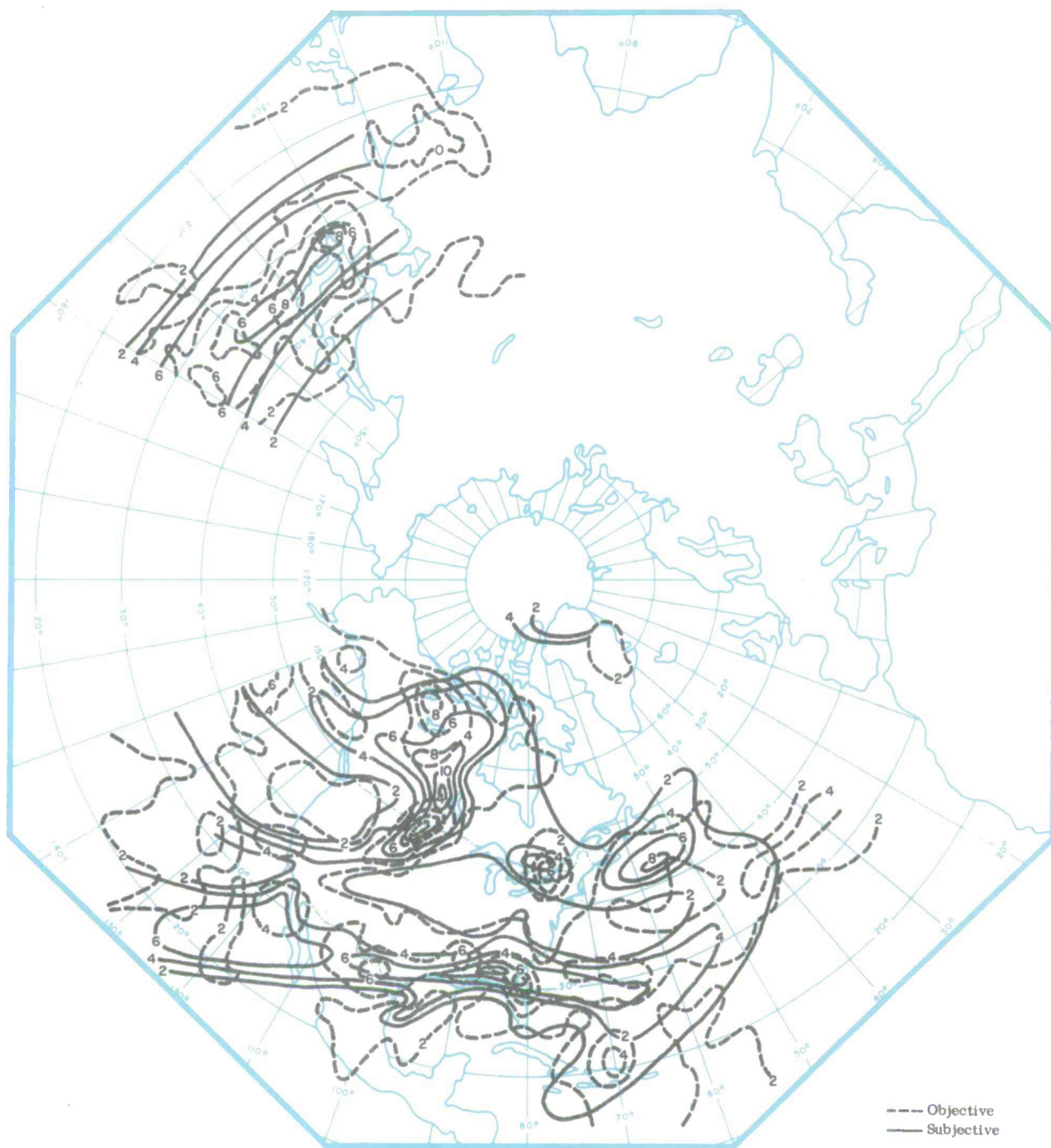
Fig. 11(b). Objective and subjective shear below the LMW analysis comparison, 1200Z, January 5, 1963 (knot 10^{-3} ft).
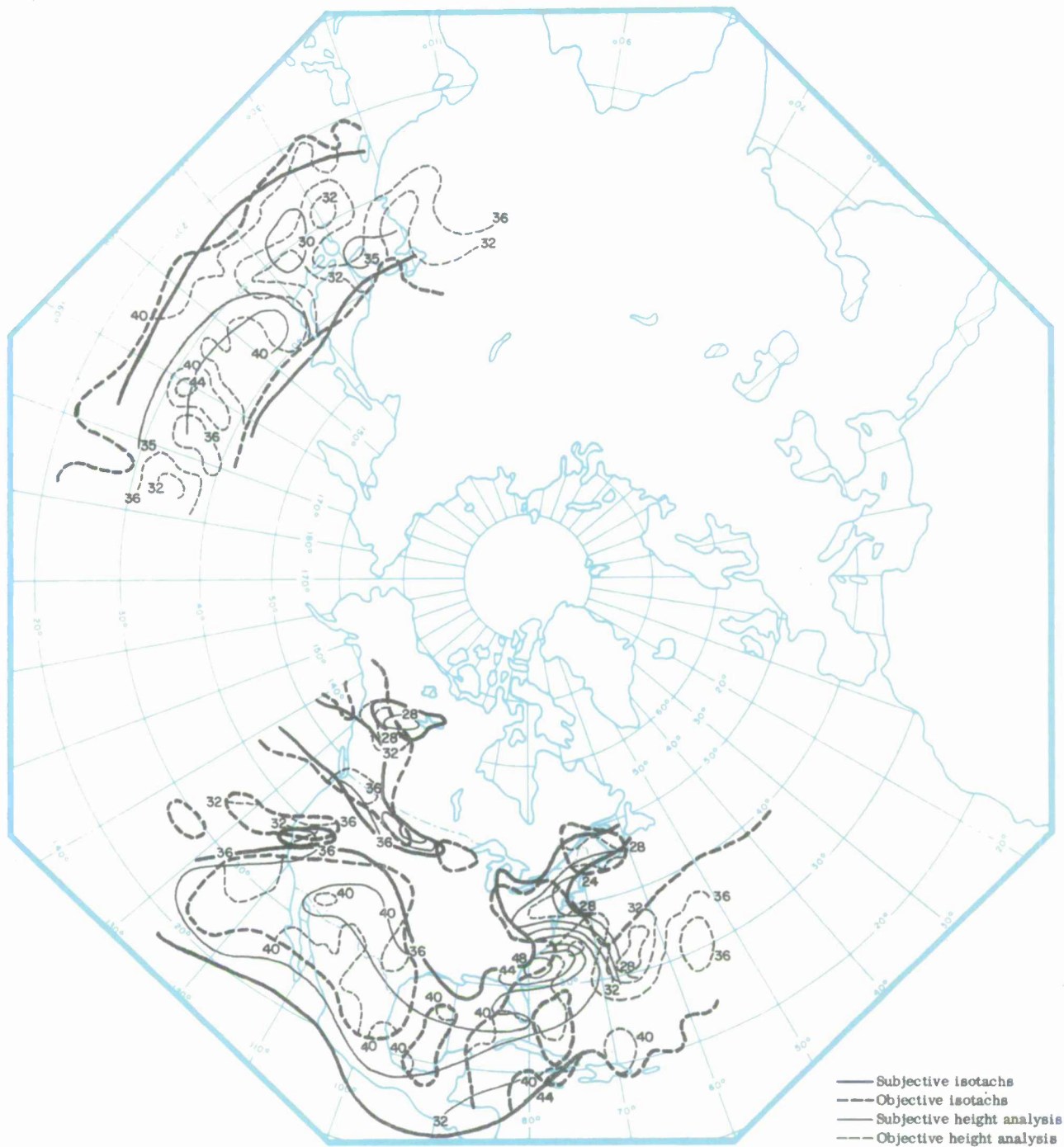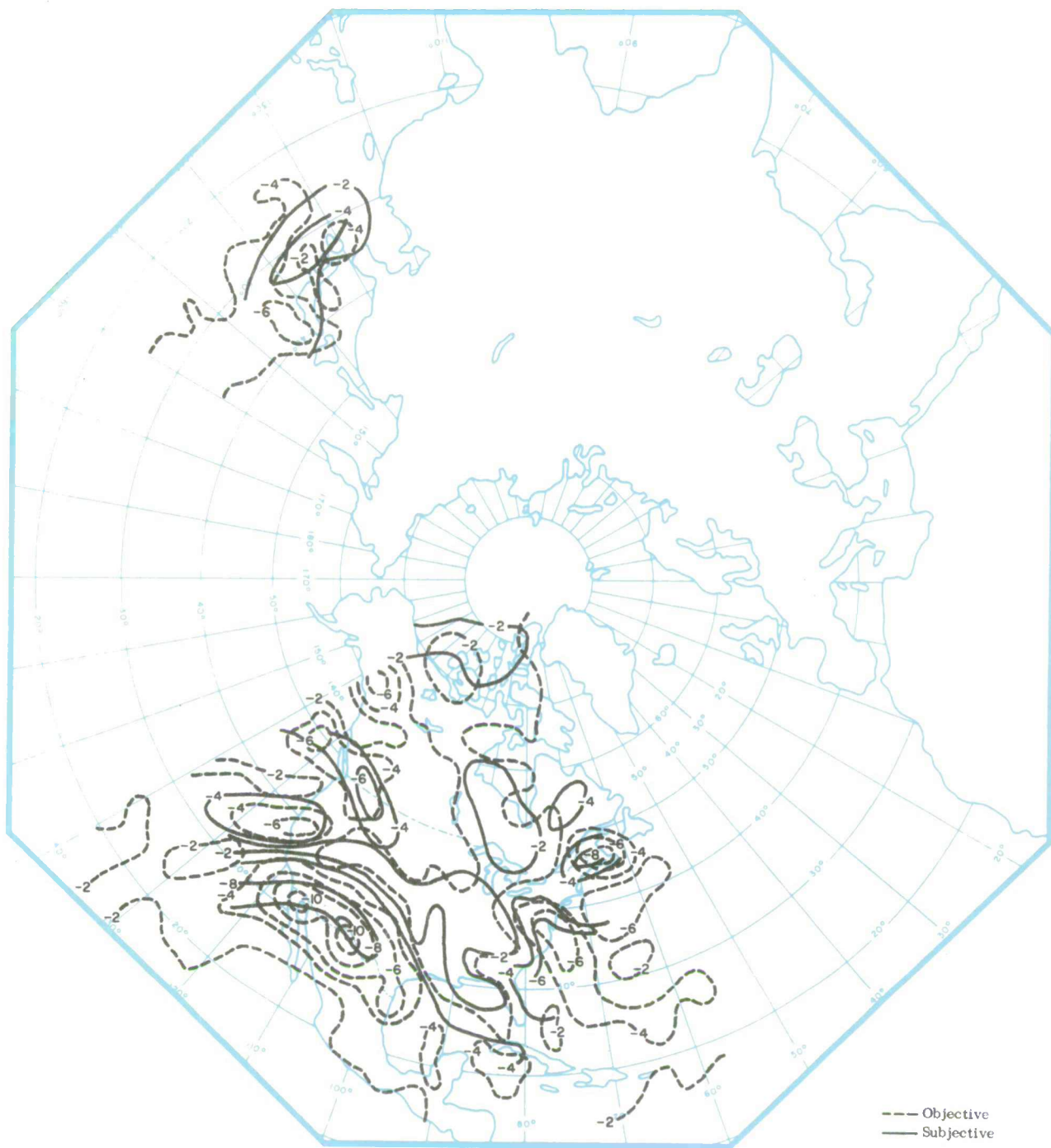
Fig. 12(a). Objective and subjective shear above the LMW analysis comparison, 1200Z, January 1, 1963 (knot 10^{-3} ft).
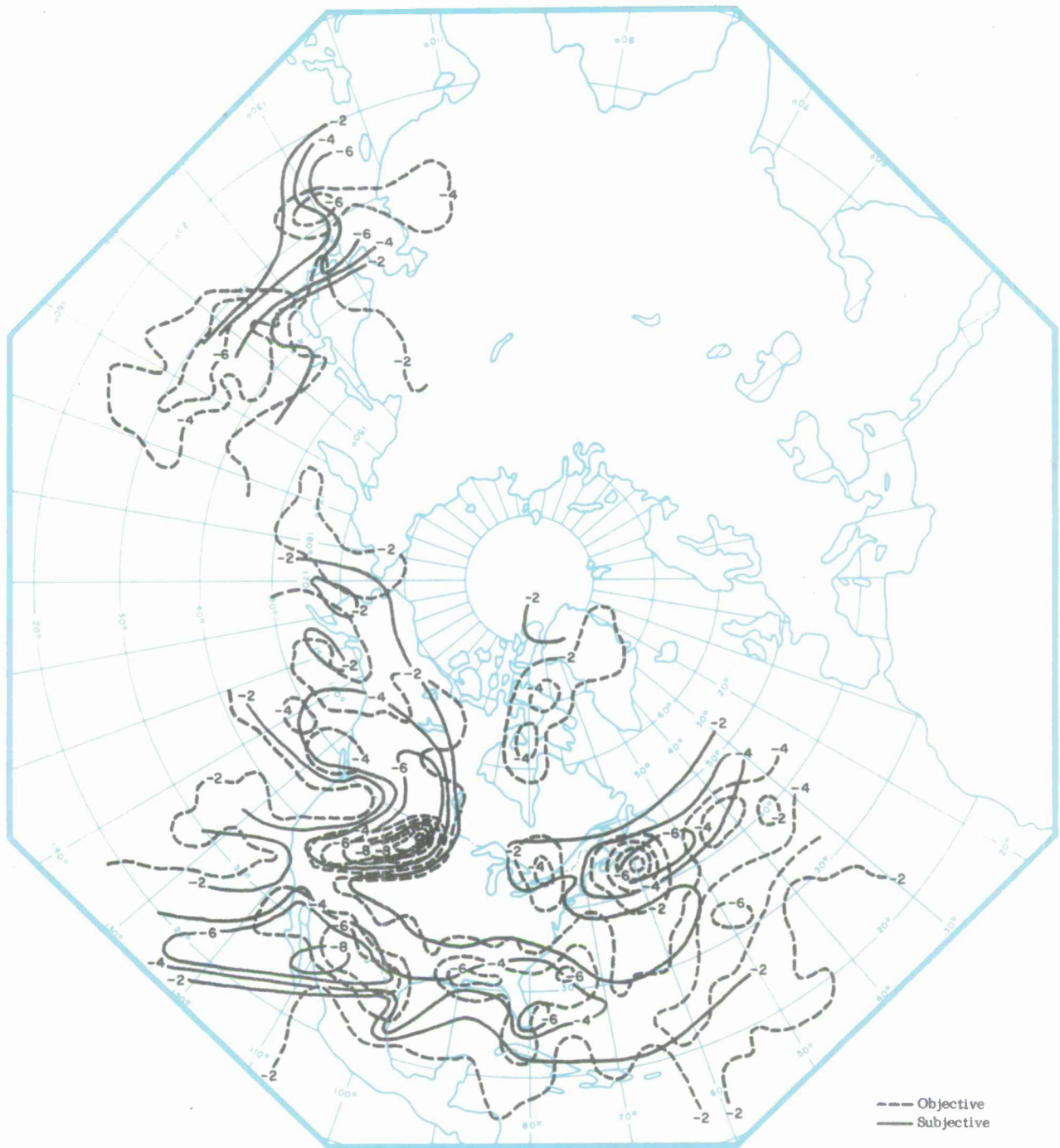
Fig. 12(b). Objective and subjective shear above the LMW analysis comparison, 1200Z, January 5, 1963 (knot 10^{-3} ft).
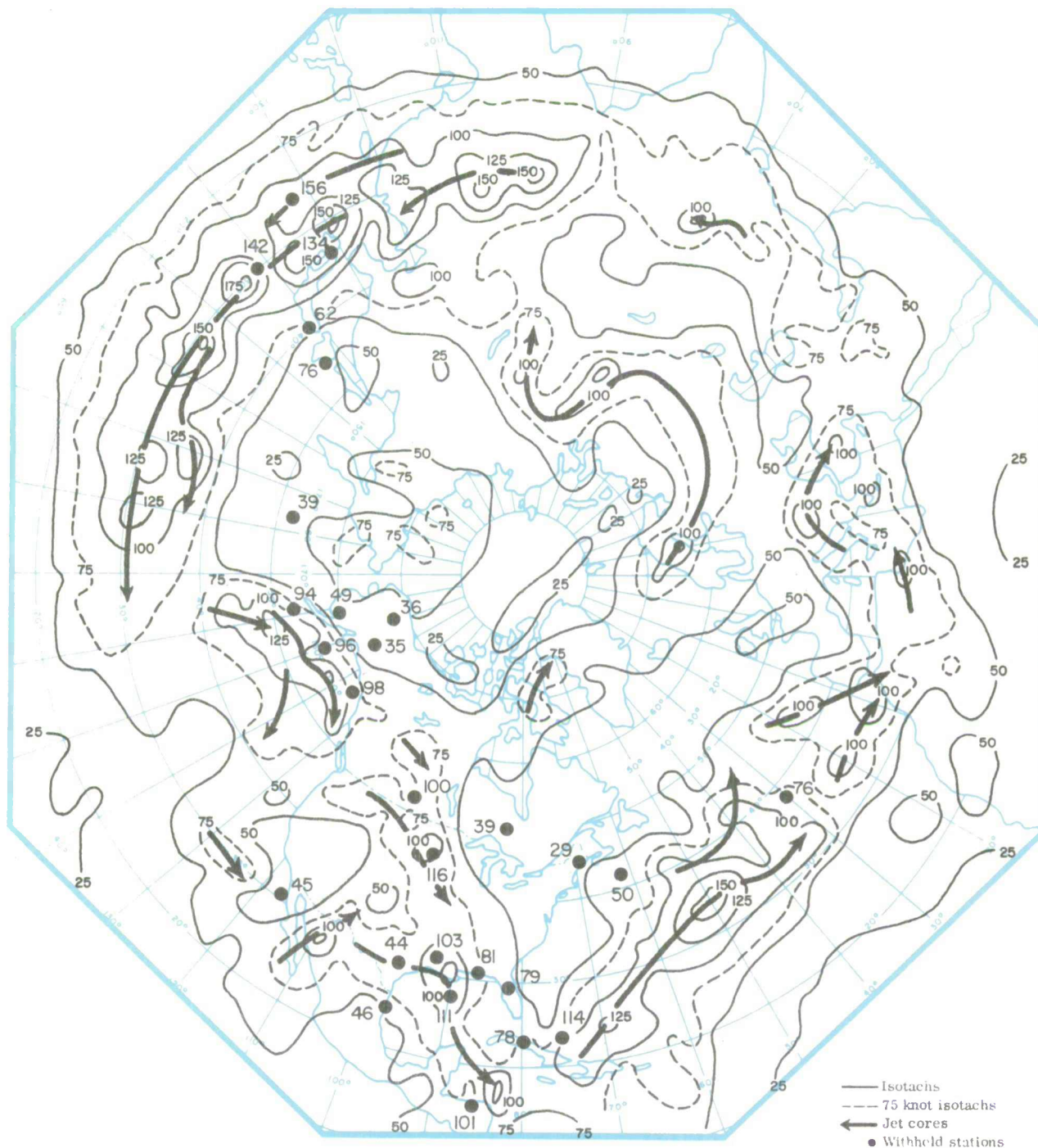
Fig. 13(a). Objective LMW wind speed, initial guess, 1200Z, January 3, 1963 (knots).

46

Fig. 13(b). Objective LMW wind speed, final pass, 1200Z, January 3, 1963 (knots).

47
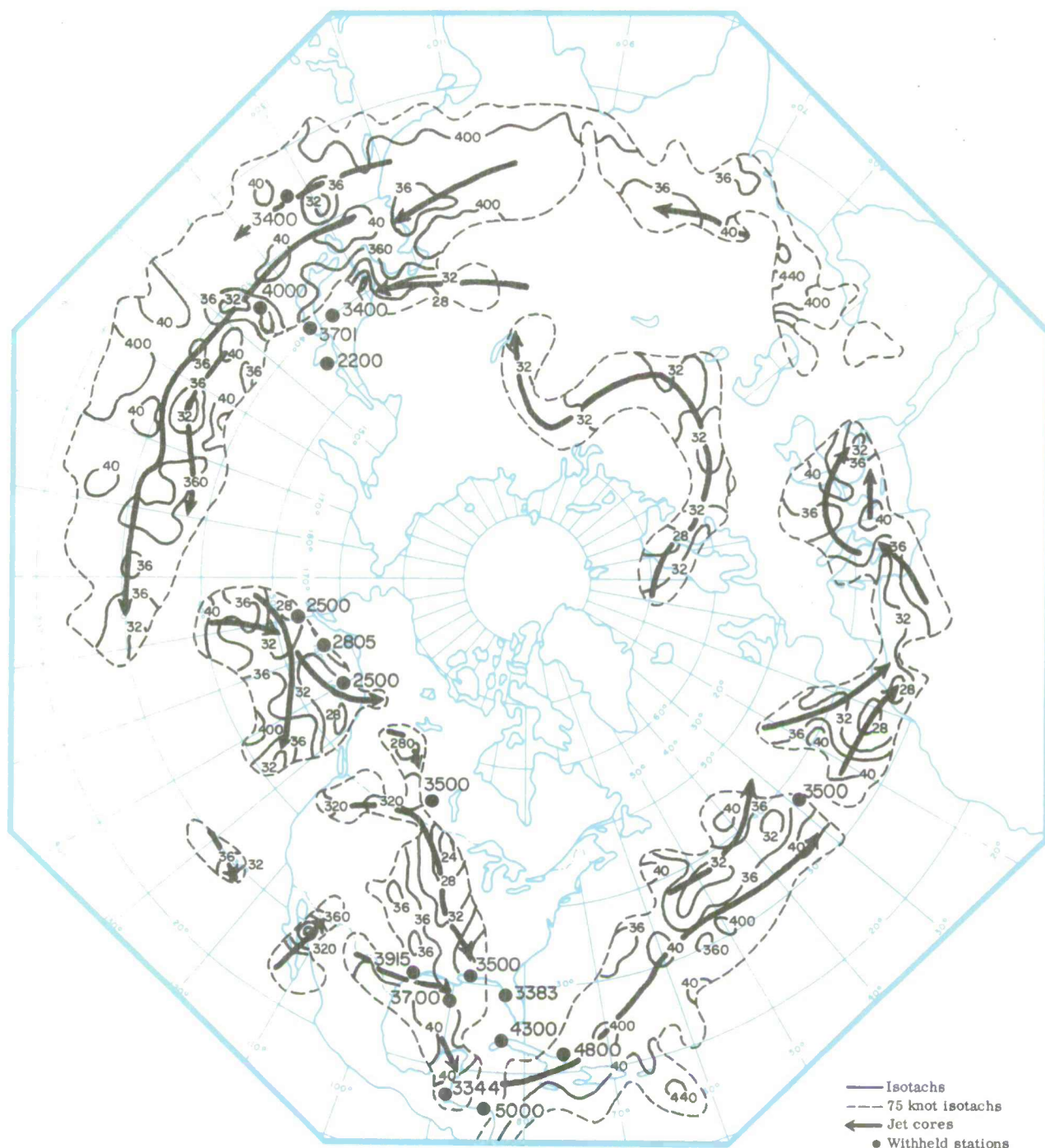
Fig. 13(c). Objective height of the LMW analysis, 1200Z, January 3, 1963 (10^3 ft).

Fig. 13(d). Objective shear below the LMW analysis, 1200Z, January 3, 1963 (knot 10^{-3} ft).
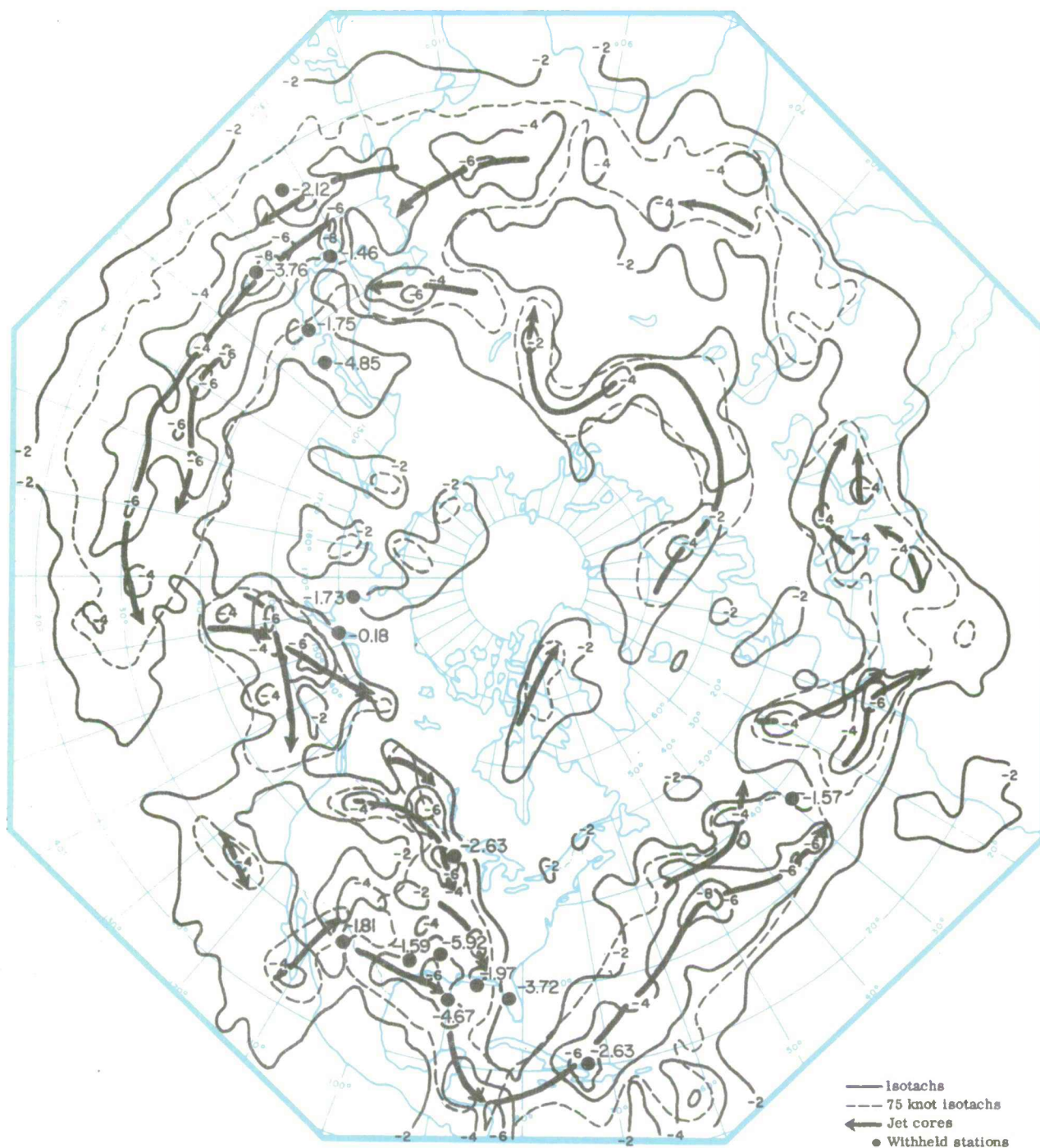
Fig. 13(e). Objective shear above the LMW analysis, 1200Z, January 3, 1963 (knot 10^{-3} ft).

maximum wind isotachs. Note the differences between the initial-guess analysis [Fig. 13(a)] and final-pass analysis [Fig. 13(b)], particularly over the areas south of Korea and north of the Dominican Republic. The jet cores were drawn taking into account the wind speed, wind direction, and generated observations along the cores.

(b) The subtropical jet (with south-southwest winds) that is shown in the central Pacific [Fig. 13(c)] meets the polar jet (with west winds) in the vicinity of 50° North and 160° West.

(c) The jets over North America are the polar jet (elevation 28—32 thousand feet), evident from central Canada southeastward to west of the Great Lakes, and the subtropical jet (elevation 36—40 thousand feet) which appears over the south central United States and runs southeastward into the southeastern Gulf of Mexico, reappearing south of Cuba and continuing on into the central Atlantic.

(d) There is a double jet in the western Pacific, with the northern one the polar jet (elevation 32—36 thousand feet) and the southern one the subtropical jet (elevation 36—40 thousand feet).

(e) Over most areas, the maximum shears [Figs. 13(d) and (e)] correspond closely to the jet cores.

SECTION V

CONCLUSIONS AND RECOMMENDATIONS

The following conclusions are drawn:

(a) The relatively-low rms errors for the LMW fields, as given by the areal-mean-error method, indicate the analyses are of high quality.

(b) An advantage of the objective technique over the subjective analysis is that it provides analyses over <u>all</u> areas of the hemisphere, including no-data and sparse-data areas. Information from data areas was incorporated into the LMW analyses over the sparse- and no-data areas in a quantitative, objective, and consistent manner by using LMW screening regression equations for seven jet-stream categories in conjunction with constant-pressure-surface fields.

(c) Over the dense data areas, the objective analyses compare favorably with the subjective analyses.

(d) The objective analyses for the LMW parameters are consistent with one another.

(e) The generated jet core "observations" tend to elongate the maximum isotachs.

(f) An apparent deficiency in the model is that vertical wind profiles exhibiting a thick <u>layer</u> of high wind speeds are not specified in the analysis of the LMW parameters. Because the analysis technique requires a <u>level</u> of maximum wind, a particular level is selected somewhere in the thick layer, although the level selected is not meaningful for these cases. The analyses and verifications of $Z(L)$, S_b, and S_a are sensitive to where the level of maximum wind is specified in the layer.

Based upon these conclusions, the following is recommended:

(a) A layer of maximum wind should be defined similar to that discussed by Reiter [4], with one of the exceptions being that the analysis of wind speed should be for the peak wind speed in the layer, rather than for the mean maximum in the layer that Reiter defines as 90% of the peak wind. The reason for analyzing for 100% of the peak wind is that the LMW analysis is applied to clear-air turbulence analysis and forecasting.

(b) The mean altitude of the <u>layer</u> of maximum wind, rather than the height of the <u>level</u> of maximum wind, should be analyzed. The thickness of the layer of maximum wind should be analyzed as an additional field that will supply more detailed information about the three-dimensional structure of the wind field in the vicinity of the jet stream.

(c) To complete the more realistic three-dimensional picture, the vector shear of the wind below and above the <u>layer</u> of maximum wind should be analyzed instead of the scalar shear below and above the <u>level</u> of maximum wind.

To accomplish the work suggested by these recommendations, it will be necessary to: (1) redefine some of the jet stream categories by considering the thickness of the layer of maximum wind as an additional criterion in the category definitions, (2) process the station data according to the LMW fields listed in the recommendations, (3) derive new LMW regression equations, based upon the new category definitions, for specifying initial guesses to the LMW parameters, and (4) add the thickness of the layer of maximum wind to the LMW analysis program.

APPENDIX

EQUATIONS FOR LMW-
PARAMETER FIRST-GUESS FIELDS

APPENDIX

EQUATIONS FOR LMW-PARAMETER FIRST-GUESS FIELDS

1. Category 1—No Jet

Conditions:

$W_s(3)$ and $W_s(2) < 50$ knots

$$Z(L) = 2908.9 + 49.977[W_s(1)] - 37.794[W_s(7)] + 23.941[T(7)]$$

$$W_s(L) = 14.190 + 0.36354[W_s(2)] + 0.36641[W_s(1)] + 0.30954[W_s(5)]$$

$$S_a = 0.013107 - 0.14963(S_b) + 0.56996[W_s(1)] + 0.067427[W_s(L)]$$

$$S_b = 2.49333 - 0.064107[W_s(L)] + 0.030697[W_s(2)] + 0.012455[W_s(5)]$$
$$+ 0.00022536[Z(L)]$$

2. Category 2—Weak to Moderate Subtropical Jet

Conditions:

(a) $W_s(3)$ or $W_s(2) = 50$—99 knots with latitude $< 30°N$, or

(b) $W_s(2) - W_s(3) > 10$ knots with latitude $\leq 45°N$

$$Z(L) = 4048.8 + 12.306[W_s(1)] - 8.0158[W_s(3)] + 12.709[T(5)]$$

$$W_s(L) = 13.504 + 0.94295[W_s(2)]$$

$$S_a = 0.80542 - 0.12514[W_s(L)] + 0.04950[W_s(1)] + 0.05469[W_s(2)]$$

$$S_b = 13.439 - 0.0037641[Z(L)] + 0.13056[W_s(L)] - 0.10909[W_s(3)]$$

3. Category 3—Strong Subtropical Jet

Conditions:

(a) $W_s(3)$ or $W_s(2) \geq 100$ knots with latitude $< 30°N$, or

(b) $W_s(2) - W_s(3) > 15$ knots with latitude $\leq 45°N$

$$Z(L) = 3822.1 - 4.8446[W_s(3)] + 3.0291[W_s(1)] + 2.7354[W_s(2)]$$

$$W_s(L) = 27.774 + 0.84052[W_s(2)]$$

$$S_a = 10.846 - 0.15284[W_s(L)] + 0.087687[W_s(2)] - 0.0026408[Z(L)]$$
$$+ 0.054073[W_s(1)]$$

57

S_b $\quad = 17.851 - 0.0046131[Z(L)] - 0.098653[W_s(3)] + 0.10677[W_s(L)]$

4. Category 4—Weak to Moderate Subtropical Polar Jet

Conditions:

$W_s(3)$ or $W_s(2) = 50$—99 knots, with $|W_s(2) - W_s(3)| \leq 10$ knots and latitude = 30—45°N

$Z(L)$ $\quad = 3604.9 + 11.855[W_s(1)] + 16.843[T(7)] - 7.4020[W_s(5)] - 34.071[W_s(3)]$

$\quad\quad\quad + 32.035[W_s(2)]$

$W_s(L)$ $\quad = 13.623 + 0.97940[W_s(2)]$

S_a $\quad = 0.35951 - 0.13492[W_s(L)] + 0.089316[W_s(3)] + 0.038302[W_s(1)]$

S_b $\quad = 8.5199 + 0.15191[W_s(L)] - 0.002418[Z(L)] - 0.10463[W_s(3)] - 0.05478[W_s(5)]$

5. Category 5—Strong Subtropical Polar Jet

Conditions:

$W_s(3)$ or $W_s(2) \geq 100$ knots with $|W_s(2)-W_s(3)| \leq 15$ knots and latitude 30°—45°N

$Z(L)$ $\quad = 3727.3 + 11.336[T(7)] + 5.3228[W_s(1)] - 22.056[W_s(3)] + 18.295[W_s(2)]$

$W_s(L)$ $\quad = 21.365 + 0.48576[W_s(3)] + 0.45093[W_s(2)]$

S_a $\quad = 9.0880 - 0.0032362[Z(L)] - 0.35472(S_b) + 0.04686[W_s(1)] - 0.080768[W_s(L)]$

$\quad\quad\quad + 0.066046[W_s(2)]$

S_b $\quad = 12.340 - 0.0038816[Z(L)] + 0.14103[W_s(L)] - 0.11350[W_s(3)]$

6. Category 6—Weak to Moderate Polar Jet

Conditions:

(a) $W_s(3)$ or $W_s(2) = 50$—99 knots with latitude > 45°N, or

(b) $W_s(3) -W_s(2) > 10$ knots with latitude > 30°N

$Z(L)$ $\quad = 3361.9 - 10.355[W_s(5)] + 16.909[W_s(2)] - 10.463[W_s(3)]$

$W_s(L)$ $\quad = 17.319 + 0.64497[W_s(3)] + 0.30167[W_s(2)]$

S_a $= 2.2800 - 0.090459[W_s(L)] + 0.054284[W_s(2)] - 0.00082532[Z(L)]$

$+ 0.033011[W_s(1)]$

S_b $= 4.8737 + 0.10729[W_s(L)] - 0.065994[W_s(5)] - 0.0015093[Z(L)]$

$- 0.038469[W_s(3)]$

7. Category 7—Strong Polar Jet

Conditions:

(a) $W_s(3)$ or $W_s(2) \geq 100$ knots with latitude $> 45°N$, or

(b) $W_s(3) - W_s(2) > 15$ knots with latitude $\geq 30°N$

$Z(L)$ $= 3794.5 + 20.950[T(5)] + 5.9493[W_s(2)] - 5.6606[W_s(3)]$

$W_s(L)$ $= 31.007 + 0.64466[W_s(3)] + 0.23493[W_s(2)]$

S_a $= 8.6349 - 0.16002[W_s(L)] + 0.090277[W_s(2)] - 0.0028288[Z(L)]$

$+ 0.060576[W_s(3)]$

S_b $= 11.040 - 0.0035587[Z(L)] + 0.083069[W_s(L)] - 0.083452[W_s(5)]$

REFERENCES

1. Cressman, G. P., 1959: "An Operational Objective Analysis System," Mo. Weath. Rev., Vol. 87, No. 10, pp. 367—374.

2. Endlich, R. M. and G. S. McLean, 1957: "The Structure of the Jet Stream Core," J. Meteorol., Vol. 14, pp. 543—552.

3. Miller, R. G., 1958: "The Screening Procedure," pp. 86—95 of Statistical Weather Prediction (T. F. Malone, ed.), Final Rpt., Contract 19(604)1590. The Travelers Weather Research Center, Hartford.

4. Reiter, E. R., 1958: "The Layer of Maximum Wind," J. Meteorol., Vol. 15, pp. 27—43.

5. Spiegler, D. B. and R. J. Ball, 1964: Detailed Program Specifications for Analysis Procedure for Level of Maximum Wind Parameters, The Travelers Research Center, Inc., Hartford.

6. Thomasell, A., 1962: The Areal-mean-error Method of Analysis Verification, Tech. Rpt. 7083-12, The Travelers Research Center, Inc., Hartford.

PART II

TECHNIQUES for PREDICTION of
LEVEL of MAXIMUM WIND PARAMETERS

by

John T. Ball
David B. Spiegler
Bernard J. Erickson
Robert J. Ball

TABLE OF CONTENTS

PART II

LIST OF ILLUSTRATIONS

64

LIST OF TABLES

INTRODUCTION

Two objective techniques for predicting level of maximum wind (LMW) parameters were developed. The first, the LMW Modeling Prediction Technique, consists simply of applying the diagnostic equations that specify LMW parameters (described in PART I) to prognoses of constant-pressure-surface fields. This results in prognoses of the following parameters:

(a) wind speed at the LMW $[W_s(L)]$

(b) wind direction at the LMW $[W_d(L)]$

(c) height of the LMW $[Z(L)]$

(d) shears above and below the LMW $[S_a$ and $S_b]$

(In PART I, the equations were used with observed fields to generate initial guesses for the LMW analyses.)

An additional feature of this technique is that it locates the forecast position of the jet core, generates "observations" along the core using horizontal profiles of jet-stream models [1], and adjusts the wind-speed grid with the successive approximation analysis technique (SAT) and the generated observations.

This technique is simply a by-product of the LMW analyses (PART I), whereas the following technique is designed specifically for predictions.

The second technique, the LMW Predictor Network Technique (PNT), is more complex and provides 12- and 24-hr prognoses of LMW parameters using a moving-coordinate prediction system. For PNT, regression equations were derived, for 12- and 24-hr prediction of the parameters or their changes, for grid points categorized according-ing to the initial-state (t_0) position of the jet stream [as indicated by the analysis of $W_s(L)$ and $W_d(L)$].

The possible predictors available for selection in the screening procedure were the five LMW parameters at t_0, their previous 12-hr changes, the wind speed at 500, 300, 200, and 100 mb (at t_0), the wind-speed shears for the 300—500-, 200—300-, and 100—200-mb levels, and their previous 12-hr changes. These predictors were selected for screening by applying a grid network oriented with the jet-stream flow to the area about the predictand point.

SECTION II

DATA PROCESSING FOR THE PREDICTOR NETWORK TECHNIQUE

Hemispheric grid-point LMW analyses (see PART I of this report) were generated from data (2 observations per day) provided by the National Meteorological Center (NMC) for 20 days, of both the months of December 1963 and January 1964. Wind speed analyses for the four constant-pressure levels used in the study were available on magnetic tape from Global Weather Central (GWC). The developmental sample consisted of the first fifteen days of data of each month. The remaining five days were used as independent data for testing.

After all basic analysis grids were obtained, the predictand points were selected on the basis of objective criteria described in Section III. The predictand points were selected only within the area shown in Fig. 1, as the main purpose of the feasibility study was to test a prediction technique that would be applicable in the area about North America. The grid network was then applied to each predictand point, and oriented according to the $W_d(L)$ at the predictand point; the predictor information from each field was extracted.
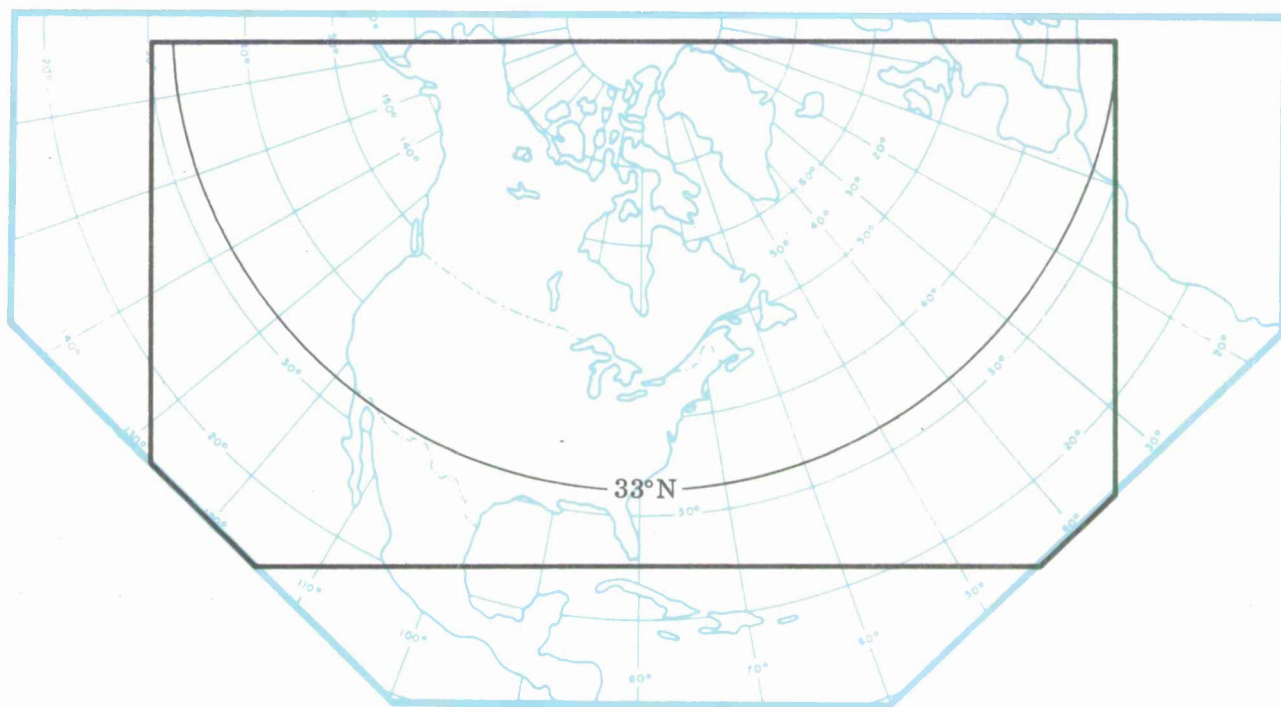
Fig. 1. Area used for North American jet-stream prediction study. Latitude 33°N is indicated as the dividing line between polar and subtropical jet stream categories.

SECTION III

THE LMW PREDICTOR NETWORK TECHNIQUE

1.   Categorization of Predictand Points

The development of this technique to predict the LMW parameters required the careful utilization of all the initial-state information that describes the parameter fields. A procedure in which prediction equations are derived for application at all grid points, such as one used in the prediction of 100-mb height change [3], did not seem a fruitful approach here because of the characteristics of the predictands. Perhaps the most important feature of any LMW prediction technique is the forecasting of the location of the jet-stream core and the corresponding wind-speed variations, or jet-maxima, located along the core. The variations in the fields of vertical wind shear above and below the LMW and the height of the LMW are closely related to the position of the jet-stream core. It followed from this that prediction equations should be developed for application to grid points which are first categorized relative to the initial-state position of the core. (The procedure for determining the core and selecting those consecutive Numerical Weather Prediction (NWP) grid points that most closely depict the core is given in PART I.)

The procedure for categorizing the NWP grid points, relative to the analyzed position of the core at time t_0, is illustrated in Fig. 2. In this figure, a solid line connects those consecutive grid points that most closely approximate the analyzed core. The arrow indicates the predominant wind direction along the core. Five categories are established. The grid point labeled "A" and circled indicates the approximate location of the jet-stream maximum. The wind speed at this grid point is greater than that at the adjacent core points upstream (the direction from which the wind is blowing) or downstream. The grid point labeled "B" is two core points upstream and the one labeled "C" is two core points down-stream. Grid point "D" is the NWP grid point closest to two grid intervals to the left of the core (using the convention of looking downstream) and grid point "E" is closest to two grid intervals to the right.

The above approach establishes five categories of grid points relative to a given jet-stream system. However, there are at least two basic types of jet-stream systems—polar and subtropical—and the characteristics and behavior of these two systems differ considerably. For example, the subtropical jet often persists in the same general location

72
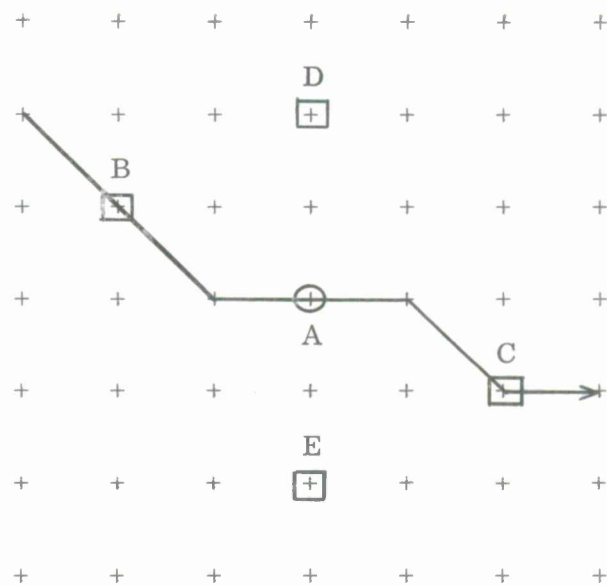
Fig. 2. Procedure for categorizing NWP grid points from the initial-state position of the jet stream core. Solid line connects the core, and the categorized grid points are marked (see text for explanation).

with predominant west to east flow that varies only moderately as jet-maxima move through the system. The winds in the polar jet, on the other hand, often have a significant north-south component of flow, develop and dissipate rapidly, and experience rapid changes in location over short periods of time. Because of the important behavioral differences in the two jet-stream types, we developed separate prediction relationships for the LMW parameters based on whether the jet-stream core was subtropical or polar (see Table I for the grid point categories).

It is obviously difficult to develop objective criteria for classifying the jet core as polar or subtropical. For this limited feasibility study, a jet core was considered polar if grid point A (wind speed maximum) of the classification model shown in Fig. 2 was located north of 33°N, and subtropical if located south of this latitude. It is recognized that a separation of the two jet types based only on latitude is rather crude. However, we felt that a more sophisticated scheme was not justified in the first attempt to examine this forecasting problem.

TABLE 1
GRID POINT CATEGORIZATION

Polar category	Subtropical category	Definition
1A	2A	Wind speed maximum
1B	2B	Second core point upstream*
1C	2C	Second core point downstream*
1D	2D	Two grid intervals to the left of core†
1E	2E	Two grid intervals to the right of core†

*Upstream is direction <u>from</u> which wind is blowing. Downstream is the direction <u>toward</u> which wind is blowing.
†Convention used is that of looking downstream.

2. Predictor Network Grid

The predictor network grid used to select predictors at NWP grid points is shown in Fig. 3. The grid interval is one NWP grid interval (381 km at 60°N). NWP grid-point analyses of all predictand and predictor fields were contained on magnetic tape. The predictand points are selected by the objective procedure described in Section 1. The predictor network grid is then applied to all predictand points. The values of the predictors are determined for all grid points of the network by a computer program. The grid is placed on each predictor field such that the predictand grid point is located at $K=5$, $L=3$, and the L axis of the grid is oriented parallel to the LMW wind direction at location (5, 3) (see Fig. 3). Other orientations of the network grid, such as the L axis always being east—west or always parallel to the basic NWP grid, were possible but we decided that the sampling of the predictor fields at locations relative to the pre-dictand point would be considerably more meaningful if the network was oriented relative to the flow of the jet-stream system.

A 7x5 (rather than a square) array was used so that rapidly moving features well upstream, such as jet-maxima or short-wave troughs, would come within the area defined by the predictor network grid.
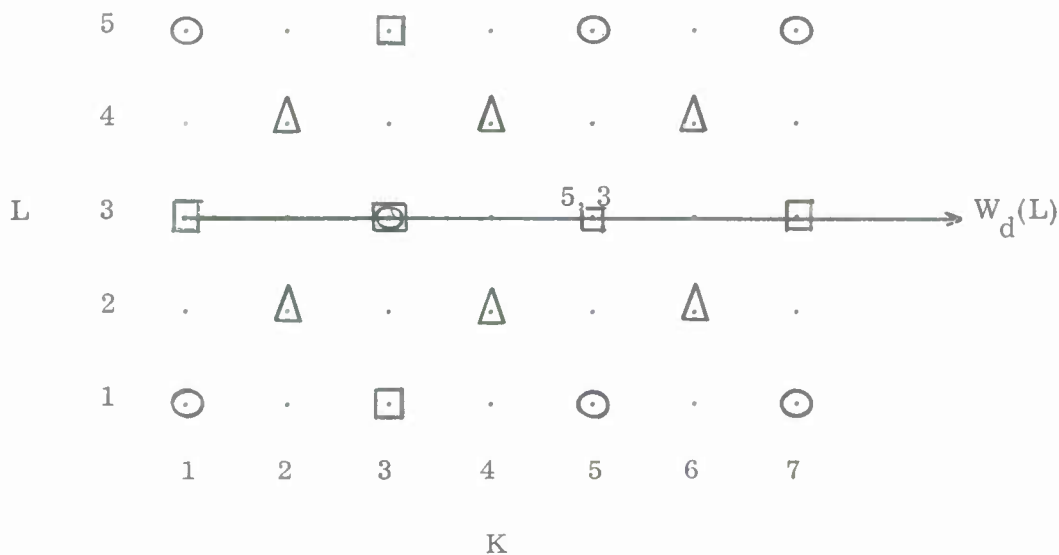
Fig. 3. Predictor network grid. Predictand point is at K=5, L=3.
[The predictor points are indicated by appropriate symbol (see Section
4. for meaning)].

3. Predictands

The predictands (the parameters being forecast) considered in this study were
the 12- and 24-hr changes, and the actual values, of the five LMW parameters [wind
direction, $W_d(L)$; wind speed, $W_s(L)$; height, $Z(L)$; and the shear above and below the
LMW, S_a and S_b]. This gives a total of twenty predictands for each of the ten categories
described in Section 1. The predictands are shown in Table II. Obviously, selectivity
was required in the feasibility study experiments. Greatest emphasis was placed on
predicting the 12- or 24-hr changes of the predictands, not on predicting their actual
value 12 or 24 hours in the future.

4. Predictors

The 7x5 network grid is applied to 20 fields of possible predictors that have been
analyzed on a NWP hemispheric grid. If every point on the grid array for each field
were utilized, there would be a total of 700 possible predictors.

Because the screening-regression technique of Miller [2], as programmed for the
IBM 7094 computer, has an upper limit of 180 possible predictors and predictands, it
was necessary to select subjectively from the original 700 predictors, a set of 160 or

TABLE II
POSSIBLE PREDICTANDS

Predictand*	Forecast interval (hr)	Predictand symbol †
$W_d(L)$	12	$\hat{W}_d(L)_{12}$
	24	$\hat{W}_d(L)_{24}$
$\Delta W_d(L)$	12	$\Delta\hat{W}_d(L)_{12}$
	24	$\Delta\hat{W}_d(L)_{24}$
$W_s(L)$	12	$\hat{W}_s(L)_{12}$
	24	$\hat{W}_s(L)_{24}$
$\Delta W_s(L)$	12	$\Delta\hat{W}_s(L)_{12}$
	24	$\Delta\hat{W}_s(L)_{24}$
$Z(L)$	12	$\hat{Z}(L)_{12}$
	24	$\hat{Z}(L)_{24}$
$\Delta Z(L)$	12	$\Delta\hat{Z}(L)_{12}$
	24	$\Delta\hat{Z}(L)_{24}$
S_b	12	$\hat{S}_{b\,12}$
	24	$\hat{S}_{b\,24}$
ΔS_b	12	$\Delta\hat{S}_{b\,12}$
	24	$\Delta\hat{S}_{b\,24}$
S_a	12	$\hat{S}_{a\,12}$
	24	$\hat{S}_{a\,24}$
ΔS_a	12	$\Delta\hat{S}_{a\,12}$
	24	$\Delta\hat{S}_{a\,24}$

*Delta (Δ) indicates "change in."

†The hat ($\hat{\ }$) is used to identify a <u>predictand</u>.
A parameter symbol without the hat would indicate
a <u>predictor</u>.

less for screening. This restriction is not very severe when one considers the high correlation that exists between values of predictors from the same field at adjacent grid points.

The number and location in the network grid of screened predictors from each field can be seen by examining Fig. 3. and Table III. The three types of distributions of predictors available for the screening-regression technique are:

(a) Selection Type A—all grid points in Fig. 3 enclosed by a circle, square or triangle.

(b) Selection Type B—all grid points in Fig. 3 enclosed by a circle or square.

(c) Selection Type C—all grid points in Fig. 3 enclosed by a square.

Table III lists each predictor field, distribution selection type, and the number of predictors screened.

TABLE III
PREDICTORS AVAILABLE FOR SCREENING

Predictor	Description	Number available	Selection type
$W_d(L)$	LMW wind direction	6	C
$W_s(L)$	LMW wind speed	18	A
$Z(L)$	LMW height	6	C
S_b	Shear below LMW	12	B
S_a	Shear above LMW	12	B
$W_s(5)^*$	500-mb wind speed	6	C
$W_s(3)$	300-mb wind speed	6	C
$W_s(2)$	200-mb wind speed	6	C
$W_s(1)$	100-mb wind speed	6	C
$\Delta W_d(L)_{-12}$	12-hr LMW wind direction change	1	Predictand point only
$\Delta W_s(L)_{-12}$	12-hr LMW wind speed change	12	B
$\Delta Z(L)_{-12}$	12-hr LMW height change	6	C
ΔS_{b-12}	12-hr shear below LMW change	12	B
ΔS_{a-12}	12-hr shear above LMW change	12	B
$S(3-5)$	300—500-mb wind speed difference	6	C
$S(2-3)$	200—300-mb wind speed difference	6	C
$S(1-2)$	100—200-mb wind speed difference	6	C
$\Delta S(3-5)_{-12}$	12-hr change of $S(3-5)$	6	C
$\Delta S(2-3)_{-12}$	12-hr change of $S(2-3)$	6	C
$\Delta S(1-2)_{-12}$	12-hr change of $S(1-2)$	6	C

*Parenthetic numbers indicate level (in hundreds of mb).

SECTION IV

RESULTS USING THE PREDICTOR NETWORK TECHNIQUE

A series of initial experiments were conducted to reduce the number of pre-
dictands and predictors used in the derivation of prediction equations for the ten grid
point categories. This experimentation was undertaken in an attempt to conserve com-
puter time, and because it is obvious that both the predictands and the predictor fields
contain redundant information. Basically, two sets of experiments were performed.
In the first set (reduction of predictands), the same set of predictors used to obtain
regression equations for the future 12- and 24-hr values of the LMW parameters were
also used to obtain equations for the 12- and 24-hr changes of these parameters. In
the second set of experiments (reduction of predictors) various sets of predictors
were used to develop regression equations to forecast the same predictand. Both sets
of experiments were undertaken using mainly grid-point categories 1D, 1E, and 2C,
which contain 336, 343 and 104 dependent cases, respectively. These categories were
tested most extensively because their associated data samples were first available.
Since the results obtained from these categories and limited testing with other cate-
gories was similar, extensive preliminary testing with all categories was not considered
necessary. The detailed results of all the initial experiments are not given here.
Rather, a summary of the results that led to the final selection of predictands and
predictors is given.

Table IV gives, for the first set of experiments, the total percent reduction of
variance (% red.) of the LMW predictands for grid-point Category 1E. The LMW wind
direction is not included in the experiment. It was found that the skill in predicting
wind direction was very low and, as good prognoses of wind direction are presently
available from NWP, we decided to discontinue experiments containing wind direction
as a predictand.

The identical predictors were screened for each predictand pair (shown in
Table IV) (12-hr LMW wind speed and 12-hr change of LMW wind speed are a pre-
dictand pair). The predictive skill, as evident in the % red., is much greater in fore-
casting 12- and 24-hr changes of LMW height, shear below, and shear above than
in forecasting their actual future values. However, in the case of the LMW wind speed,

79

TABLE IV

REDUCTION OF PREDICTANDS

[Comparison of percent reductions of LMW predictands
using same predictor set (Category 1E)]

Predictand	% red.	
	12-hr prediction	24-hr prediction
$\hat{W}_s(L)$	57	52
$\Delta\hat{W}_s(L)$	33	36
$\hat{Z}(L)$	34	27
$\Delta\hat{Z}(L)$	43	51
$\hat{S}_b$	19	10
$\Delta\hat{S}_b$	48	38
$\hat{S}_a$	29	24
$\Delta\hat{S}_a$	45	46

a larger % red. is obtained using the actual value, rather than the change, for both 12-
and 24-hr prediction intervals. The summary results shown in Table IV are similar
to those obtained for Categories 1D and 2C, except that all values of % red. were higher
for Category 2C due to the greater persistence of the subtropical jet stream.

It is certainly not surprising that the predictors are better related (higher linear
correlations) to the change of height or wind shears rather than to the actual values.
For example, a LMW height value of 35000 ft could correspond to a wide variety of
meteorological conditions, while an LMW height change of -3500 ft would frequently
be associated with an approaching trough or wind speed maximum. In the case of wind
speed, however, the actual value clearly defines the jet stream and associated core
maximum and is, therefore, well correlated to potential predictors. On the basis of
the initial testing of the three categories, we decided to use the actual value of LMW
wind speed and the changes of the LMW height and wind shear fields as predictands to

80

develop 12- and 24-hr prediction equations for the ten grid-point categories.

An example of the results from the second set of experiments is shown in Table V which gives, for Category 2C, the total percent reduction of variance of the 12- and 24-hr LMW wind speed, and changes, when (1) all predictors are screened and (2) the fields containing wind-speed differences between constant pressure surfaces, and the 12-hr changes of these differences, are excluded. Note that the change in % red. is very small when the predictor fields $S(3-5)$, $S(2-3)$, and $S(1-2)$, and their 12-hr changes, are eliminated from consideration in obtaining the regression equations. On the basis of the experiments summarized in Table V, and many similar experiments, we decided to exclude the prediction fields containing the actual values and the previous 12-hr changes of the wind-speed differences in the development of the regression equations for the ten grid-point categories.

Various other initial prediction experiments were attempted, with different combinations of predictor fields being included for screening. The general conclusion was that the actual values and 12-hr changes of the LMW predictors, and wind speed at constant pressure surfaces, all contain significant predictive information, the relative importance of which depends on the category, forecast interval and LMW predictand. These predictors were used to develop the prediction equations for all categories.

TABLE V
REDUCTION OF PREDICTORS

[Comparison of percent reduction of $\hat{W}_S(L)$ for different predictor sets (Category 2C)]

Predictand	% red. using	
	All predictors	All except $S(3-5)$, $S(2-3)$ $S(1-2)$, and their changes
$\hat{W}_S(L)_{12}$	76	73
$\Delta\hat{W}_S(L)_{12}$	52	47
$\hat{W}_S(L)_{24}$	59	59
$\Delta\hat{W}_S(L)_{24}$	46	45

5.   Polar Jet Stream—Dependent Data Results

The dependent sample size for each of the five polar jet-stream categories was approximately 350 cases. The dependent sample was obtained from 54 observation times within the two intervals 12Z   Dec. 1—12Z   Dec. 14, 1963 and 00Z   Jan. 2— 00Z   Jan. 15, 1964. Table VI lists the predictors selected for each of the eight predictands for each grid-point category, and the total percent reduction of variance (% red.) of the predictand for the predictors selected. In examining the lists of variables selected, the most obvious repetitive feature is that the first predictor selected for both 12- and 24-hr prognoses of the four LMW parameters was, in most instances, the initial-state value at the predictand point $(5, 3)$ of the LMW parameter being predicted. For example, in all five categories, for 12- and 24-hr predictions of height change, the first predictor selected was $Z(L)$ $(5, 3)$.

A second feature to be noted is that very few 12-hr change predictors were selected. This indicates that the 12-hr changes prior to t_0 (initial state) are not highly correlated (linearly) to the 12- and 24-hr LMW predictands. This again reflects the fact that the polar jet streams are rapidly-changing (non-linearly) systems. It will be seen that the 12-hr change predictors contain more useful information when forecasting the subtropical jet-stream LMW predictands.

Two additional general comments can be made. First, aside from the predictand point $(5, 3)$, the selected predictors are most frequently located at a point upstream from the predictand point. (The parenthetic numbers separated by a comma, given with each selected predictor, indicate the location on the predictor grid. When the first of the two numbers is between 1 and 4, an upstream location is indicated; the numbers 6 and 7 indicate a downstream location). This is true for all categories, and is certainly reasonable because it would be expected that most of the useful predictor information would be found upstream (particularly in the case of rapidly changing jet-stream systems). Also note that the type of predictor most frequently selected is the wind speed either at the LMW or a constant pressure surface. This result is also quite reaonsable because, of the predictor fields considered in the feasibility study, the wind speed most clearly defines the jet-stream systems, and therefore contains the most useful prediction information.

TABLE VI
SELECTED PREDICTORS FOR POLAR JET-STREAM CATEGORIES
(Results on dependent data)

(a) Category 1A (350 cases)

Predictand	Predictors in order of selection	% red.	Std. dev.	rms error	Units
$\hat{W}_s(L)_{12}$	$W_s(2)(3,3), W_s(L)(4,2), \Delta S_b(7,1)$	40.7	33.2	25.5	knots
$\Delta\hat{Z}(L)_{12}$	$Z(L)(5,3), \Delta Z(L)(5,3)$	27.0	5430	4641	ft
$\Delta\hat{S}_{b\,12}$	$S_b(5,3), W_s(L)(4,2)$	52.9	2.7	1.8	knots 10^{-3} ft^{-1}
$\Delta\hat{S}_{a\,12}$	$S_a(5,3), W_s(L)(2,2)$	53.2	2.8	1.9	knots 10^{-3} ft^{-1}
$\hat{W}_s(L)_{24}$	$W_s(L)(3,3), W_s(2)(3,1), S_b(3,3)$	34.9	32.4	26.1	knots
$\Delta\hat{Z}(L)_{24}$	$Z(L)(5,3), Z(L)(1,3), W_s(1)(5,3)$	30.8	7043	5860	ft
$\Delta\hat{S}_{b\,24}$	$S_b(5,3), W_s(2)(3,1)$	64.1	2.6	1.6	knots 10^{-3} ft^{-1}
$\Delta\hat{S}_{a\,24}$	$S_a(5,3), W_s(2)(3,1)$	56.9	2.9	1.9	knots 10^{-3} ft^{-1}

(b) Category 1B (355 cases)

Predictand	Predictors in order of selection	% red.	Std. dev.	rms error	Units
$\hat{W}_s(L)_{12}$	$W_s(L)(3,3), W_s(5)(5,3), W_s(L)(6,2),$ $W_s(1)(5,3)$	48.7	33.3	23.8	knots
$\Delta\hat{Z}(L)_{12}$	$Z(L)(5,3), Z(L)(3,3), W_s(2)(3,1),$ $W_s(5)(5,3), W_s(L)(5,5)$	37.5	5858	4631	ft
$\Delta\hat{S}_{b\,12}$	$S_b(5,3), W_s(L)(6,2)$	59.2	2.6	1.6	knots 10^{-3} ft^{-1}
$\Delta\hat{S}_{a\,12}$	$S_a(5,3), W_s(3)(3,3), W_s(5)(5,3)$	53.1	2.6	1.8	knots 10^{-3} ft^{-1}
$\hat{W}_s(L)_{24}$	$W_s(L)(3,3), W_s(L)(6,2), W_s(2)(3,5)$	35.0	34.7	28.0	knots
$\Delta\hat{Z}(L)_{24}$	$Z(L)(5,3), Z(L)(3,1), \Delta Z(L)(7,3)$	38.3	6623	5201	ft
$\Delta\hat{S}_{b\,24}$	$S_b(5,3), W_s(L)(6,2), W_s(1)(3,1)$	61.8	2.6	1.6	knots 10^{-3} ft^{-1}
$\Delta\hat{S}_{a\,24}$	$S_a(5,3), W_s(2)(3,3), S_b(7,1),$ $W_s(1)(3,3), Z(L)(3,1)$	58.6	2.8	1.8	knots 10^{-3} ft^{-1}

TABLE VI (Continued)

(c) Category 1C (366 cases)

Predictand	Predictors in order of selection	% red.	Std. dev.	rms error	Units
$\hat{W}_s(L)_{12}$	$W_s(L)(5,3), W_s(L)(3,3), S_a(5,3),$ $W_s(L)(4,2)$	43.2	29.6	22.3	knots
$\Delta\hat{Z}(L)_{12}$	$Z(L)(5,3), Z(L)(3,3), Z(L)(7,3),$ $W_s(L)(5,1)$	35.7	5373	4309	ft
$\Delta\hat{S}_{b\,12}$	$S_b(5,3), W_s(L)(4,2)$	41.6	2.3	1.8	knots 10^{-3} ft^{-1}
$\Delta\hat{S}_{a\,12}$	$S_a(5,3), W_s(3)(3,3)$	48.4	2.5	1.8	knots 10^{-3} ft^{-1}
$\hat{W}_s(L)_{24}$	$W_s(1)(5,3), W_s(3)(1,3), W_s(L)(6,4),$ $W_s(3)(3,3), W_s(5)(3,5), W_s(2)(3,1)$	37.9	32.4	25.5	knots
$\Delta\hat{Z}(L)_{24}$	$Z(L)(5,3),\ Z(L)(7,3),\ Z(L)(3,3)$	33.6	6726	5482	ft
$\Delta\hat{S}_{b\,24}$	$S_b(5,3), W_s(L)(6,4), W_s(3)(1,3)$	55.1	2.4	1.6	knots 10^{-3} ft^{-1}
$\Delta\hat{S}_{a\,24}$	$S_a(5,3), W_s(L)(2,4), \Delta W_s(L)(3,5)$	52.9	2.6	1.8	knots 10^{-3} ft^{-1}

(d) Category 1D (336 cases)

Predictand	Predictors in order of selection	% red.	Std. dev.	rms error	Units
$\hat{W}_s(L)_{12}$	$W_s(2)(5,3), W_s(L)(4,2), \Delta W_s(L)(3,3),$ $W_s(L)(6,4)$	47.2	30.6	22.2	knots
$\Delta\hat{Z}(L)_{12}$	$Z(L)(5,3), Z(L)(3,3), W_s(3)(7,3)$	46.2	7563	5548	ft
$\Delta\hat{S}_{b\,12}$	$S_b(5,3), W_s(L)(4,2), \Delta W_s(L)(3,3),$ $W_s(2)(5,3)$	41.3	2.0	1.6	knots 10^{-3} ft^{-1}
$\Delta\hat{S}_{a\,12}$	$S_a(5,3), W_s(L)(4,2), \Delta W_s(L)(3,3),$ $W_s(3)(5,3)$	30.2	2.2	1.8	knots 10^{-3} ft^{-1}
$\hat{W}_s(L)_{24}$	$W_s(2)(3,3), W_s(L)(5,1), \Delta W_s(L)(3,3),$ $W_s(2)(5,3)$	32.9	31.7	26.0	knots
$\Delta\hat{Z}(L)_{24}$	$Z(L)(5,3), W_s(1)(3,3), \Delta Z(L)(5,3)$	53.5	8228	5611	ft
$\Delta\hat{S}_{b\,24}$	$S_b(5,3), \Delta W_s(L)(7,5), W_s(L)(4,2)$	41.5	2.2	1.7	knots 10^{-3} ft^{-1}
$\Delta\hat{S}_{a\,24}$	$S_a(5,3), W_s(2)(3,3)$	23.7	2.2	2.0	knots 10^{-3} ft^{-1}

TABLE VI (Continued)

(e) Category 1E (343 cases)

Predictand	Predictors in order of selection	% red.	Std. dev.	rms error	Units
$\hat{W}_s(L)_{12}$	$W_s(L)(5,3)$, $W_s(L)(4,2)$, $W_s(L)(7,5)$, $W_s(3)(3,3)$	50.2	28.4	20.1	knots
$\Delta\hat{Z}(L)_{12}$	$Z(L)(5,3)$, $Z(L)(3,3)$, $\Delta Z(L)(5,3)$	38.5	6901	5414	ft
$\Delta\hat{S}_{b\,12}$	$S_b(5,3)$, $W_s(L)(3,3)$	40.9	1.9	1.5	knots 10^{-3} ft^{-1}
$\Delta\hat{S}_{a\,12}$	$S_a(5,3)$, $S_a(7,5)$, $W_s(3)(3,3)$	38.1	1.9	1.5	knots 10^{-3} ft^{-1}
$\hat{W}_s(L)_{24}$	$W_s(L)(5,3)$, $W_s(L)(2,4)$, $W_s(L)(6,2)$, $S_a(7,5)$	46.6	30.6	22.4	knots
$\Delta\hat{Z}(L)_{24}$	$Z(L)(5,3)$, $Z(L)(3,3)$, $W_s(1)(7,3)$	49.4	7502	5339	ft
$\Delta\hat{S}_{b\,24}$	$S_b(5,3)$, $S_a(7,5)$	36.3	2.0	1.6	knots 10^{-3} ft^{-1}
$\Delta\hat{S}_{a\,24}$	$S_a(5,3)$, $S_a(7,5)$, $W_s(L)(1,1)$	42.7	2.0	1.5	knots 10^{-3} ft^{-1}

An interesting variation is found for the most frequent location on the predictor grid of the selected variables when category 1D (two grid intervals to the left of the jet core) is compared with Category 1E (two grid intervals to the right of the jet core). The second of the two numbers in parentheses given with each selected variable indicates whether the network grid point is on the upper portion of the grid (numbers 4 and 5) or the lower portion (numbers 1 and 2). For Category 1D, more predictors are selected from the lower portion of the grid, while for Category 1E, more predictors are selected from the upper portion. Thus, for both categories, the selected variables are located on that part of the predictor network grid that lies closest to the jet-stream core. Changes which take place in this region are normally most rapid and will have the greatest overall influence on the future patterns of the LMW predictands. The above-described selection preference, therefore, seems quite logical from the meteorological viewpoint.

6.   Subtropical Jet Stream—Dependent Data Results

The dependent sample size was considerably smaller for the subtropical jet-stream categories than for the polar categories. Table VII lists the predictors selected for each of the eight predictands for each grid-point category, and the total percent reduction of variance (% red.) of the predictand for the predictors selected. Examination of the selected predictors leads to several general comments concerning the selection. First, as was the case with the polar jet stream, the first predictor usually selected for both 12- and 24-hr prognoses was the initial-state value at the predictand point (5, 3) of the LMW parameter being predicted. A second comment, however, points to a significant difference between the predictors selected for the two jet-stream types. A much greater number of 12-hr change predictors were selected for the subtropical categories. In many instances the change parameter is the second predictor selected, indicating the importance of the predictor contribution to the percent reduction of the predictand. The fact that 12-hr change information is more useful, in predicting LMW parameters associated with the subtropical jet stream, is not surprising when one considers that the movement of these systems is much more regular than the polar jet-stream motion and, therefore, previous 12-hr changes in predictor fields should have a higher linear correlation with future 12- and 24-hr changes of the predictand.

As would be expected, aside from the predictand point (5, 3), the selected predictors are most frequently located at a point upstream from the predictand point for all categories except 2A. Because grid points in this category fall close to the center of the initial-state location of the wind speed maximum, it might be suggested that with a symmetrical shaped subtropical maximum, predictor information downstream would be similar to that upstream, and, hence, as likely to be selected. This situation would be much less likely to occur in the case of the polar jet stream where more rapid changes in jet-stream intensity, shape, and location occur.

7.   Independent-data Testing

The equations (see the Appendix) obtained with the selected variables described in Sections 5 and 6, were tested on independent data. The independent data were obtained from 14 observation times within the intervals 12Z December 16—12Z December 19, 1963 and 00Z January 17—00Z January 20, 1964. The root-mean-square (rms) errors

86

TABLE VII
SELECTED PREDICTORS FOR SUBTROPICAL JET-STREAM CATEGORIES
(Results on dependent data)

(a) Category 2A (104 cases)

Predictand	Predictors in order of selection	% red.	Std. dev.	rms error	Units
$\hat{W}_s(L)_{12}$	$W_s(L)(5,3), W_s(3)(5,3)$	47.0	32.4	23.6	knots
$\Delta\hat{Z}(L)_{12}$	$Z(L)(5,3), W_s(5)(3,3), W_s(1)(1,3),$ $W_s(L)(7,3), \Delta Z(L)(1,3), \Delta W_s(L)(7,1)$	68.9	4711	2629	ft
$\Delta\hat{S}_{b\,12}$	$S_b(5,3)$	50.4	3.1	2.2	knots 10^{-3} ft^{-1}
$\Delta\hat{S}_{a\,12}$	$S_a(5,3), W_s(3)(5,3), \Delta S_b(5,3)$	54.2	3.4	2.3	knots 10^{-3} ft^{-1}
$\hat{W}_s(L)_{24}$	$W_s(L)(6,2)$	26.3	33.4	28.7	knots
$\Delta\hat{Z}(L)_{24}$	$Z(L)(5,3), W_s(3)(3,3), S_a(7,3)$	51.1	5720	4000	ft
$\Delta\hat{S}_{b\,24}$	$S_b(5,3), \Delta W_s(L)(5,3)$	51.7	3.4	2.4	knots 10^{-3} ft^{-1}
$\Delta\hat{S}_{a\,24}$	$S_a(5,3)$	41.7	3.7	2.8	knots 10^{-3} ft^{-1}

(b) Category 2B (90 cases)

Predictand	Predictors in order of selection	% red.	Std. dev.	rms error	Units
$\hat{W}_s(L)_{12}$	$W_s(L)(5,3), W_s(L)(4,2)$	60.7	30.9	19.4	knots
$\Delta\hat{Z}(L)_{12}$	$Z(L)(5,3), W_s(L)(2,2)$	38.8	4458	3487	ft
$\Delta\hat{S}_{b\,12}$	$\Delta S_b(5,3), \Delta W_s(L)(1,3), \Delta W_s(L)(7,5),$ $S_b(5,3), W_s(L)(4,2)$	58.5	2.3	1.5	knots 10^{-3} ft^{-1}
$\Delta\hat{S}_{a\,12}$	$S_a(5,3), W_s(2)(5,3)$	33.6	1.7	1.4	knots 10^{-3} ft^{-1}
$\hat{W}_s(L)_{24}$	$W_s(L)(4,2), W_s(L)(5,3), \Delta S_b(3,1), S_a(3,3)$	60.0	28.8	18.2	knots
$\Delta\hat{Z}(L)_{24}$	$Z(L)(5,3), \Delta S_b(7,5), \Delta S_b(3,1),$ $S_a(7,3), S_a(5,3)$	49.2	4550	3243	ft
$\Delta\hat{S}_{b\,24}$	$S_b(5,3), S_a(3,1)$	52.5	2.3	1.6	knots 10^{-3} ft^{-1}
$\Delta\hat{S}_{a\,24}$	$S_a(5,3), W_s(L)(4,2)$	28.8	1.8	1.5	knots 10^{-3} ft^{-1}

TABLE VII (Continued)

(c) Category 2C (104 cases)

Predictand	Predictors in order of selection	% red.	Std. dev.	rms error	Units
$\hat{W}_s(L)_{12}$	$W_s(L)(5,3)$, $W_s(L)(5,1)$	58.7	31.3	20.1	knots
$\Delta\hat{Z}(L)_{12}$	$\Delta Z(L)(5,3)$, $W_s(5)(3,3)$, $Z(L)(5,3)$ $\Delta W_s(L)(3,5)$	45.7	5121	3773	ft
$\Delta\hat{S}_{b\,12}$	$S_b(5,3)$, $\Delta S_a(7,3)$	40.6	2.7	2.1	knots 10^{-3} ft^{-1}
$\Delta\hat{S}_{a\,12}$	$S_a(5,3)$, $S_a(5,1)$	43.8	2.5	1.9	knots 10^{-3} ft^{-1}
$\hat{W}_s(L)_{24}$	$W_s(2)(5,3)$, $W_s(L)(5,1)$, $W_s(L)(3,5)$, $S_b(5,1)$	46.3	32.7	24.0	knots
$\Delta\hat{Z}(L)_{24}$	$Z(L)(5,3)$	26.6	5024	4308	ft
$\Delta\hat{S}_{b\,24}$	$S_b(5,3)$, $W_s(2)(5,3)$, $\Delta S_a(1,3)$, $\Delta Z(L)(3,3)$, $\Delta S_a(1,1)$, $W_s(3)(3,1)$	55.9	2.8	1.8	knots 10^{-3} ft^{-1}
$\Delta\hat{S}_{a\,24}$	$S_a(5,3)$	42.2	2.6	2.0	knots 10^{-3} ft^{-1}

(d) Category 2D (138 cases)

Predictand	Predictors in order of selection	% red.	Std. dev.	rms error	Units
$\hat{W}_s(L)_{12}$	$W_s(L)(5,3)$, $W_s(2)(3,3)$, $W_s(5)(5,3)$	59.3	30.3	19.3	knots
$\Delta\hat{Z}(L)_{12}$	$Z(L)(5,3)$, $Z(L)(3,3)$	20.8	4788	4261	ft
$\Delta\hat{S}_{b\,12}$	$S_b(5,3)$, $S_b(3,3)$	31.7	1.9	1.6	knots 10^{-3} ft^{-1}
$\Delta\hat{S}_{a\,12}$	$S_a(5,3)$, $W_s(L)(3,3)$	46.1	2.0	1.4	knots 10^{-3} ft^{-1}
$\hat{W}_s(L)_{24}$	$W_s(L)(4,2)$, $W_s(2)(3,3)$	38.4	34.2	26.8	knots
$\Delta\hat{Z}(L)_{24}$	$Z(L)(5,3)$, $W_s(5)(1,3)$	33.0	5770	4757	ft
$\Delta\hat{S}_{b\,24}$	$S_b(5,3)$, $W_s(L)(4,2)$	37.3	2.3	1.9	knots 10^{-3} ft^{-1}
$\Delta\hat{S}_{a\,24}$	$S_a(5,3)$, $W_s(L)(4,2)$	46.9	2.4	1.7	knots 10^{-3} ft^{-1}

TABLE VII (Continued)

(e) Category 2E (98 cases)

Predictand	Predictors in order of selection	% red.	Std. dev.	rms error	Units
$\hat{W}_s(L)_{12}$	$W_s(3)(5,3), W_s(1)(7,3), W_s(5)(3,3)$	50.6	26.3	18.5	knots
$\Delta\hat{Z}(L)_{12}$	$Z(L)(5,3), W_s(3)(5,3), Z(L)(3,3),$ $W_s(5)(5,3), W_s(L)(3,3)$	57.6	5046	3284	ft
$\Delta\hat{S}_{b\,12}$	$S_b(5,3)$	29.2	2.4	2.0	knots 10^{-3} ft^{-1}
$\Delta\hat{S}_{a\,12}$	$S_a(5,3), W_s(5)(7,3)$	57.8	3.1	2.0	knots 10^{-3} ft^{-1}
$\hat{W}_s(L)_{24}$	$W_s(3)(5,3), W_s(L)(6,4), \Delta Z(L)(3,3)$	53.1	26.1	17.9	knots
$\Delta\hat{Z}(L)_{24}$	$Z(L)(5,3)$	46.8	5524	4027	ft
$\Delta\hat{S}_{b\,24}$	$S_b(5,3), \Delta S_a(3,3), \Delta W_s(L)(3,3)$	52.7	2.2	1.5	knots 10^{-3} ft^{-1}
$\Delta\hat{S}_{a\,24}$	$S_a(5,3), \Delta S_a(5,3)$	51.5	2.0	1.4	knots 10^{-3} ft^{-1}

of the equations for 12- and 24-hour prognoses are compared with persistence (forecast of no change) for all categories of the polar jet stream in Table VIII. The independent sample size for the five grid-point categories varies between 82 and 85 cases. The grid points in the independent data at which the prognoses are made are selected for each category with the same objective procedure that was used for the dependent data sample.

The prognoses obtained from the derived equations are superior to persistence (lower rms error) for all categories, both time intervals, and each predictand. In most instances, the rms error is significantly lower than persistence. The most outstanding example is found in the Category 1A, 24-hr prognoses of wind speed, shear above, and shear below; here, the rms errors of the equations are all less than half that of persistence. The persistence rms errors are highest for this category and forecast interval. This is to be expected, as the position and intensity of the wind speed maximum can change drastically in a 24-hr period.

If the independent-data equation rms errors shown in Table VIII are compared to the dependent-data rms errors it is seen that the two sets of error statistics are very

TABLE VIII
Rms ERRORS ON INDEPENDENT DATA FOR
POLAR JET-STREAM CATEGORIES

(a) Category 1A (84 cases)

Predictand	Prediction rms error	Persistence rms error	Units
$\hat{W}_s(L)_{12}$	26.2	48.4	knots
$\Delta\hat{Z}(L)_{12}$	4785	5624	ft
$\Delta\hat{S}_{b\,12}$	1.7	3.1	knots 10^{-3} ft^{-1}
$\Delta\hat{S}_{a\,12}$	1.9	3.6	knots 10^{-3} ft^{-1}
$\hat{W}_s(L)_{24}$	30.4	61.9	knots
$\Delta\hat{Z}(L)_{24}$	5101	7041	ft
$\Delta\hat{S}_{b\,24}$	1.4	3.6	knots 10^{-3} ft^{-1}
$\Delta\hat{S}_{a\,24}$	2.0	4.1	knots 10^{-3} ft^{-1}

(b) Category 1B (84 cases)

Predictand	Prediction rms error	Persistence rms error	Units
$\hat{W}_s(L)_{12}$	24.5	34.2	knots
$\Delta\hat{Z}(L)_{12}$	3731	4974	ft
$\Delta\hat{S}_{b\,12}$	1.6	2.5	knots 10^{-3} ft^{-1}
$\Delta\hat{S}_{a\,12}$	1.7	2.8	knots 10^{-3} ft^{-1}
$\hat{W}_s(L)_{24}$	26.9	42.9	knots
$\Delta\hat{Z}(L)_{24}$	4928	6064	ft
$\Delta\hat{S}_{b\,24}$	1.6	2.7	knots 10^{-3} ft^{-1}
$\Delta\hat{S}_{a\,24}$	1.9	3.3	knots 10^{-3} ft^{-1}

TABLE VIII (Continued)

(c) Category 1C (85 cases)

Predictand	Prediction rms error	Persistence rms error	Units
$\hat{W}_s(L)_{12}$	23.9	28.0	knots
$\Delta \hat{Z}(L)_{12}$	4770	5520	ft
$\Delta \hat{S}_{b\,12}$	1.7	2.2	knots $10^{-3} ft^{-1}$
$\Delta \hat{S}_{a\,12}$	2.1	2.7	knots $10^{-3} ft$
$\hat{W}_s(L)_{24}$	32.3	38.7	knots
$\Delta \hat{Z}(L)_{24}$	4218	5380	ft
$\Delta \hat{S}_{b\,24}$	2.2	2.6	knots $10^{-3} ft^{-1}$
$\Delta \hat{S}_{a\,24}$	2.2	3.2	knots $10^{-3} ft^{-1}$

(d) Category 1D (83 cases)

Predictand	Prediction rms error	Persistence rms error	Units
$\hat{W}_s(L)_{12}$	24.0	30.1	knots
$\Delta \hat{Z}(L)_{12}$	5727	7837	ft
$\Delta \hat{S}_{b\,12}$	1.5	2.2	knots $10^{-3} ft^{-1}$
$\Delta \hat{S}_{a\,12}$	1.4	1.8	knots $10^{-3} ft^{-1}$
$\hat{W}_s(L)_{24}$	33.6	40.0	knots
$\Delta \hat{Z}(L)_{24}$	5714	8022	ft
$\Delta \hat{S}_{b\,24}$	2.2	2.7	knots $10^{-3} ft^{-1}$
$\Delta \hat{S}_{a\,24}$	2.2	2.4	knots $10^{-3} ft^{-1}$

TABLE VIII (Continued)

(e) Category 1E (82 cases)

Predictand	Prediction rms error	Persistence rms error	Units
$\hat{W}_s(L)_{12}$	17.6	19.0	knots
$\Delta\hat{Z}(L)_{12}$	5353	5604	ft
$\Delta\hat{S}_{b\,12}$	1.3	1.7	knots 10^{-3} ft^{-1}
$\Delta\hat{S}_{a\,12}$	1.5	1.7	knots 10^{-3} ft^{-1}
$\hat{W}_s(L)_{24}$	23.4	25.3	knots
$\Delta\hat{Z}(L)_{24}$	5059	5323	ft
$\Delta\hat{S}_{b\,24}$	1.6	2.0	knots 10^{-3} ft^{-1}
$\Delta\hat{S}_{a\,24}$	1.5	1.9	knots 10^{-3} ft^{-1}

similar, indicating the stability of the relationships on the independent-data sample tested.

The rms errors on independent data, obtained with the 12- and 24-hr subtropical jet-stream prediction equations for all categories, are given in Table IX. The sample size varies between 17 and 28 cases and, because of the limited size, the results must be interpreted cautiously. However, the results appear consistent with a priori meteorological reasoning and will be presented in this light.

The persistence rms errors for 24-hr prediction of wind speed, shear above, and shear below are again highest in the wind speed maxima category (2A). The 24-hr persistence rms errors for wind speed and height are, for most categories, lower for the subtropical jet stream than those obtained for the polar jet stream. This result is consistent with the more regular behavior and persistence of the subtropical jet stream. However, no consistent difference can be noted between the rms errors for the two types of jet streams, when considering shear above and below persistence forecasts.

The rms errors obtained from the prediction equations are lower than persistence with only one exception. The rms error for the 12-hr forecast of shear above for Category 2B is the same as persistence. A comparison of the independent-data rms errors given in Table IX with the dependent-data rms errors in Table VII shows that, in general, the rms errors obtained with independent data are similar, although much higher or lower errors do occur in some categories. These fluctuations are very likely a result of the small sample size of the independent data.

A final series of experiments was conducted with the independent data to consider the usefulness of the categorization that was employed in this feasibility study. Specifically, the three features investigated were: (1) separation into polar and subtropical jet-stream classes, (2) the use of exclusive categories to the right and the left of the jet core and (3) the breakdown of categories along the core.

Table X gives the rms errors that occur when the equation developed for one category is tested on the independent data cases of a different category. A comparison with the rms error statistics shown in Tables VIII and IX is required in the interpretation of the results.

Parts (a) and (b) of Table X provide information concerning items (1) and (2) above. The equations developed for Category 1D (two grid intervals to the left of the polar jet-

93

TABLE IX
Rms ERRORS ON INDEPENDENT DATA FOR
SUBTROPICAL JET-STREAM CATEGORIES

(a) Category 2A (20 cases)

Predictand	Prediction rms error	Persistence rms error	Units
$\hat{W}_s(L)_{12}$	24.9	41.0	knots
$\Delta\hat{Z}(L)_{12}$	3187	4897	ft
$\Delta\hat{S}_{b\,12}$	1.7	3.2	knots $10^{-3} ft^{-1}$
$\Delta\hat{S}_{a\,12}$	1.9	3.3	knots $10^{-3} ft^{-1}$
$\hat{W}_s(L)_{24}$	27.9	40.3	knots
$\Delta\hat{Z}(L)_{24}$	3353	4856	ft
$\Delta\hat{S}_{b\,24}$	2.3	3.4	knots $10^{-3} ft^{-1}$
$\Delta\hat{S}_{a\,24}$	2.6	4.1	knots $10^{-3} ft^{-1}$

(b) Category 2B (20 cases)

Predictand	Prediction rms error	Persistence rms error	Units
$\hat{W}_s(L)_{12}$	28.6	32.8	knots
$\Delta\hat{Z}(L)_{12}$	3100	3668	ft
$\Delta\hat{S}_{b\,12}$	2.7	3.2	knots $10^{-3} ft^{-1}$
$\Delta\hat{S}_{a\,12}$	2.4	2.4	knots $10^{-3} ft^{-1}$
$\hat{W}_s(L)_{24}$	21.8	29.3	knots
$\Delta\hat{Z}(L)_{24}$	3327	4853	ft
$\Delta\hat{S}_{b\,24}$	2.1	2.9	knots $10^{-3} ft^{-1}$
$\Delta\hat{S}_{a\,24}$	1.5	1.9	knots $10^{-3} ft^{-1}$

TABLE IX   (Continued)

(c)   Category 2C (18 cases)

Predictand	Prediction rms error	Persistence rms error	Units
$\hat{W}_s(L)_{12}$	28.2	33.4	knots
$\Delta\hat{Z}(L)_{12}$	4180	5780	ft
$\Delta\hat{S}_{b\,12}$	1.8	2.2	knots 10^{-3} ft^{-1}
$\Delta\hat{S}_{a\,12}$	1.9	2.5	knots 10^{-3} ft^{-1}
$\hat{W}_s(L)_{24}$	27.5	37.6	knots
$\Delta\hat{Z}(L)_{24}$	4770	6800	ft
$\Delta\hat{S}_{b\,24}$	2.0	3.3	knots 10^{-3} ft^{-1}
$\Delta\hat{S}_{a\,24}$	1.9	2.8	knots 10^{-3} ft^{-1}

(d)   Category 2D (28 cases)

Predictand	Prediction rms error	Persistence rms error	Units
$\hat{W}_s(L)_{12}$	20.3	25.1	knots
$\Delta\hat{Z}(L)_{12}$	4616	5904	ft
$\Delta\hat{S}_{b\,12}$	1.4	2.0	knots 10^{-3} ft^{-1}
$\Delta\hat{S}_{a\,12}$	1.5	2.3	knots 10^{-3} ft^{-1}
$\hat{W}_s(L)_{24}$	25.1	31.4	knots
$\Delta\hat{Z}(L)_{24}$	4570	6508	ft
$\Delta\hat{S}_{b\,24}$	1.9	2.5	knots 10^{-3} ft^{-1}
$\Delta\hat{S}_{a\,24}$	1.6	2.5	knots 10^{-3} ft^{-1}

TABLE IX (Continued)

(e) Category 2E (17 cases)

Predictand	Prediction rms error	Persistence rms error	Units
$\hat{W}_s(L)_{12}$	21.5	22.3	knots
$\Delta\hat{Z}(L)_{12}$	5022	6933	ft
$\Delta\hat{S}_{b\,12}$	1.6	2.2	knots $10^{-3}\,\text{ft}^{-1}$
$\Delta\hat{S}_{a\,12}$	1.5	2.6	knots $10^{-3}\,\text{ft}^{-1}$
$\hat{W}_s(L)_{24}$	23.9	28.1	knots
$\Delta\hat{Z}(L)_{24}$	2992	4011	ft
$\Delta\hat{S}_{b\,24}$	1.7	3.0	knots $10^{-3}\,\text{ft}$
$\Delta\hat{S}_{a\,24}$	1.9	3.0	knots $10^{-3}\,\text{ft}$

(a) Category 1A Data (84 cases)

Predictand	Rms error		Units
	Category 1D equation	Category 2A equation	
$\hat{W}_s(L)_{12}$	30.5	32.5	knots
$\Delta\hat{Z}(L)_{12}$	5121	5703	ft
$\Delta\hat{S}_{b\,12}$	1.9	1.8	knots 10^{-3} ft^{-1}
$\Delta\hat{S}_{a\,12}$	2.1	2.4	knots 10^{-3} ft^{-1}
$\hat{W}_s(L)_{24}$	34.9	38.8	knots
$\Delta\hat{Z}(L)_{24}$	5235	5412	ft
$\Delta\hat{S}_{b\,24}$	1.4	1.6	knots 10^{-3} ft^{-1}
$\Delta\hat{S}_{a\,24}$	2.2	2.1	knots 10^{-3} ft^{-1}

(b) Category 1D Data (83 cases)

Predictand	Rms error		Units
	Category 1A equation	Category 1E equation	
$\hat{W}_s(L)_{12}$	35.4	27.4	knots
$\Delta\hat{Z}(L)_{12}$	6293	6060	ft
$\Delta\hat{S}_{b\,12}$	1.6	1.6	knots 10^{-3} ft^{-1}
$\Delta\hat{S}_{a\,12}$	1.9	1.6	knots 10^{-3} ft^{-1}
$\hat{W}_s(L)_{24}$	39.8	35.0	knots
$\Delta\hat{Z}(L)_{24}$	6144	6501	ft
$\Delta\hat{S}_{b\,24}$	2.3	2.3	knots 10^{-3} ft^{-1}
$\Delta\hat{S}_{a\,24}$	2.4	2.2	knots 10^{-3} ft^{-1}

TABLE X (Continued)

(c) Category 1B Data (84 cases) and
Category 1C Data (85 cases)*

Predictand	Rms error		Units
	Category 1C equation	Category 1B equation	
$\hat{W}_s(L)_{12}$	22.6	25.4	knots
$\Delta\hat{Z}(L)_{12}$	3537	5106	ft
$\Delta\hat{S}_{b\,12}$	1.5	1.7	knots 10^{-3} ft^{-1}
$\Delta\hat{S}_{a\,12}$	1.7	2.0	knots 10^{-3} ft^{-1}
$\hat{W}_s(L)_{24}$	25.7	33.3	knots
$\Delta\hat{Z}(L)_{24}$	5196	4311	ft
$\Delta\hat{S}_{b\,24}$	1.6	2.2	knots 10^{-3} ft^{-1}
$\Delta\hat{S}_{a\,24}$	1.9	2.4	knots 10^{-3} ft^{-1}

(d) Combined Data of Categories 2A, 2B, and 2C (56 cases)

Predictand	Rms error			Units
	Category 2A equation	Category 2B equation	Category 2C equation	
$\hat{W}_s(L)_{12}$	29.1	29.6	28.0	knots
$\Delta\hat{Z}(L)_{12}$	3954	3628	3882	ft
$\Delta\hat{S}_{b\,12}$	2.1	2.4	2.4	knots 10^{-3} ft^{-1}
$\Delta\hat{S}_{a\,12}$	2.0	2.5	2.2	knots 10^{-3} ft^{-1}
$\hat{W}_s(L)_{24}$	26.6	26.3	28.4	knots
$\Delta\hat{Z}(L)_{24}$	3777	4104	4178	ft
$\Delta\hat{S}_{b\,24}$	2.2	2.2	2.5	knots 10^{-3} ft^{-1}
$\Delta\hat{S}_{a\,24}$	2.0	2.2	2.0	knots 10^{-3} ft^{-1}

*Category 1B equation tested on Category 1C data, and vice versa.

stream core) and Category 2A (subtropical wind speed maximum) are tested on inde-
pendent data for Category 1A (polar wind speed maximum). The rms errors for these
two equations [Table X(a)] are consistently higher for all predictands than the rms errors
for the Category 1A equation [Table VIII(a)]. For example, the rms errors for 24-hr prog-
noses of wind speed are 30.4 for the Category 1A equation, 34.9 for the Category 1D
equation, and 38.8 for the Category 2A equation. Thus, the equations developed for the
wind-speed maximum category of the subtropical jet and for a category off the polar
jet core yielded inferior results when tested on independent data for the polar jet-
stream wind-speed maximum category.

The rms errors obtained when the Category 1A equation and Category 1E equation
(developed for two grid intervals to the right of the polar jet-stream core) are tested on
Category 1D independent data are given in Table X(b). A comparison with the rms errors
obtained with the Category 1D equation [Table VIII(d)] shows that higher rms errors resulted
for all predictands using both the Category 1A and Category 1E equations. Taking the 24-hr
wind speed as an example again, the rms errors are 33.6 for the Category 1D equation,
39.8 for the Category 1A equation, and 35.0 for the Category 1E equation. It is seen,
therefore, that the equations (Category 1A equation) developed for a category on the core
yield increased rms errors when applied to an area removed from the core. Furthermore,
when the equations developed for the category to the right of the core are applied to data
to the left of the core, higher rms errors result. The above results indicate that the
stratification of the data into polar and subtropical systems, each being further separated
into grid points on the core or to the right or left of the core, was worthwhile.

Rms errors that occur when the Category 1C equation (two grid points downstream
from the wind speed maximum) is applied to Category 1B independent data, and vice
versa, are given in Table X(c). If the classification procedure used along the core has
merit, considerably higher rms errors should result when the equation developed for the
category upstream from the wind speed maximum is applied to independent data down-
stream. A comparison with Table VIII(b) and (c) shows that this is not the case. The rms
errors differ very little, and for some predictands are actually lower. This result may
be due to the fact that wind speed and shear variations along the core are much smaller
than the variations which occur to the right and left of the core. The obvious conclusion

99

to be drawn from the above is that a single category of grid points located on the jet-stream core should replace the three categories used. The results shown in Table X(d) further substantiate this conclusion. The sets of equations for the three subtropical core categories are applied to all grid points along the subtropical jet core, with little difference noted in the rms errors.

An example of the predictions obtained from the LMW Predictor Network Technique (PNT) is given in Fig. 4(a)—(h). The initial-state distribution of W_s(L) on 00Z December 17, 1963 is given in Fig. 4(a). The subsequent 12- and 24-hr distributions (analyses obtained from observations) are shown in Fig. 4(b) and (d). The corresponding 12- and 24-hr prognoses are given in Fig. 4(c) and (e). The isopleths for these maps and Fig. 4(f), (g) and (h) (24-hr prognoses of height, shear below, and shear above) are all drawn subjectively. The isopleths were, however, based on grid-point values of the parameters that were obtained objectively from the prediction equations or, in the case of the LMW wind-speed analyses, from a SAT analysis of the observations. The jet-stream cores shown on the LMW wind speed analyses and prognoses are drawn in subjectively, based on the grid-point values of wind speed and the isotach analysis. Both the predicted and analyzed jet cores are shown on the maps depicting the 24-hr predictions of LMW height, shear above and shear below.

An examination of the initial-state LMW wind speed map shows that three major, intense jet-stream systems with wind maxima greater than 125 knots are to be found. The system over the southeastern North Pacific Ocean curves southeastward toward the equator. A second strong system defines an upper-level ridge centered just off the Pacific coast of the U.S. and southwest Canada. The isotach maximum is moving across the top of the ridge and is located at the Canadian border. The third system is a major east-west jet stream extending from the eastern United States across the Atlantic just south of 40°N latitude. An intense wind-speed maximum of 200 knots is noted at 50°W longitude.

The major changes that occur after 24 hours are: (1) the jet stream over the southeastern North Pacific Ocean intensifies upstream at the edge of the map and begins to curve slightly north of east, tending to be linked with the system over the west coast of the United States, (2) the jet stream near the west coast of the U.S. is displaced north-

ward at the crest of the ridge, but the jet maximum plunges into the northern plains, and (3) the jet stream in the Atlantic maintains position but the intensity is somewhat diminished.

The corresponding 24-hr prognoses (1) correctly forecast the change in curvature of the Pacific Ocean jet stream and the tendency to "link" with the west coast jet-stream system, but do not indicate the increased intensity upstream, (2) correctly indicate the departure of the Pacific Coast wind-speed maximum south-eastward, but do not displace the jet-stream northward and (3) correctly maintains the position and reduces the intensity of the Atlantic jet stream system, but does not indicate the jet maximum in the extreme eastern Atlantic Ocean.

In general then, it can be said that the prediction equations for the LMW wind speeds yield quite reasonable prognoses. A weakness in the prediction technique is, however, clearly illustrated by these series of maps. A need exists to make predictions further downstream from the initial-state location of the jet-stream wind-speed maximum than was undertaken with the technique developed in this feasibility study (no predictions were made over most of the western and central United States because no predictand points were located in those areas; this resulted in the LMW parameters being undefined in this region of the prognoses).

Figure 4(f), (g) and (h) shows the 24-hr predictions of the LMW shear below, shear above and height of the LMW with the actual and forecast jet cores superimposed on the analyses. Generally, the most intense shears above the LMW are located close to or just south of the jet core, while the most intense shears below the LMW are located close to or just north of the core. The LMW height prognoses are shown only within the area defined by the predicted 75-knot isotach.

To summarize, Fig. 4 shows that reasonable forecasts are obtained for a particular series of maps. The series of maps also helps to emphasize the point that additional categories of predictand points over areas where there are no jets at initial time (t_0) would be required before developing an operationally-useful set of prediction equations.
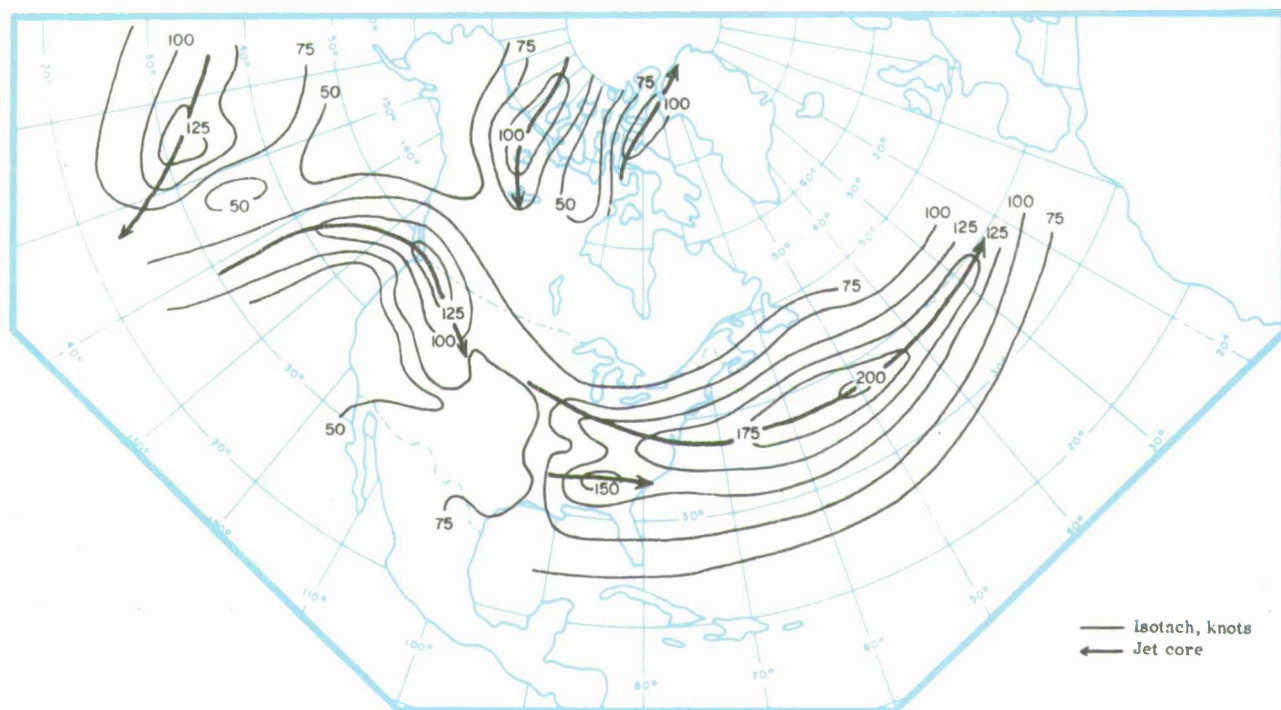
101

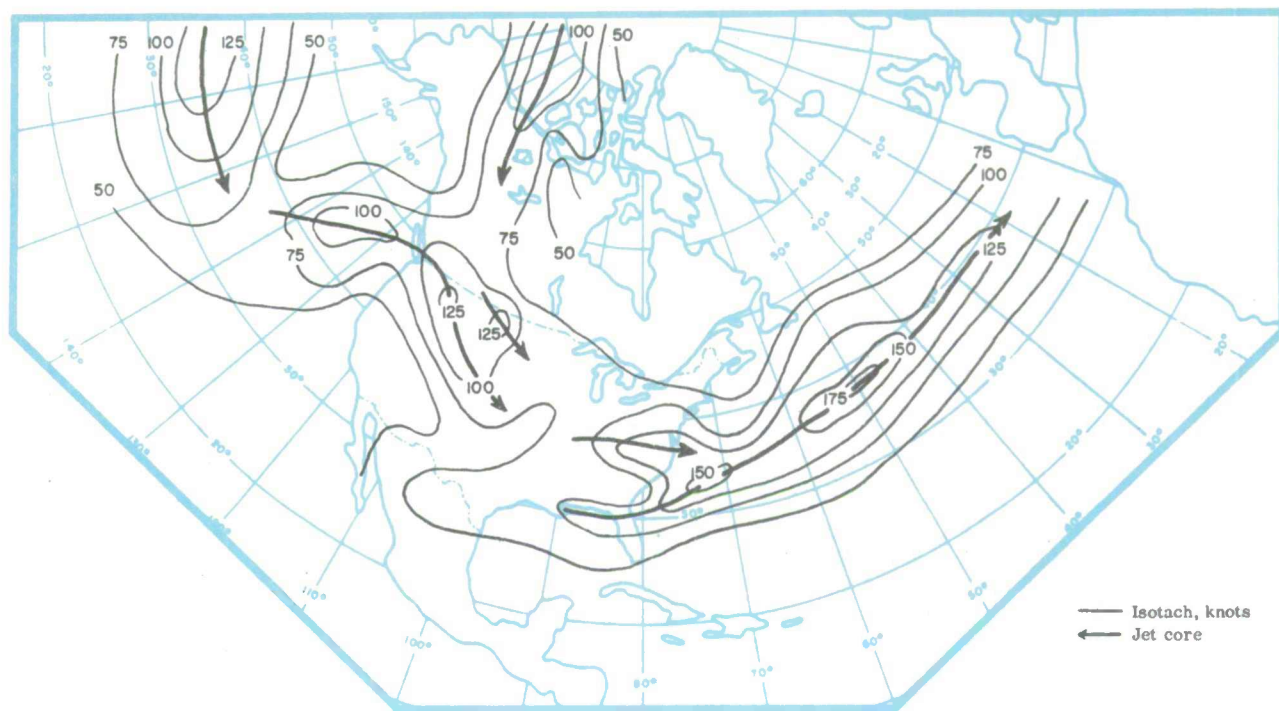Fig. 4(a). W_s(L) analysis, 00Z December 17, 1963.

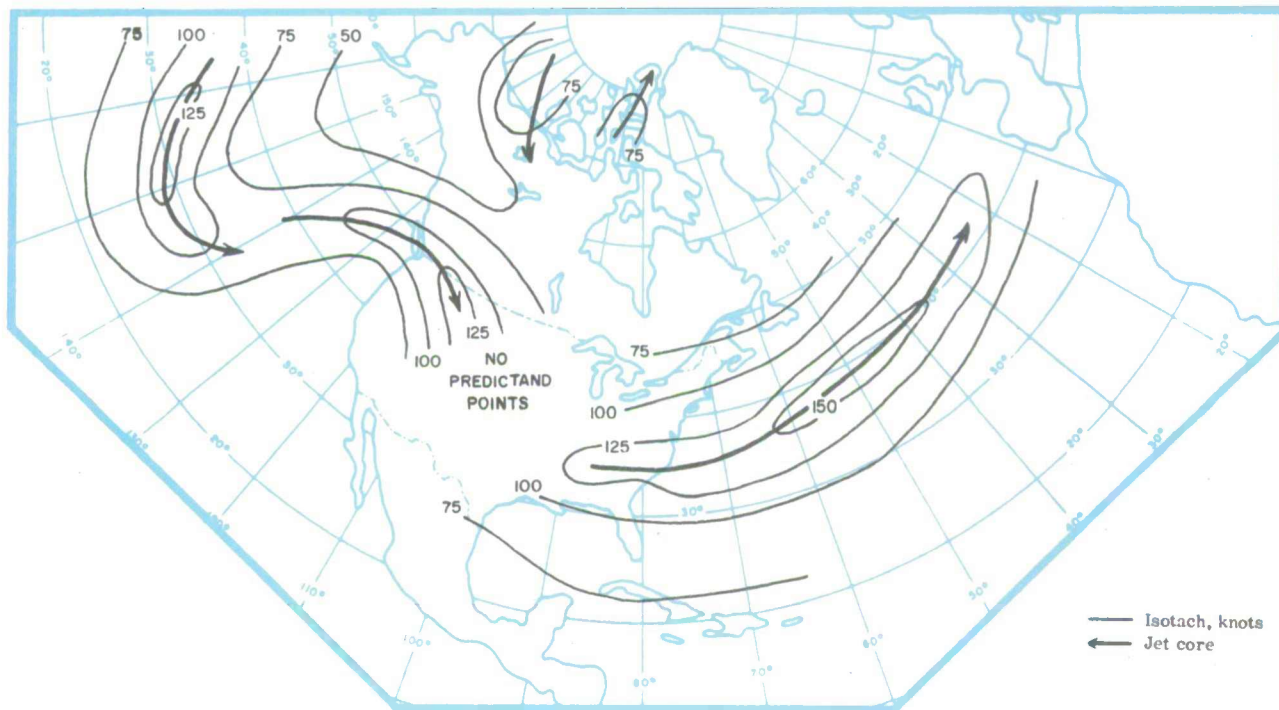Fig. 4(b). W_s(L) analysis, 12Z December 17, 1963.

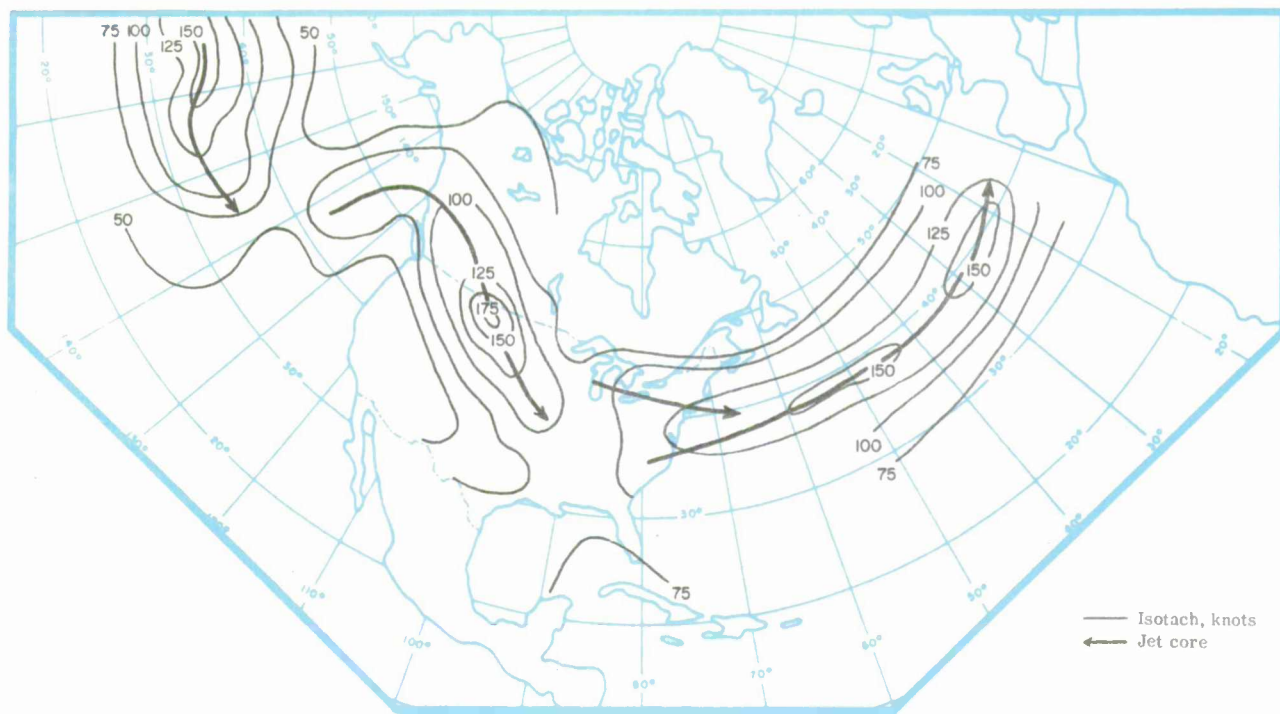Fig. 4(c). W_s(L) 12-hr prognosis valid 12Z December 17, 1963.

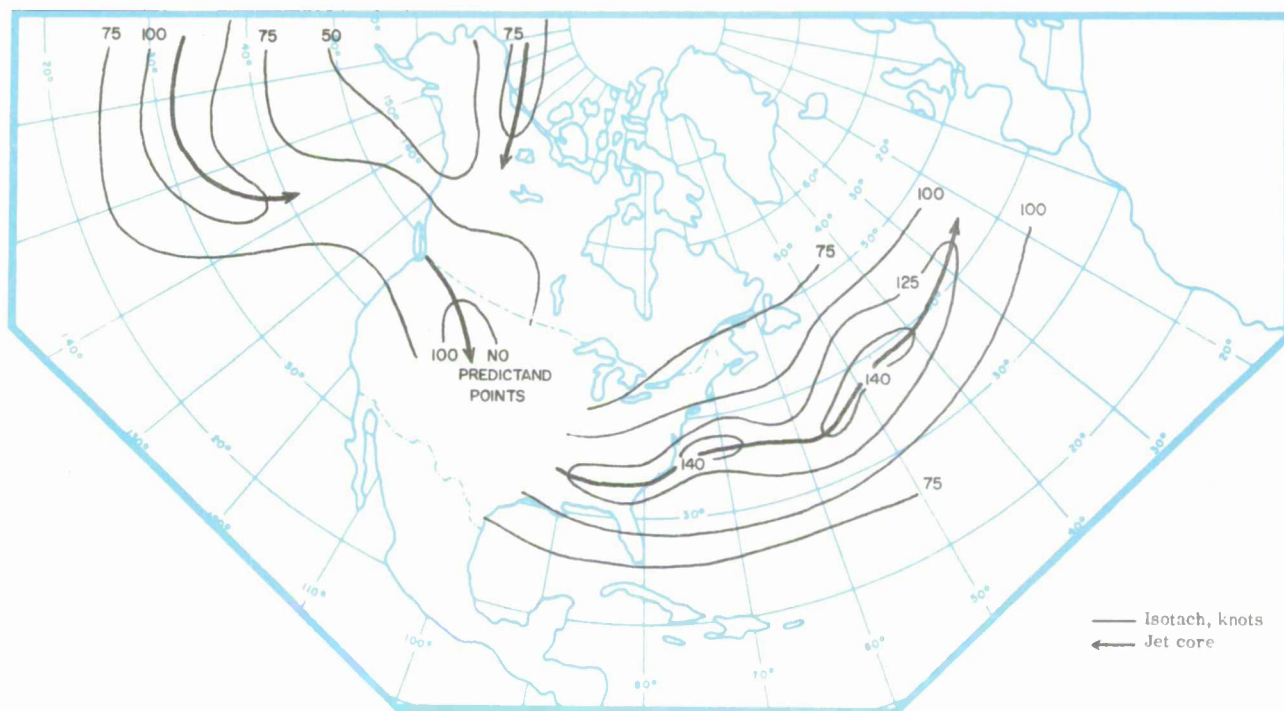Fig. 4(d). $W_s(L)$ analysis, 00Z December 18, 1963.

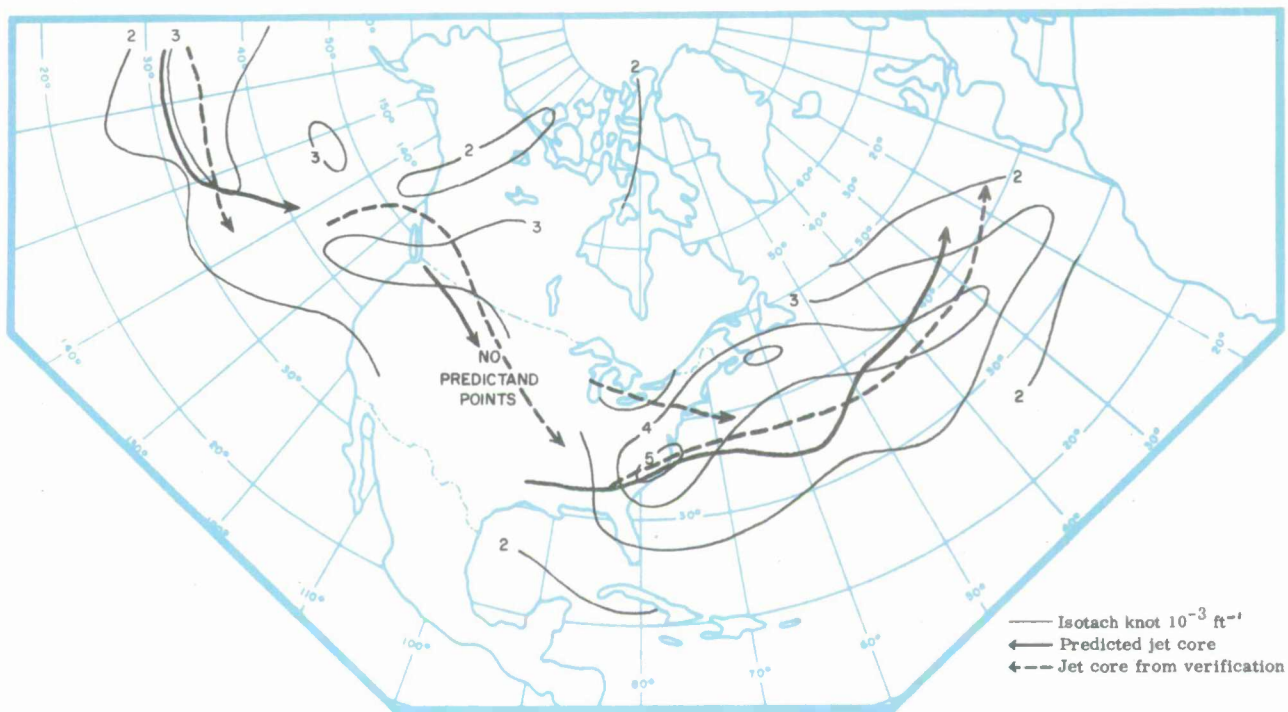Fig. 4(e). $W_s(L)$ 24-hr prognosis valid 00Z December 18, 1963.

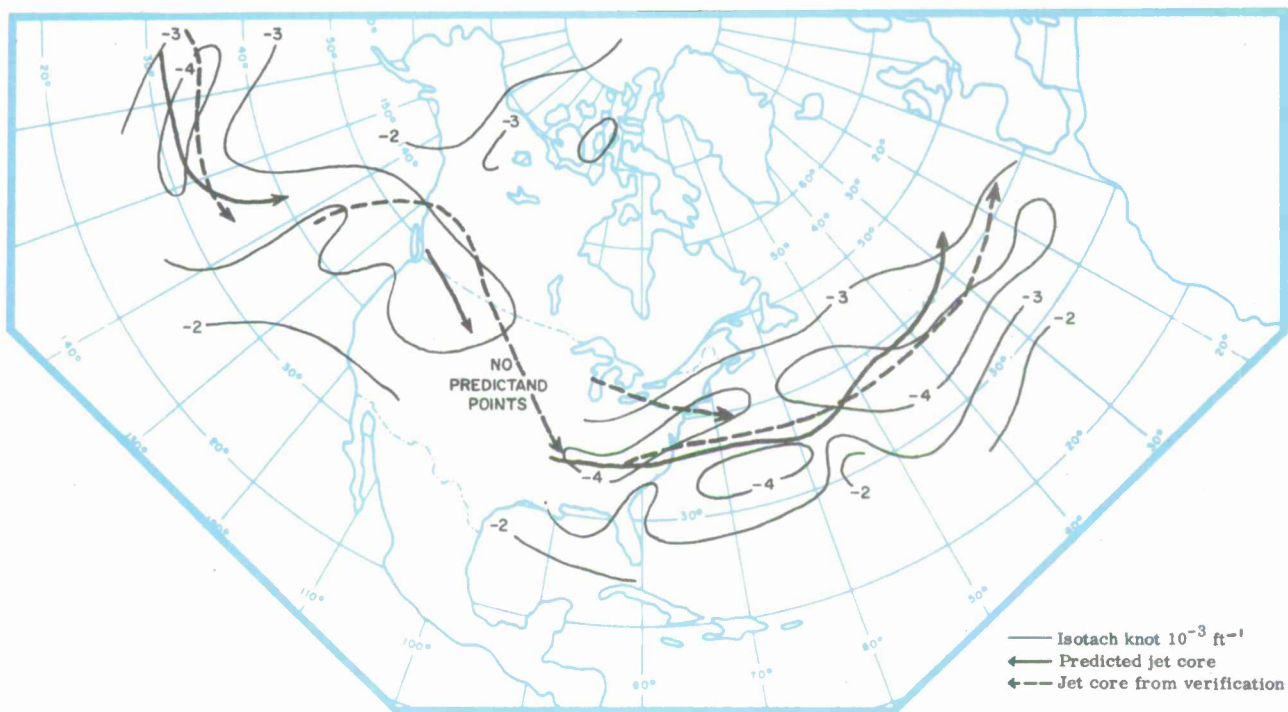Fig. 4(f). S_b 24-hr prognosis valid 00Z December 18, 1963.

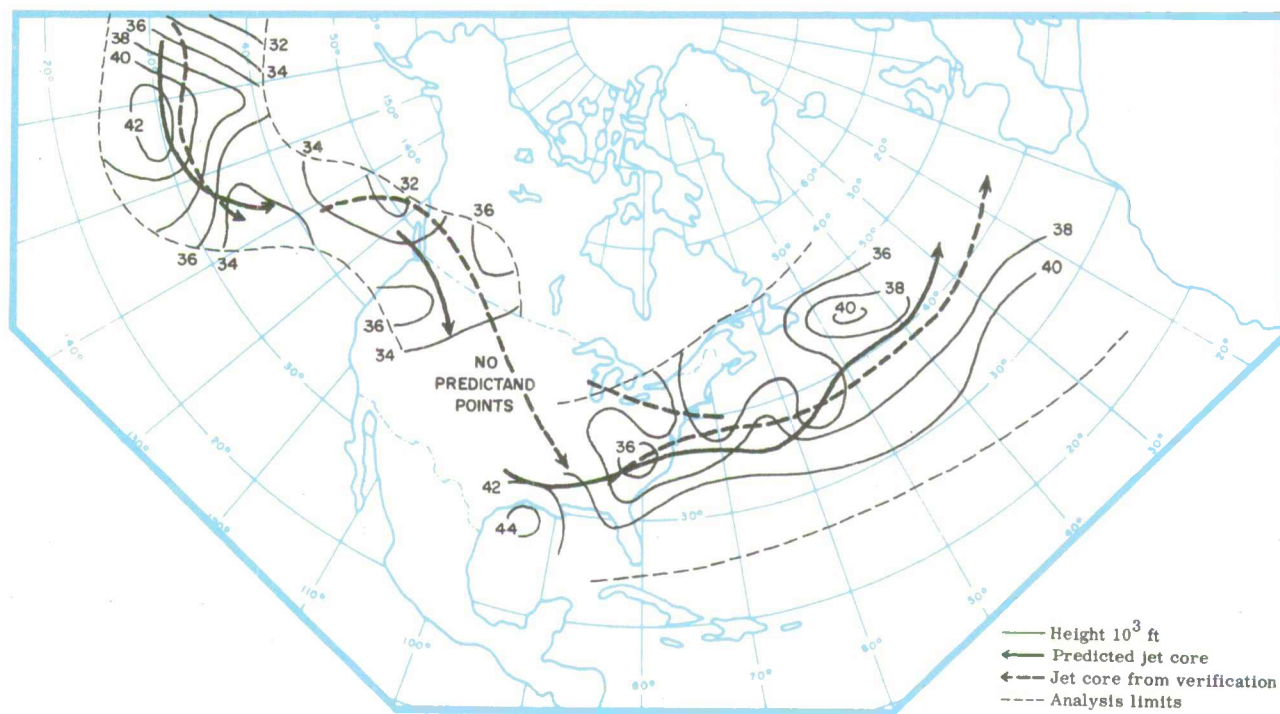Fig. 4(g). S_a 24-hr prognosis valid 00Z December 18, 1963.

Fig. 4(h). Z(L) 24-hr prognosis valid 00Z December 18, 1963.

SECTION V

RESULTS USING THE MODELING PREDICTION TECHNIQUE

The LMW Predictor Network Technique was developed from a two-month winter data sample, a portion of which was set aside as independent data for testing the technique. Prognostic constant-pressure-surface charts were not included as part of this data sample. Thus, it was necessary to acquire a special collection of numerical prognoses for the LMW Modeling Prediction Technique, which requires using constant-pressure-surface prognostic charts in conjunction with the diagnostic LMW equations. Third Weather Wing personnel (Offutt Air Force Base, Omaha, Nebraska) supplied us with a five-day sample of prognostic charts and analyses (9—14 December 1964) for testing.

Ten sets of 12-, 24-, 36-, and 48-hr constant-pressure-surface prognoses of height, temperature, and wind were used with the diagnostic (as opposed to the prognostic equations discussed in the previous section) LMW equations, beginning with the set that was generated from initial data at 00Z December 9, 1964. Analyses of height, temperature, and wind from 00Z December 9 to 00Z December 14 were used with the diagnostic LMW equations to obtain LMW analyses for verification purposes (the analyses were not "corrected" by station data and the successive approximation analysis technique as described in PART I of this report, because station data were not on hand). Because analyses were not available after 00Z December 14, ten 12-hr, nine 24-hr, eight 36-hr, and seven 48-hr LMW prognoses were verified with the analyses.

Root-mean-square errors were computed (at grid points) for each forecast LMW parameter for each observation time, and overall rms errors were computed for each LMW parameter for the 12-, 24-, 36-, and 48-hr prognosis groups. As was expected, the errors increased with increasing length of the forecast interval. Table XI presents the overall error statistics.

The measure of error by rms errors for the prognoses of the LMW parameters is not a particularly good indicator of their accuracy, because of the nature of the horizontal variations of the fields of LMW parameters.

TABLE XI

OVERALL rms ERRORS FOR LMW PROGNOSES

Predictand	rms errors				Units
	12-hr	24-hr	36-hr	48-hr	
$\hat{W}_s(L)$	12.8	15.7	18.6	21.0	knots
$\hat{Z}(L)$	4598	5289	5924	6491	ft
$\hat{S}_b$	0.98	1.04	1.09	1.13	knots 10^{-3}ft^{-1}
$\hat{S}_a$	0.92	1.01	1.11	1.20	knots 10^{-3}ft^{-1}

To obtain a clearer picture of the usefulness, the prognoses were examined with regard to: (1) location of the jet-stream axes, (2) the intensity of the maxima along the axes, (3) the extent of the areas of wind speeds in excess of 100 knots, and (4) the height of the LMW and the vertical shears below and above the LMW over those areas where wind speeds were observed in excess of 100 knots. The evaluation based on this type of examination was necessarily subjective in nature. Accuracy of the predictions of each of the LMW parameters is discussed separately.

8.   Wind speed at the LMW [$W_s(L)$]

The 12-hr prognoses of $W_s(L)$ were considered very good, based on the first three criteria listed above, i.e. (1) the location of the jet-stream axes was generally forecast quite well with only occasional maximum errors in position of the jet-cores of 100—150 miles, (2) errors for the intensity of the maxima along the isotachs ranged from near zero to 25% (% error = $|\frac{\text{Fcst minus observed}}{\text{observed}}| \times 100$) with the average errors about 10%, and (3) the extent of the areas of wind speeds in excess of 100 knots was specified very well over most areas of the hemisphere for the 12-hr prognoses.

The 24-hr prognoses of $W_s(L)$ were judged, in general, to be fair-to-good or good. The locations of the jet-stream axes were forecast well over most areas of the hemisphere during most of the five-day period, but over central and eastern Asia and the western Pacific, where there were large-amplitude trough—ridge systems in the planetary waves, causing the jet-streams axes to have a markedly meridional character, the extent of the meridional air flow was usually under-forecast, although

the relative longitudinal positions of the troughs and ridges were forecast accurately. Errors for the intensity of the maxima were somewhat higher than for the 12-hr forecasts, ranging up to 40% occasionally, but averaging 15—20%.

The area of winds in excess of 100 knots was specified fairly accurately over most areas of the hemisphere, with no apparent systematic error. At times, there were areas where winds were forecast to be in excess of 100 knots, but were not observed to be and the converse was true at other times. In other words, there was no noticeable bias in the forecasts.

The 36-hr and 48-hr prognoses of $W_s(L)$ showed considerable deterioration from the 12- and 24-hr prognoses, although two prognoses in each group were considered to be good, with the remainder only fair to fair-to-good. The largest errors in the forecasts occurred over central and eastern Asia where large amplitude planetary waves were evident, and over an area near Hawaii in the vicinity of a cut-off closed cyclonic circulation that was quasi-stationary for half the five-day period and then began to move northeastward. Over the North Atlantic Ocean, where a wide area of strong zonal (westerly) winds (≥ 100 knots) was observed for most of the five-day period, the 36- and 48-hr prognoses were judged to be good.

Figure 5(a) through (e) is the observed and 12-, 24-, 36-, and 48-hr $W_s(L)$ prognoses valid at 00Z December 13. These prognoses were judged to be fair-to-good. Figure 6(a) through (e) is the 12-, 24-, 36-, and 48-hr prognoses valid at 00Z December 14—a series of prognoses that were considered to be generally good-to-excellent.

9. Height of the LMW [Z(L)]

The areas where the wind speeds were observed in excess of 100 knots were examined on the prognosis charts of $Z(L)$ and compared with the observed chart of $Z(L)$. It was evident from the comparison that the errors in the prognoses were relatively low—generally less than 2000 ft and rarely more than 5000 ft for the 12- and 24-hr prognoses and somewhat higher (2000—4000 ft and only occasionally as high as 8000—10000 ft) for the 36- and 48-hr prognoses. In general, the prognoses of $Z(L)$ for all forecast intervals were considered to be good. Figure 7(a) through (d) shows the error fields for $Z(L)$ prognoses [over areas where $W_s(L)$ was observed as ≥ 100 knots] valid at 00Z December 13, 1964, and Fig. 8(a) through (d) shows the

109

Z(L) error fields for prognoses valid 24 hr later. (These sets of error fields correspond to the verification times for the W_s(L) prognoses discussed in the previous section.) It is evident that the general conclusion stated for all the Z(L) prognoses in the five-day series is valid for these specific observation times.

10.   Shear below the LMW (S_b)

Within the 100-knot wind-speed isotach, S_b errors generally averaged about 1.5 knots per thousand feet for the 12-hr prognoses and close to 2 knots per thousand feet for the 24-hr prognoses except for very small areas where the errors were sometimes as high as 3 to 6 knots per thousand feet. It should be emphasized that the areas where these larger errors occurred comprised only about 5% of the areas enclosed by the 100-knot isotachs. For the 36- and 48-hr prognoses, the average errors over the areas within the 100-knot isotach increased to 2 to 3 knots per thousand feet, but maximum errors of 4 to 6 knots occurred only over a small portion (3—5%) of the total area outlined by the observed 100-knot isotach. In contrast, the total rms errors for the hemisphere for all forecast intervals was near 1 knot per thousand feet, because over the major portion of the hemisphere winds are less than 100 knots at the LMW, vertical shears are less, and it follows that the errors are quite small. The areas of maximum errors of S_b appear to be highly correlated to the maximum errors of wind speed at the LMW.

Figure 9(a) through (d) and Fig 10. (a) through (d) present the error distribution of forecast fields of S_b within the observed 100-knot isotach for the same time periods as for W_s(L) and Z(L).

11.   Shear Above the LMW (S_a)

The statements in the discussion of the shear below the LMW apply for S_a, except that there were a few cases at isolated grid points where maximum errors were 8 and 9 knots per thousand feet. Figure 11(a) through (d) and Fig 12. (a) through (d) are the error fields within the 100-knot wind-speed isotach of S_a prognoses valid at 00Z December 13 and 00Z December 14.
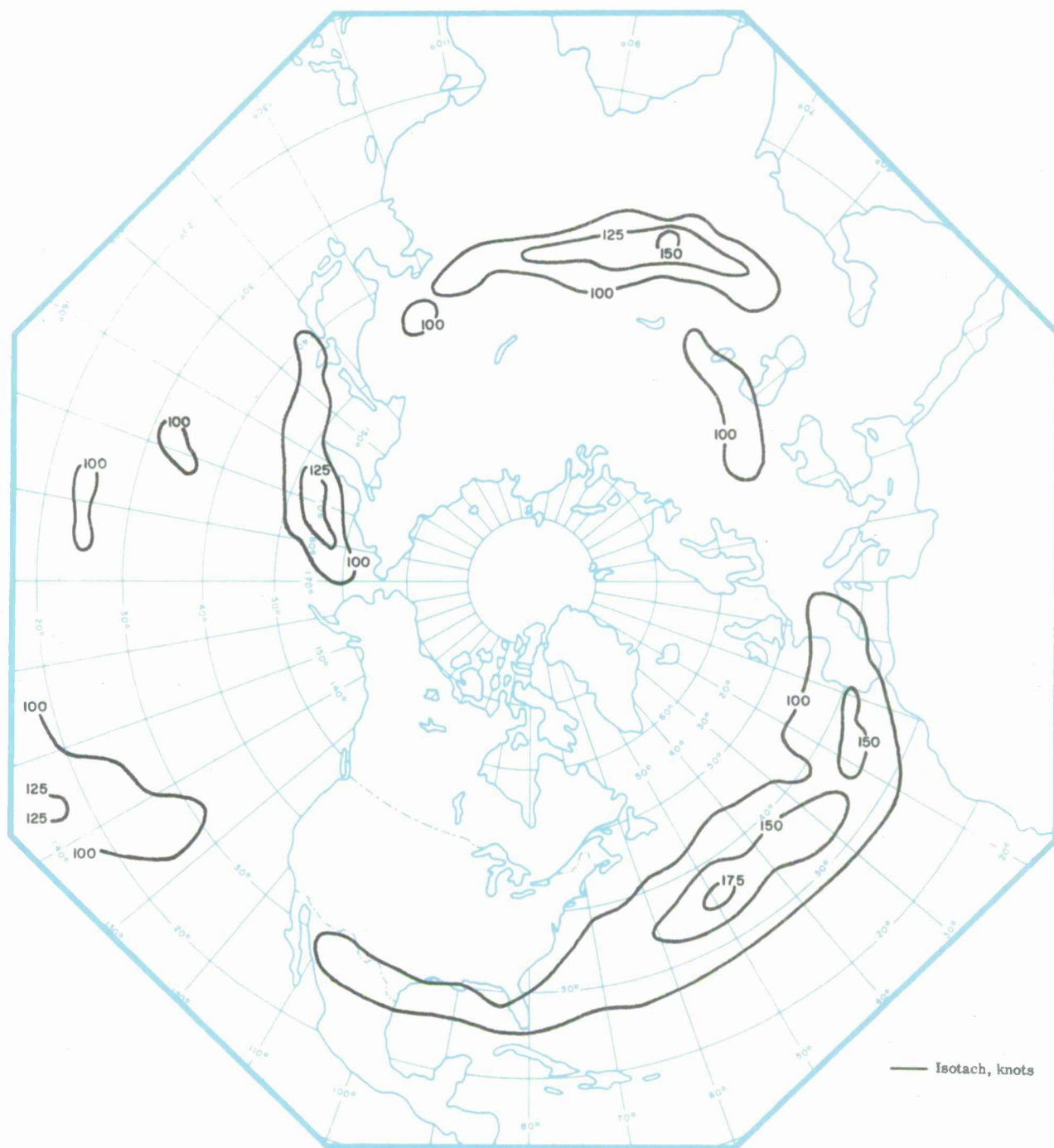
Fig. 5(a). W_s(L) analysis 00Z December 13, 1964

Fig. 5(b). W_s(L) 12-hr prognosis valid 00Z December 13, 1964.
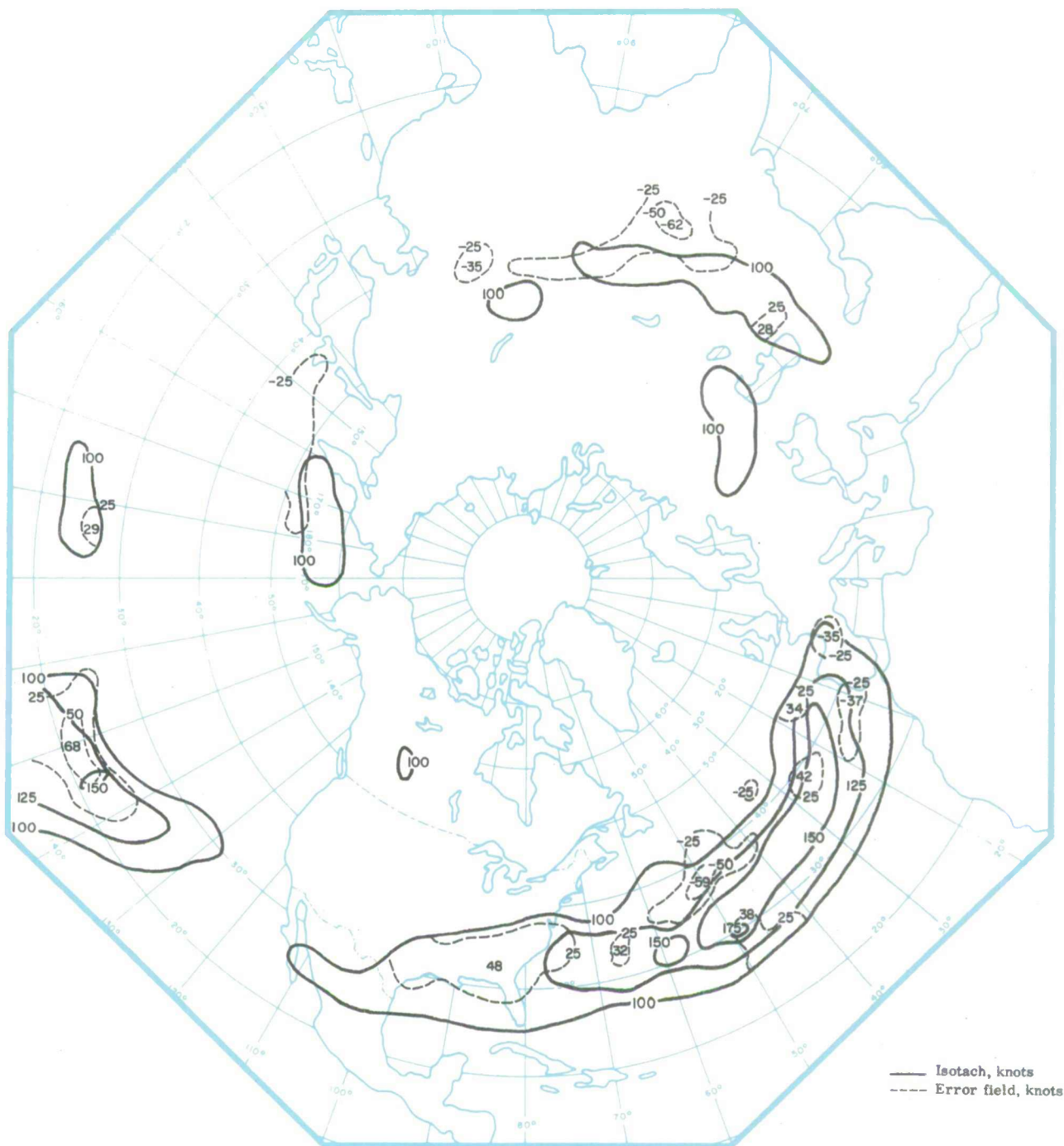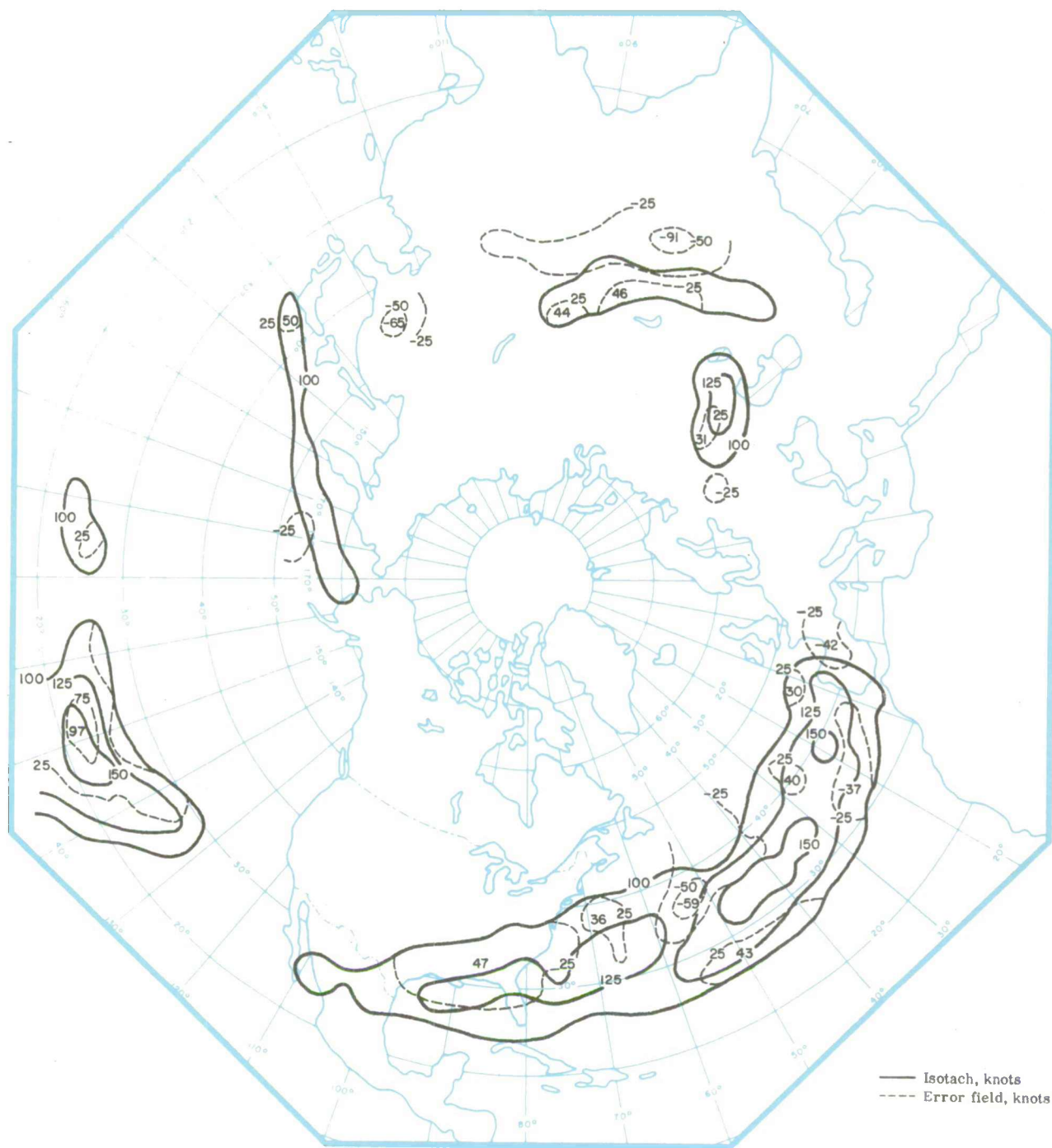
112

Fig. 5(c). $W_s(L)$ 24-hr prognosis valid 00Z December 13, 1964.

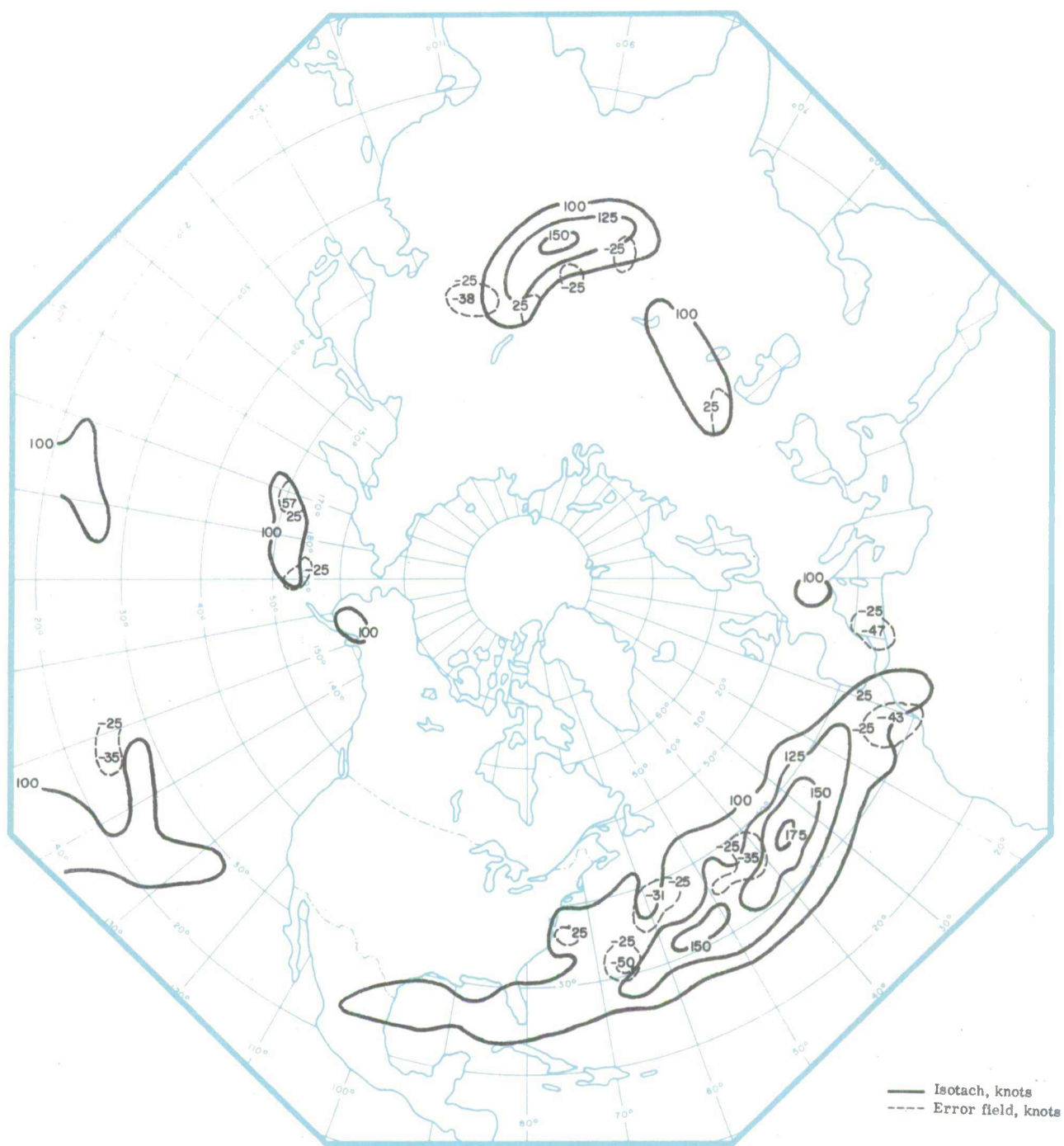Fig. 5(d). $W_s(L)$ 36-hr prognosis valid 00Z December 13, 1964.

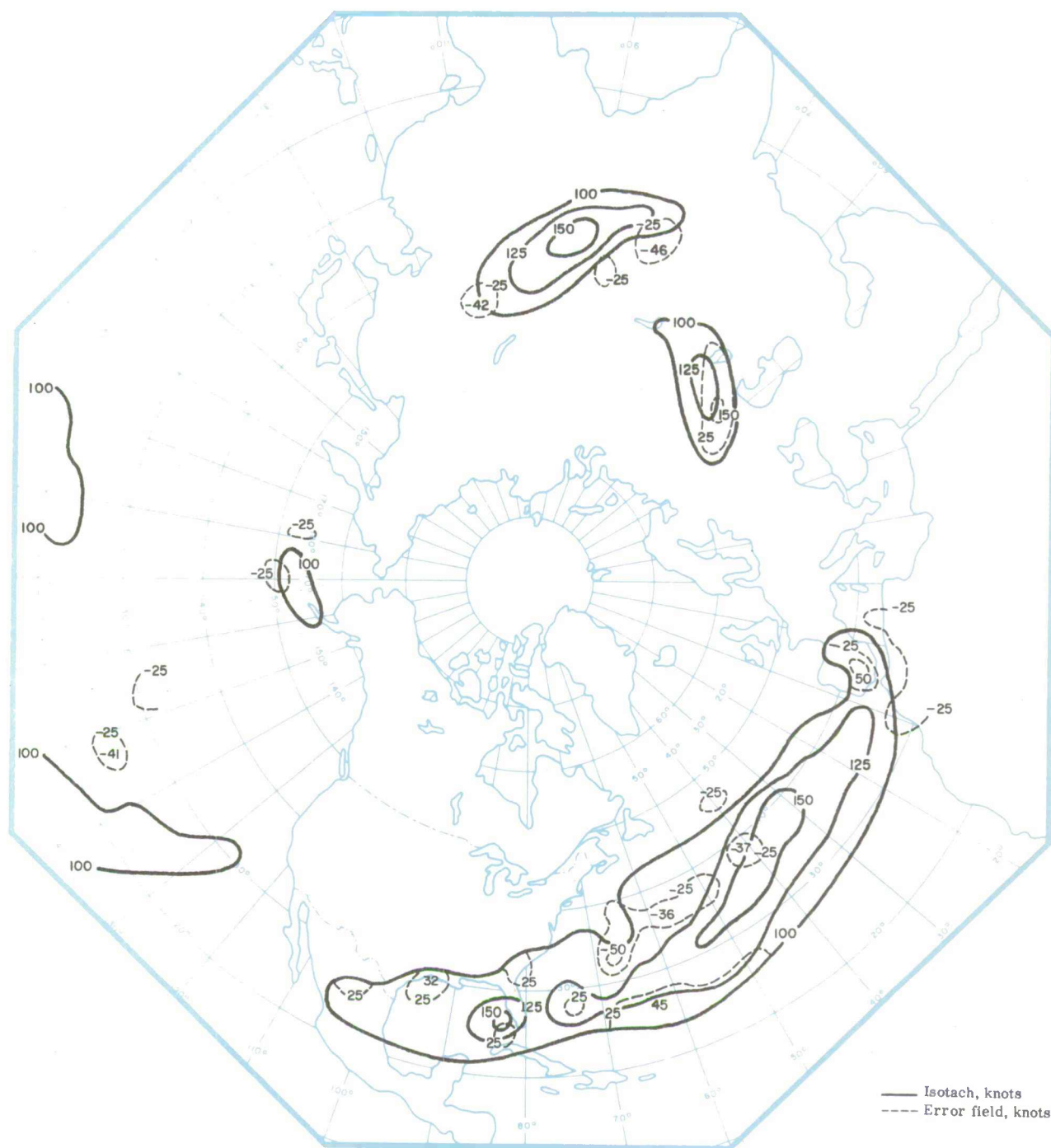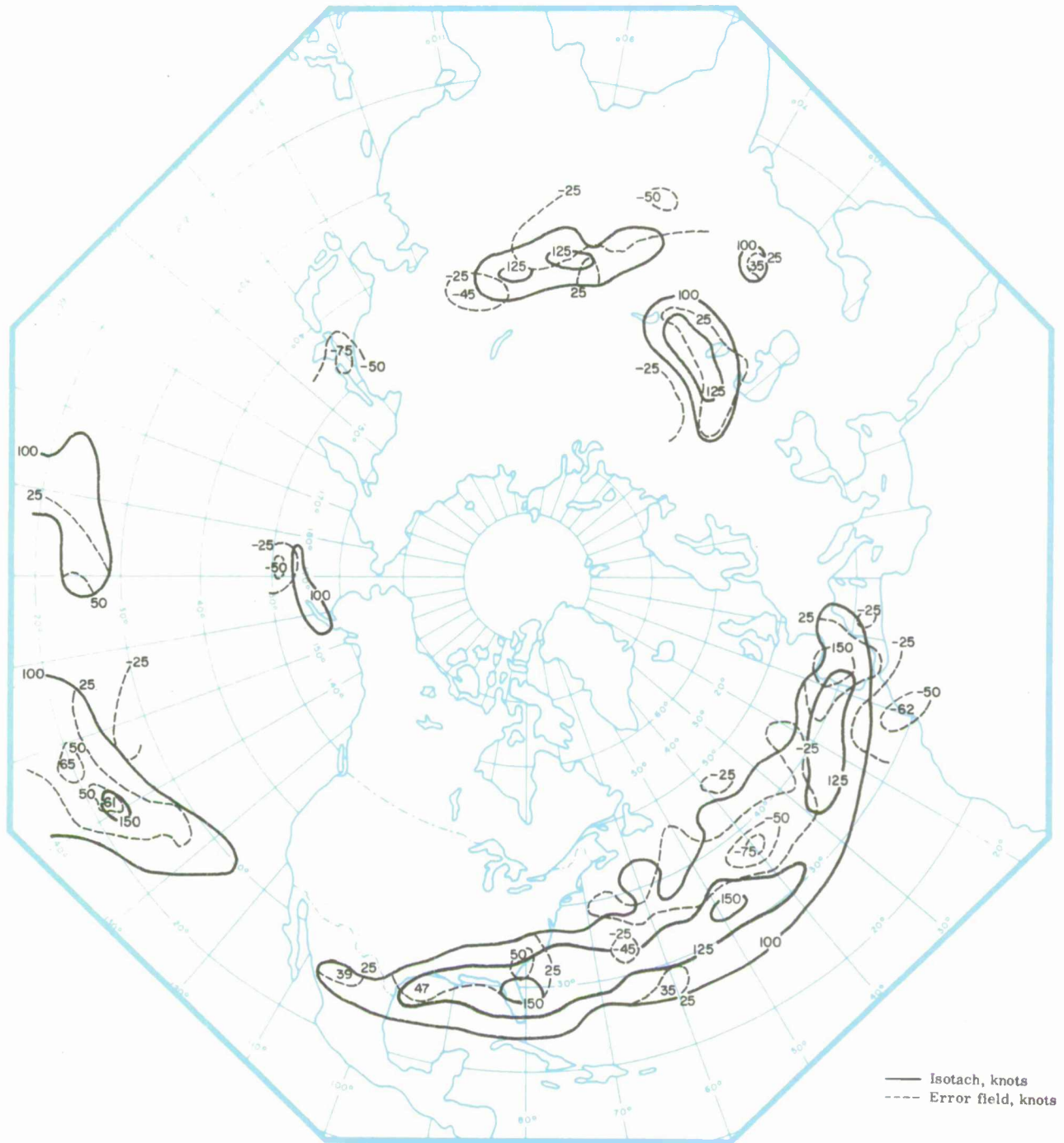Fig. 5(e). $W_s(L)$ 48-hr prognosis valid 00Z December 13, 1964.

115

Fig. 6(a). $W_s(L)$ analysis, 00Z December 14, 1964.

116

Fig. 6(b). $W_s(L)$ 12-hr prognosis valid 00Z December 14, 1964.

Fig. 6(c). $W_s(L)$ 24-hr prognosis valid 00Z December 14, 1964.

Fig. 6(d). $W_S(L)$ 36-hr prognosis valid 00Z December 14, 1964.

Fig. 6(e). $W_s(L)$ 48-hr prognosis valid 00Z December 14, 1964.
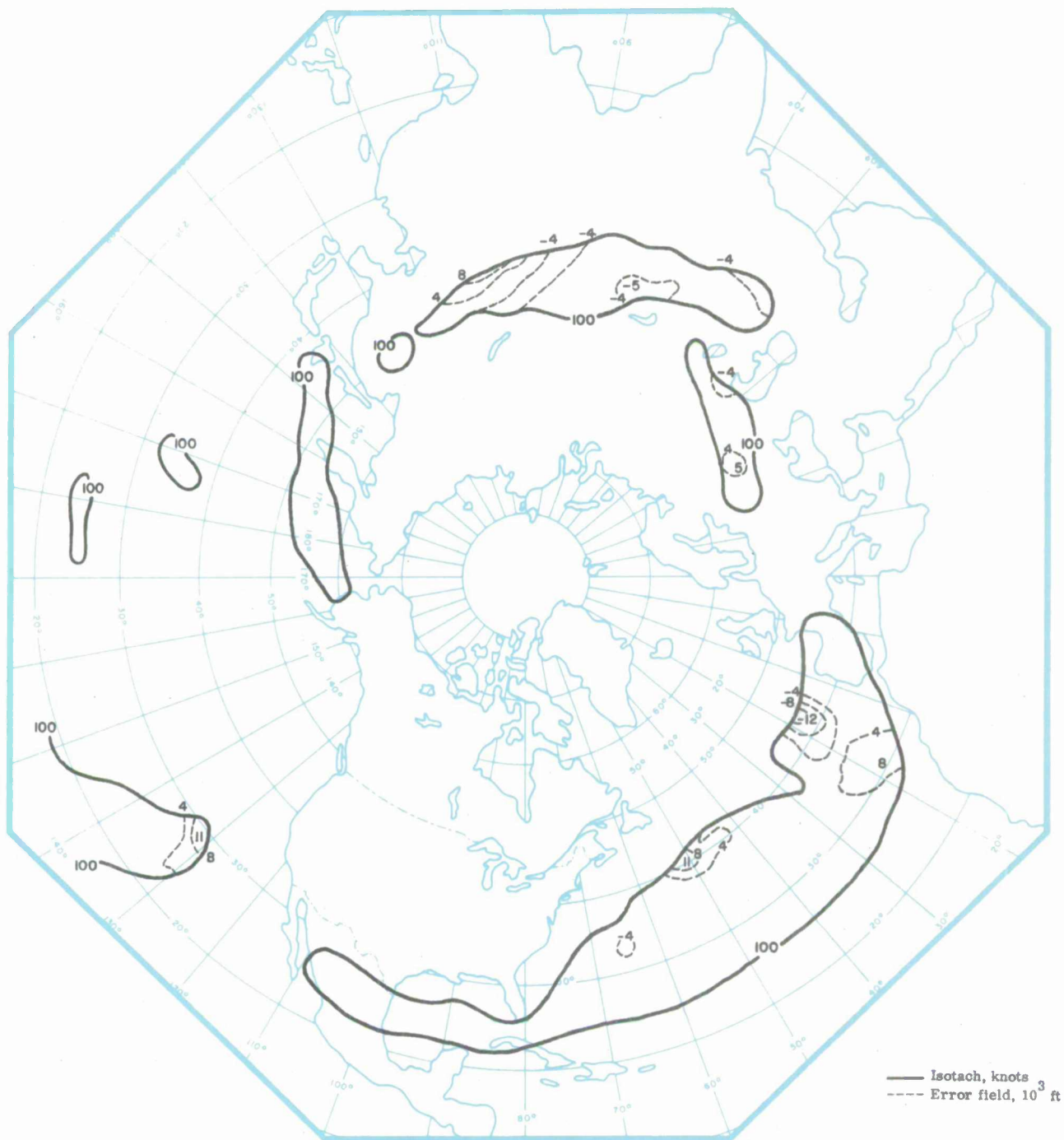
Fig. 7(a). Z(L) 12-hr prognosis (valid 00Z December 13, 1964) error field
[(forecast minus observed) over areas where $W_S(L)$ observed as > 100 knots)].

Fig. 7(b). Z(L) 24-hr prognosis (valid 00Z December 13, 1964) error field [(forecast minus observed) over areas where $W_s(L)$ observed as > 100 knots)].
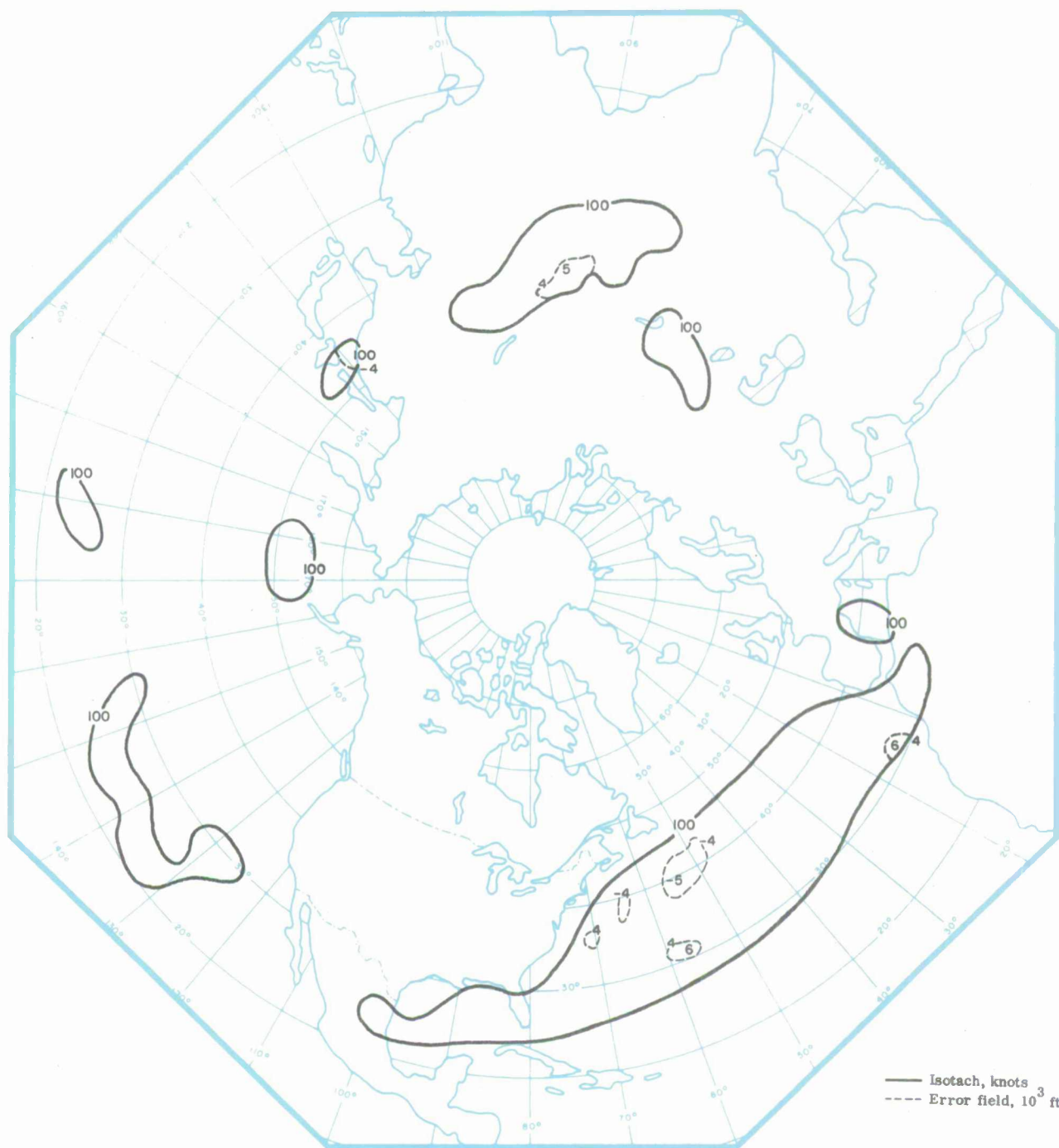
Fig. 7(c). Z(L) 36-hr prognosis (valid 00Z December 13, 1964) error field
[(forecast minus observed) over areas where $W_s(L)$ observed as > 100 knots)].

Fig. 7(d). Z(L) 48-hr prognosis (valid 00Z December 13, 1964) error field [(forecast minus observed) over areas where W_s(L) observed as > 100 knots)].

Fig. 8(a). Z(L) 12-hr prognosis (valid 00Z December 14, 1964) error field [(forecast minus observed) over areas where W_s(L) observed as > 100 knots)].
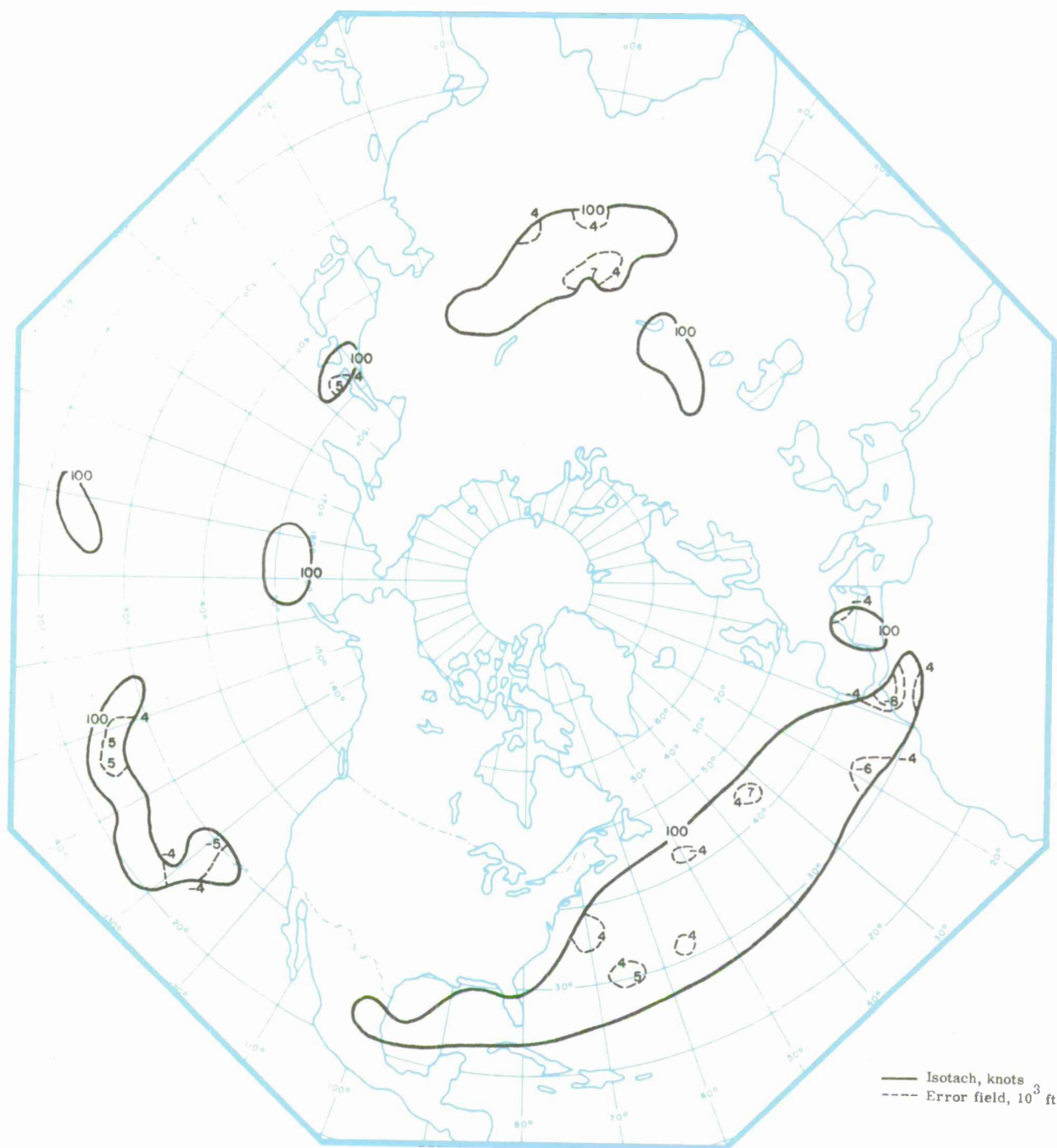
Fig. 8(b). Z(L) 24-hr prognosis (valid 00Z December 14, 1964) error field
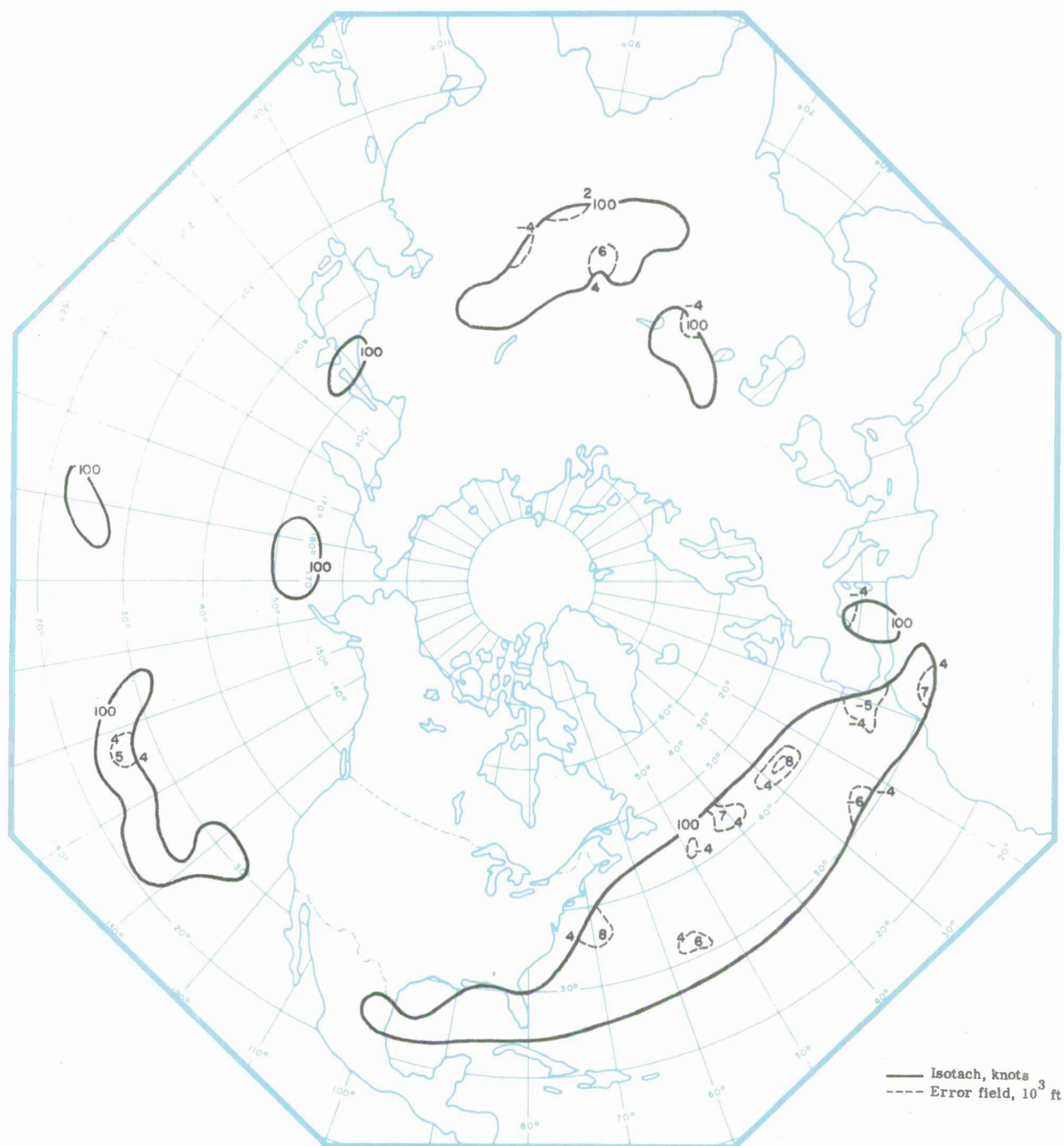[(forecast minus observed) over areas where $W_s(L)$ observed as > 100 knots)].

Fig. 8(c). Z(L) 36-hr prognosis (valid 00Z December 14, 1964) error field [(forecast minus observed) over areas where $W_s(L)$ observed as > 100 knots)].

Fig. 8(d). Z(L) 48-hr prognosis (valid 00Z December 14, 1964) error field [(forecast minus observed) over areas where $W_s(L)$ observed as > 100 knots)].
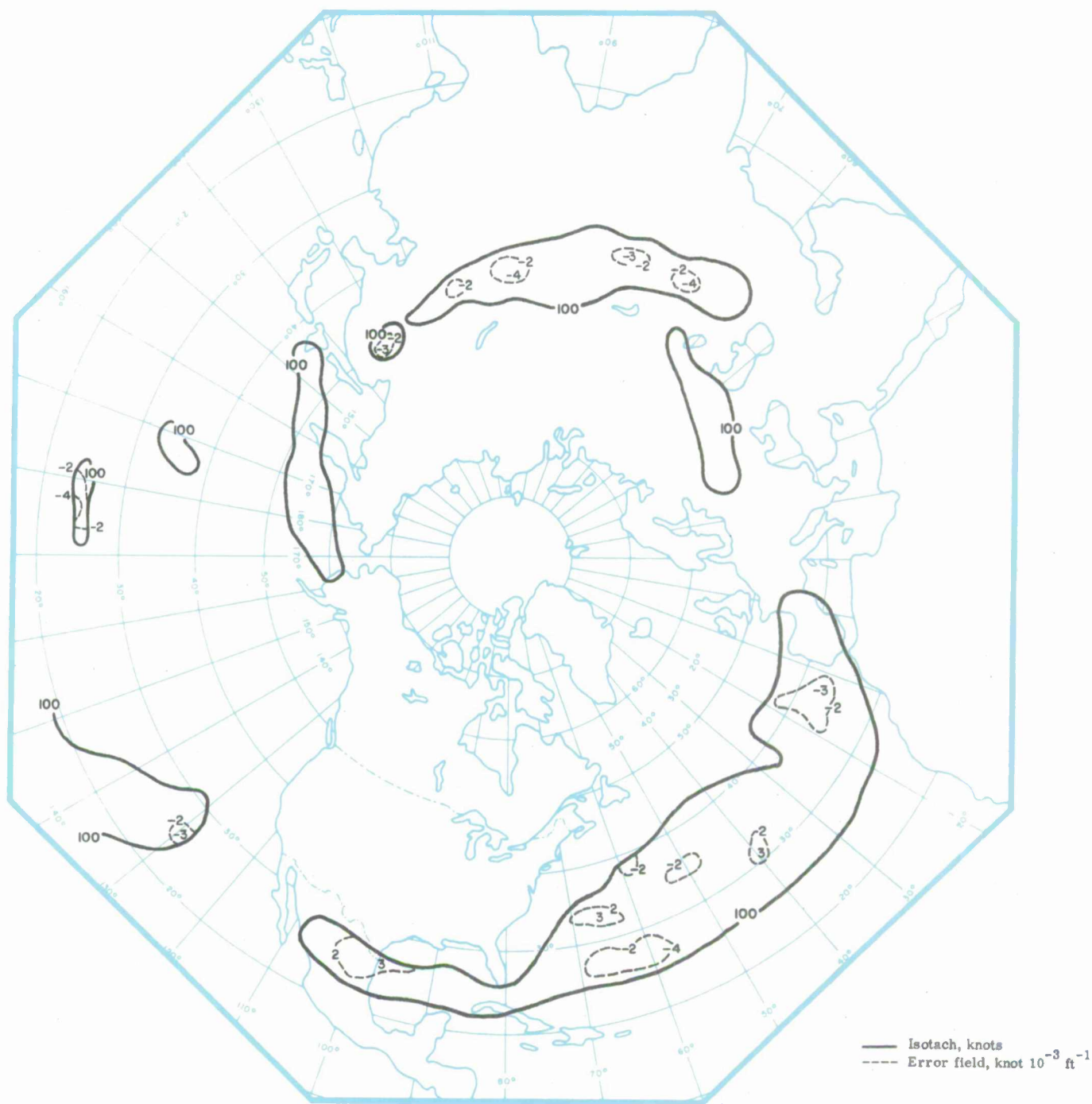
Fig. 9(a). S_b 12-hr prognosis (valid 00Z December 13, 1964) error field
[(forecast minus observed) over areas where W_s (L) observed as > 100 knots)].
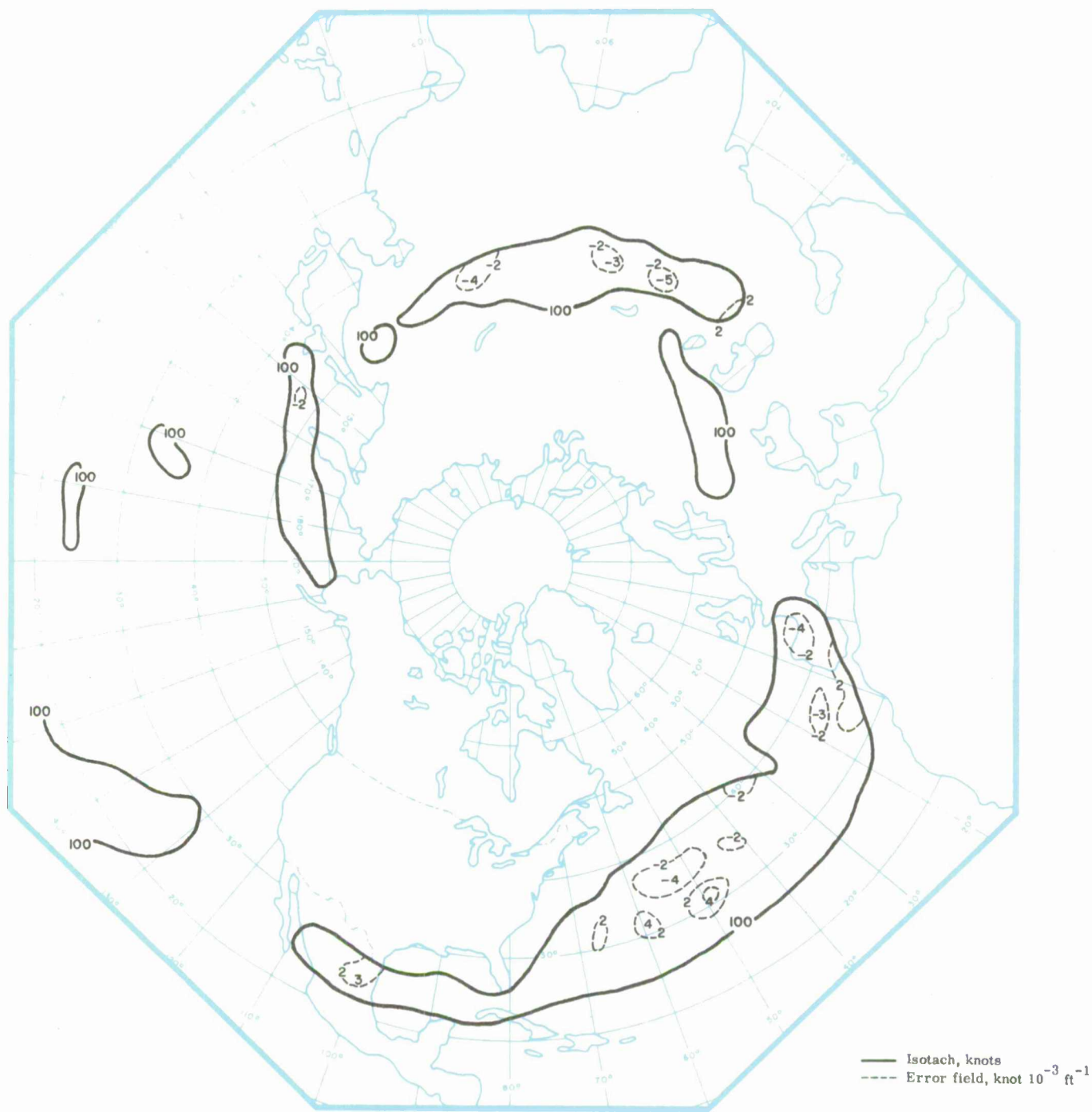
Fig. 9(b). S_b 24-hr prognosis (valid 00Z December 13, 1964) error field [(forecast minus observed) over areas where $W_s(L)$ observed as > 100 knots)].

Fig. 9(c). S_b 36-hr prognosis (valid 00Z December 13, 1964) error field
[(forecast minus observed) over areas where $W_s(L)$ observed as > 100 knots)].

131

Fig. 9(d). S_b 48-hr prognosis (valid 00Z December 13, 1964) error field
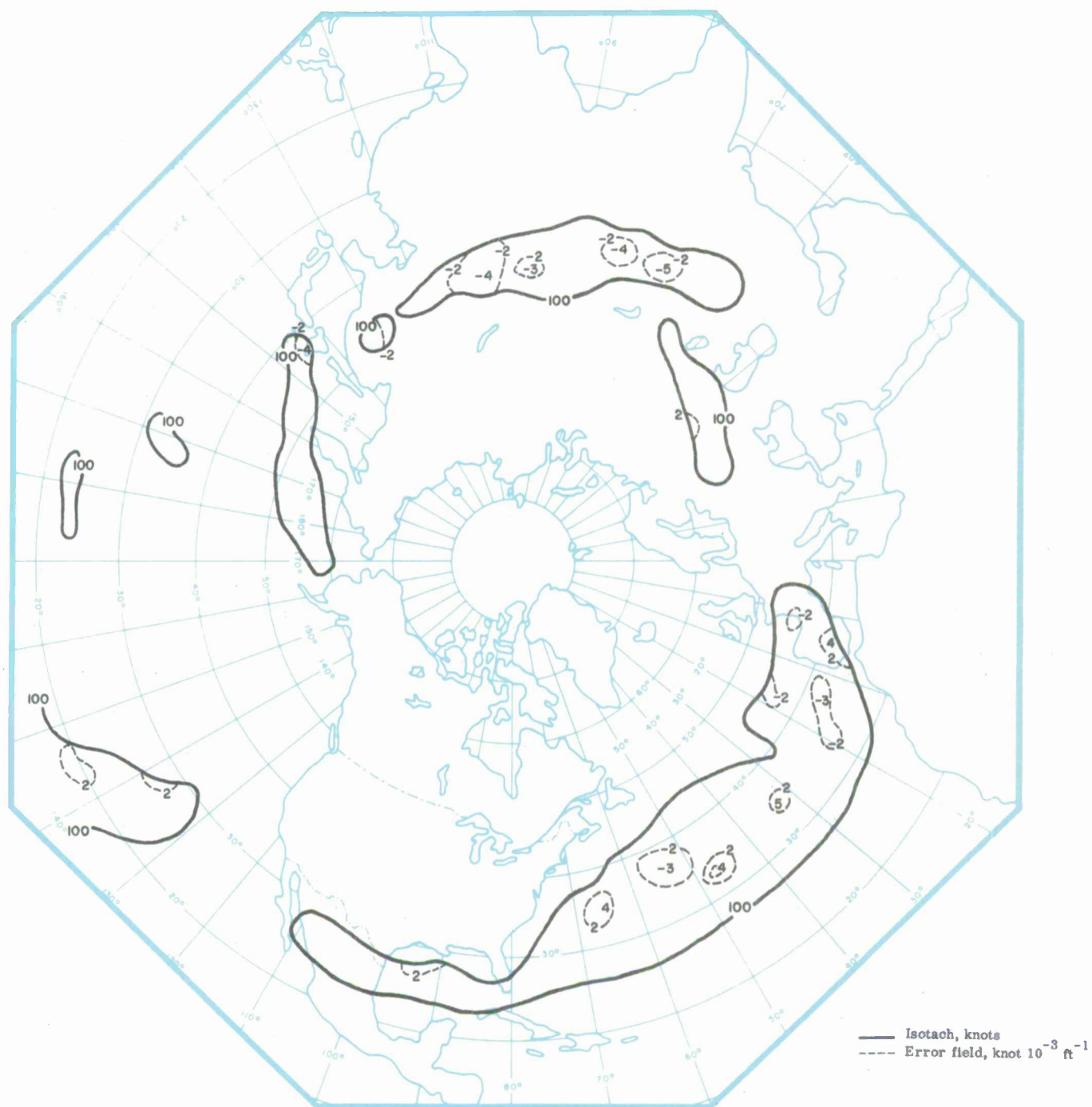[(forecast minus observed) over areas where $W_s(L)$ observed as > 100 knots)].

Fig. 10(a). S_b 12-hr prognosis (valid 00Z December 14, 1964) error field [(forecast minus observed) over areas where W_s(L) observed as > 100 knots)].

Fig. 10(b). S_b 24-hr prognosis (valid 00Z December 14, 1964) error field [(forecast minus observed) over areas where $W_s(L)$ observed as > 100 knots)].

Fig. 10(c). S_b 36-hr prognosis (valid 00Z December 14, 1964) error field
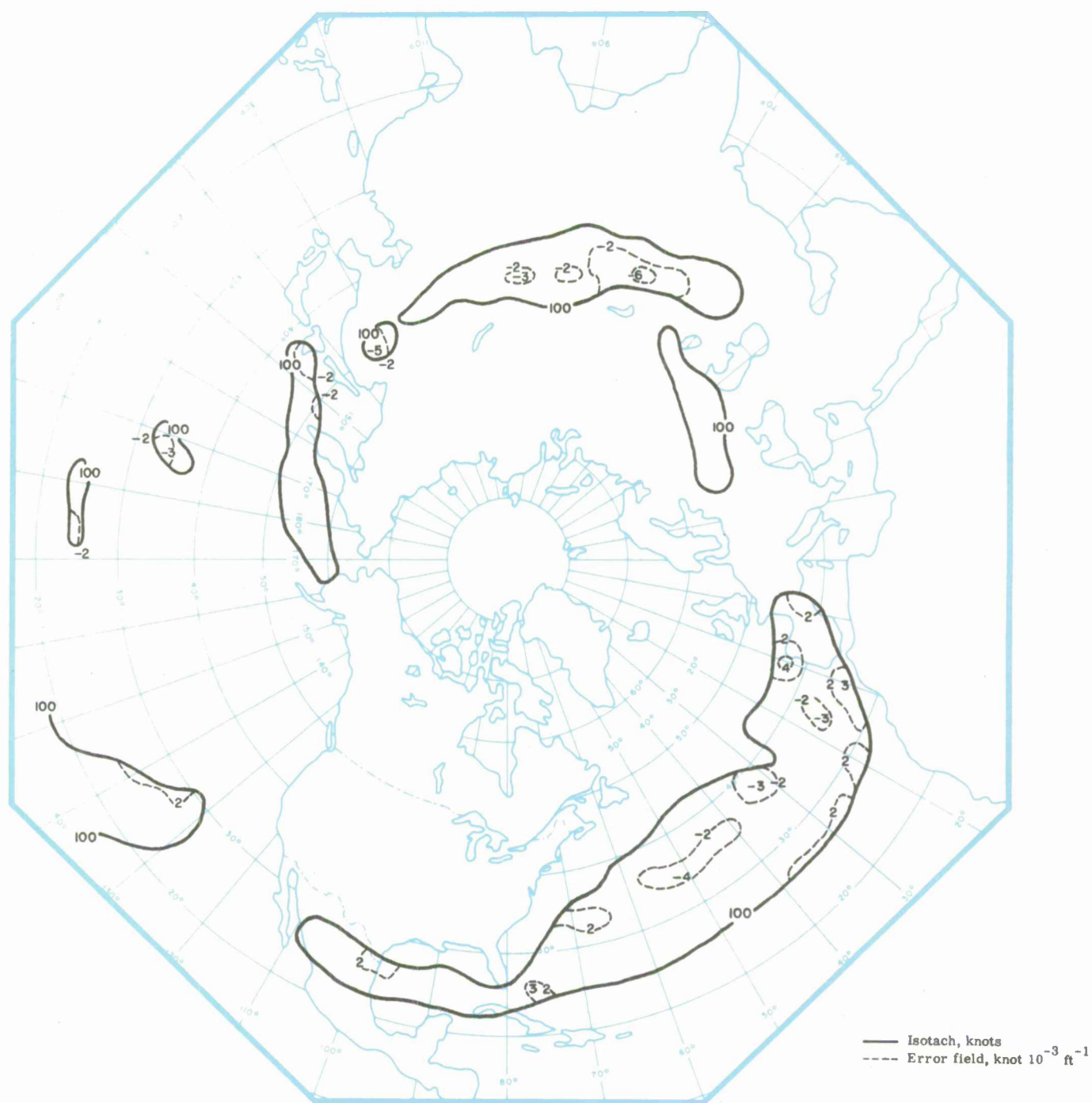[(forecast minus observed) over areas where W_s(L) observed as > 100 knots)].

Fig. 10(d). S_b 48-hr prognosis (valid 00Z December 14, 1964) error field [(forecast minus observed) over areas where $W_s(L)$ observed as > 100 knots)].

Fig. 11(a). S_a 12-hr prognosis (valid 00Z December 13, 1964) error field
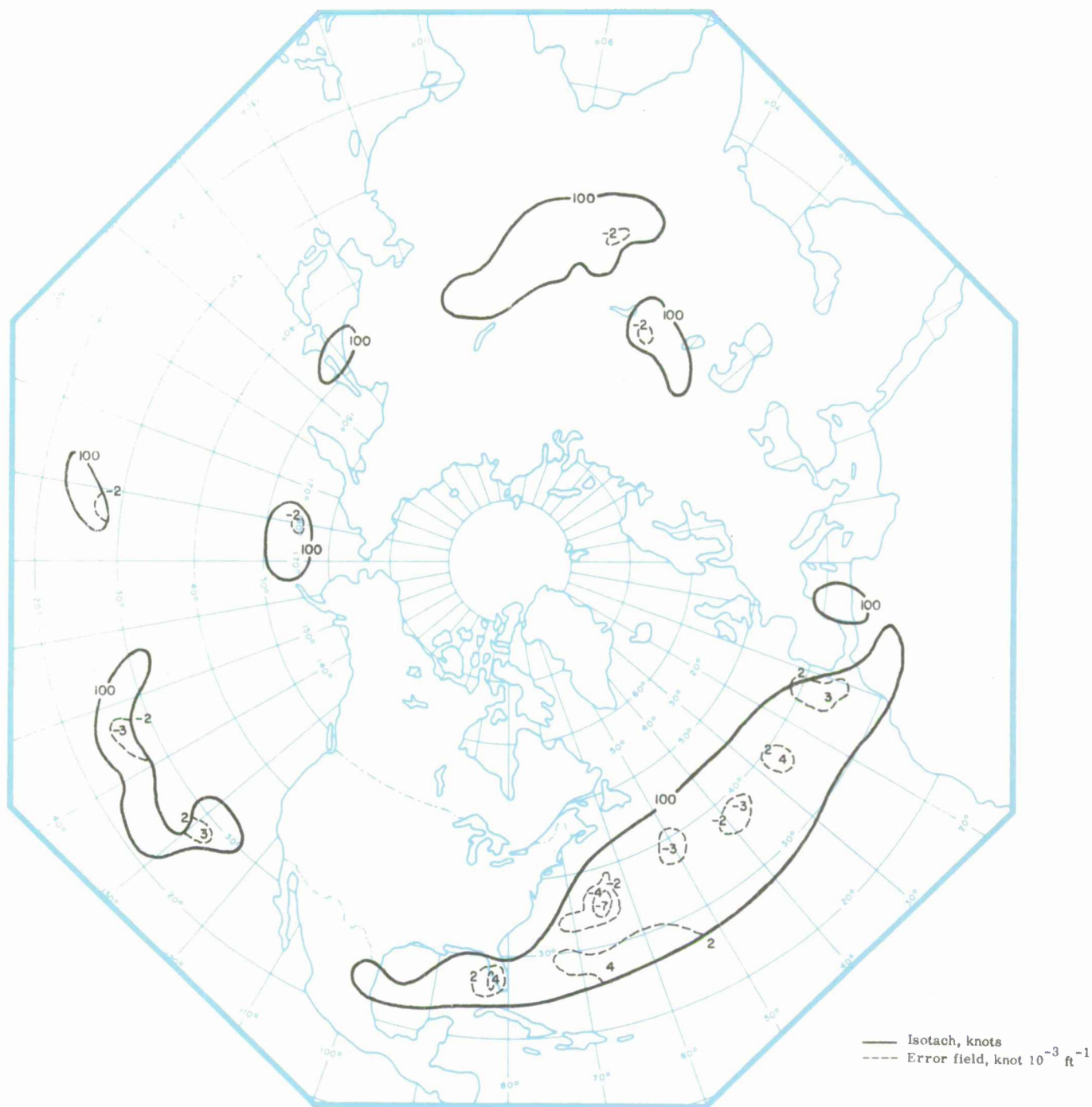[(forecast minus observed) over areas where $W_s(L)$ observed as > 100 knots)].

137

Fig. 11(b). S_a 24-hr prognosis (valid 00Z December 13, 1964) error field [(forecast minus observed) over areas where $W_s(L)$ observed as > 100 knots)].
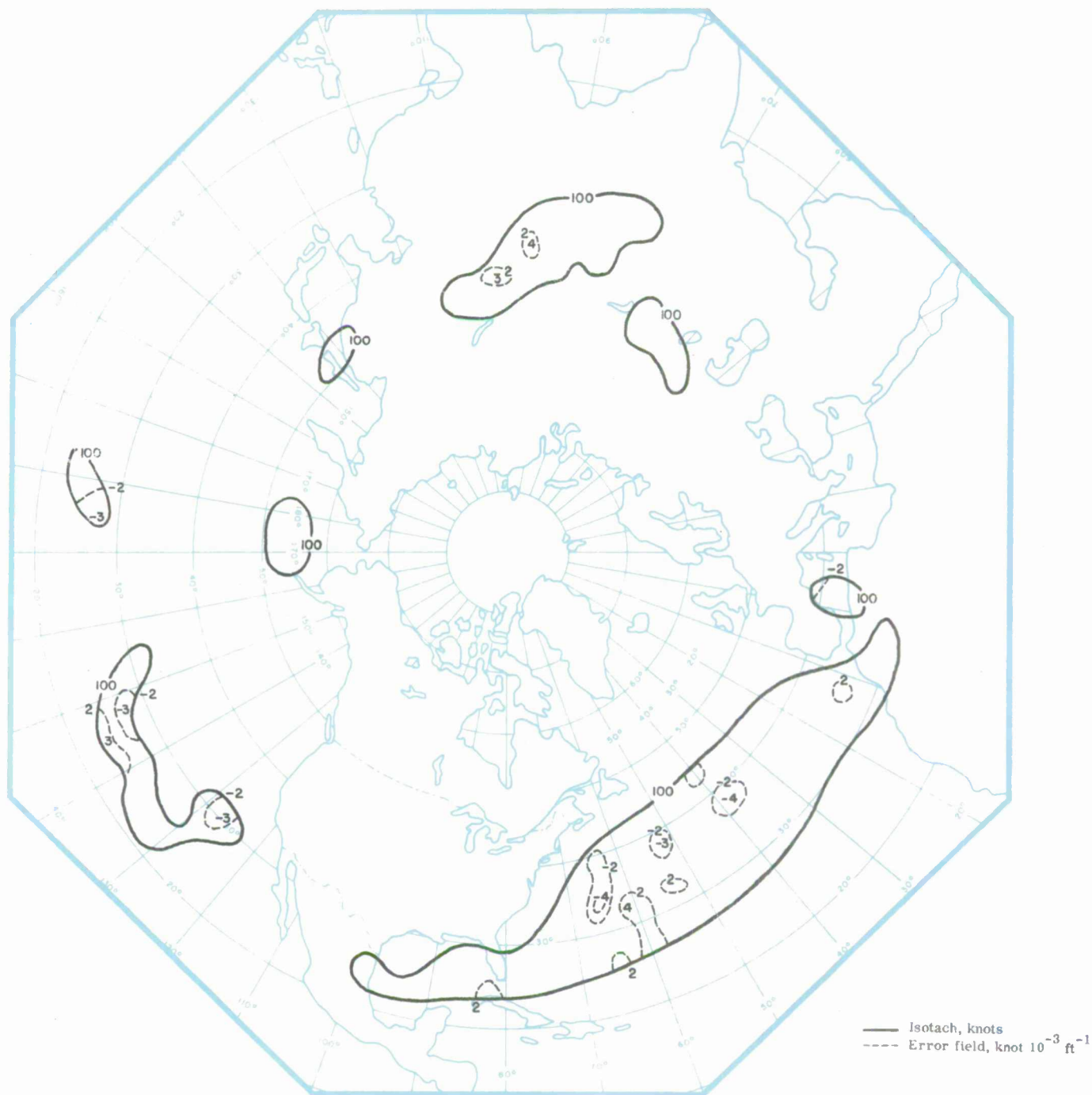
138

Fig. 11(c). S_a 36-hr prognosis (valid 00Z December 13, 1964) error field
[(forecast minus observed) over areas where $W_s(L)$ observed as > 100 knots)].
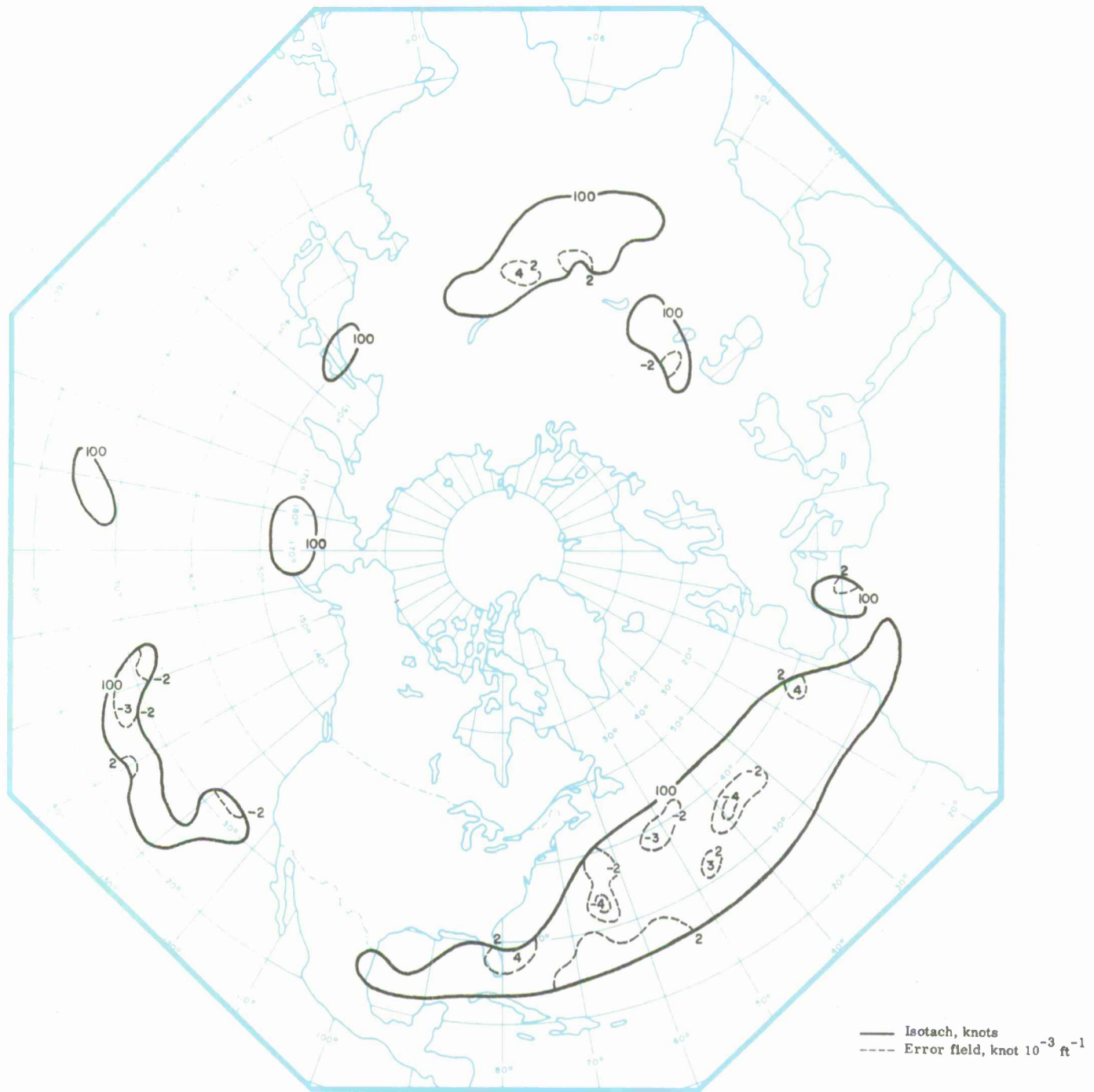
Fig. 11(d). S_a 48-hr prognosis (valid 00Z December 13, 1964) error field
[(forecast minus observed) over areas where $W_s(L)$ observed as > 100 knots)].

140

Fig. 12(a). S_a 12-hr prognosis (valid 00Z December 14, 1964) error field [(forecast minus observed) over areas where $W_s(L)$ observed as > 100 knots)].

Fig. 12(b). S$_a$ 24-hr prognosis (valid 00Z December 14, 1964) error field
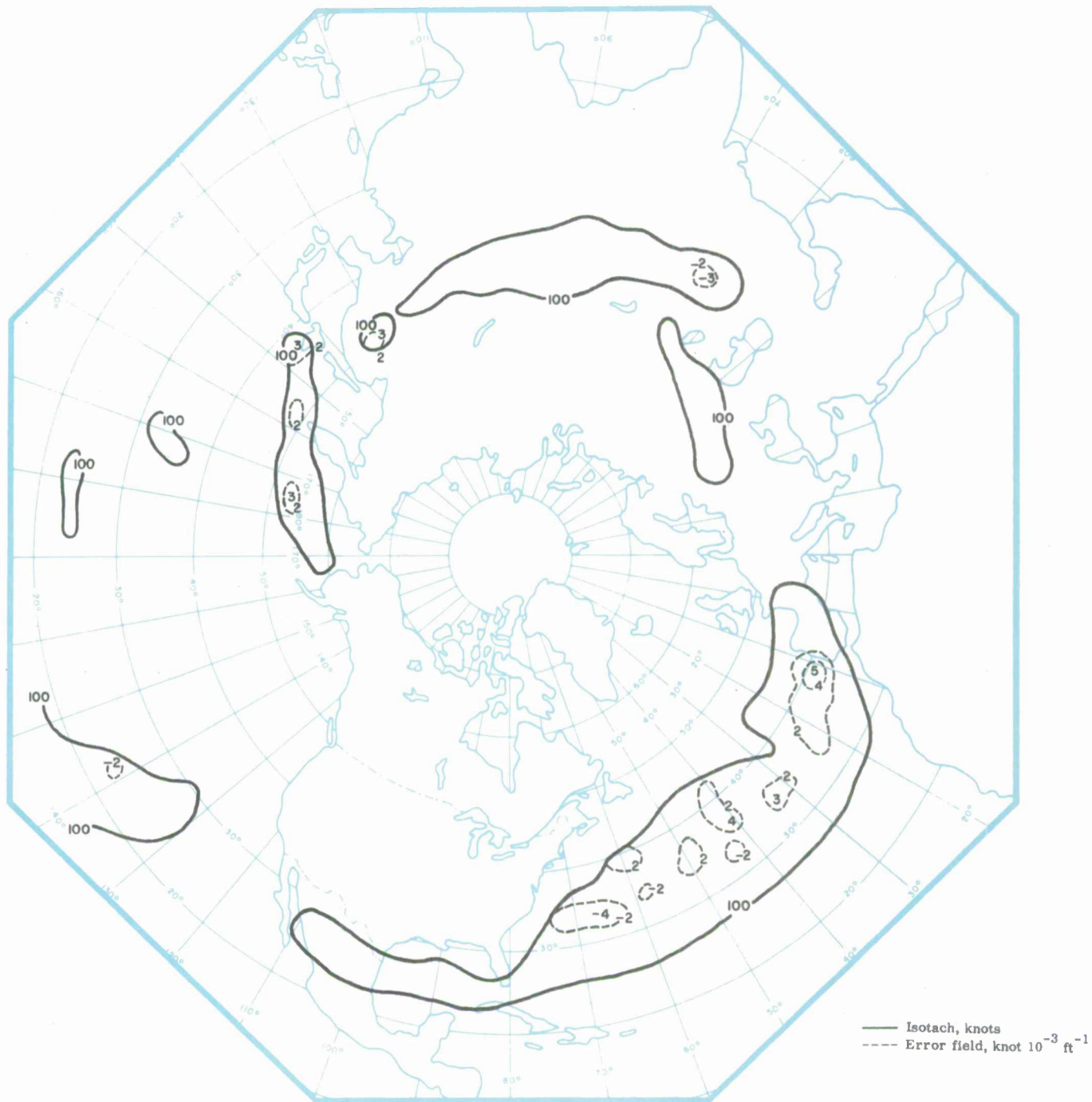[(forecast minus observed) over areas where W$_s$(L) observed as > 100 knots)].

Fig. 12(c). S_a 36-hr prognosis (valid 00Z December 14, 1964) error field [(forecast minus observed) over areas where $W_s(L)$ observed as > 100 knots)].
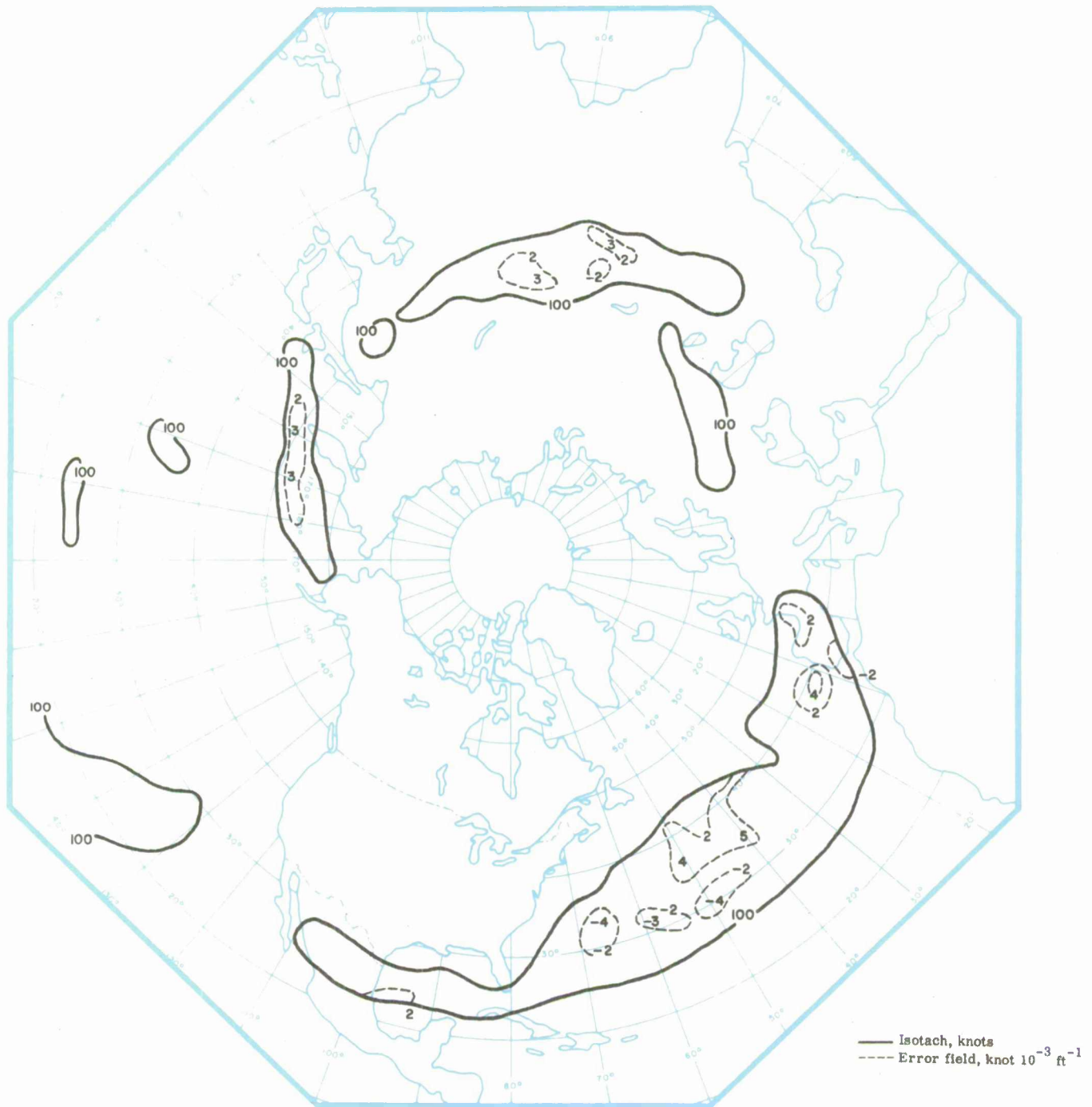
143

Fig. 12(d). S_a 48-hr prognosis (valid 00Z December 14, 1964) error field
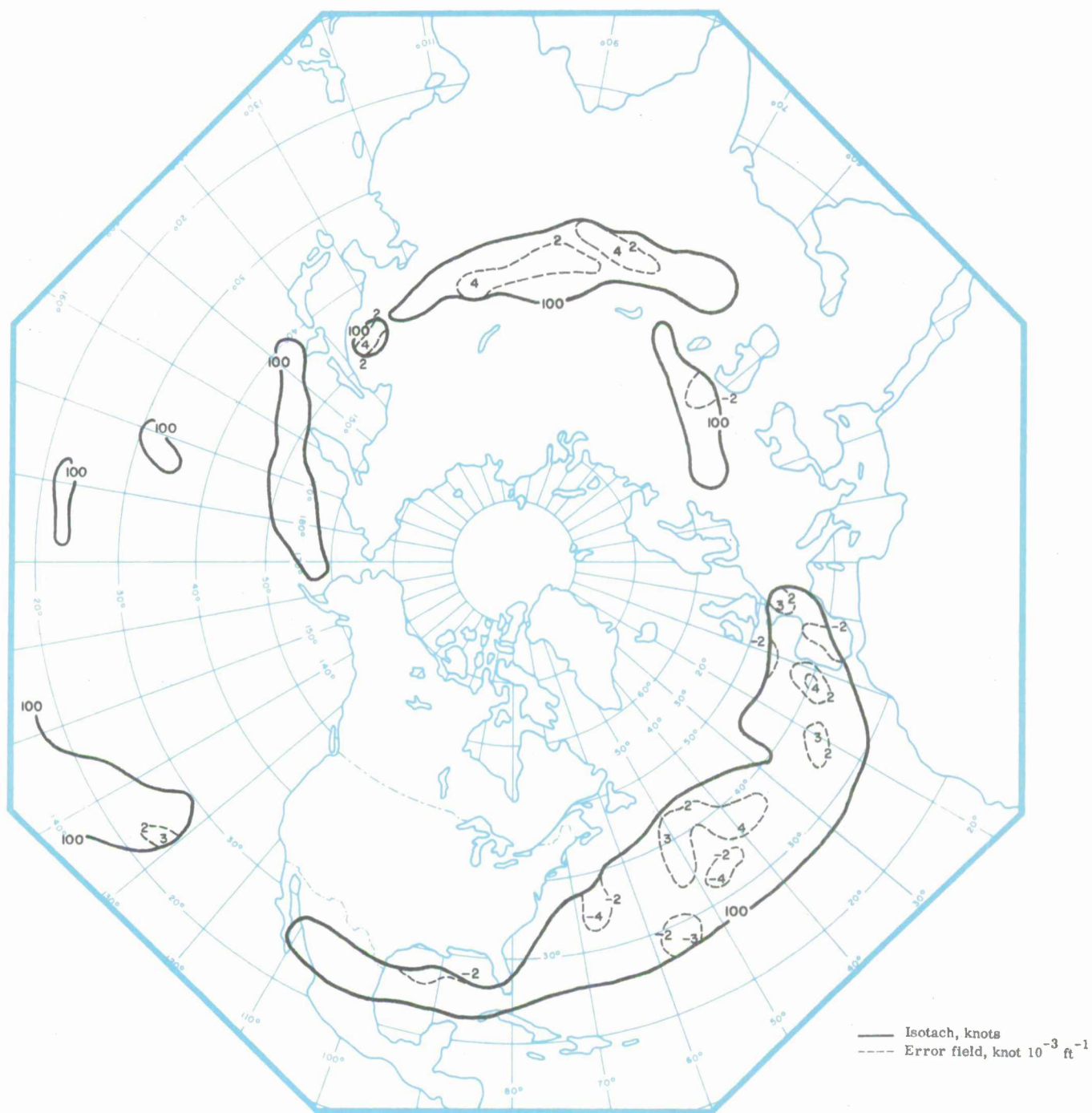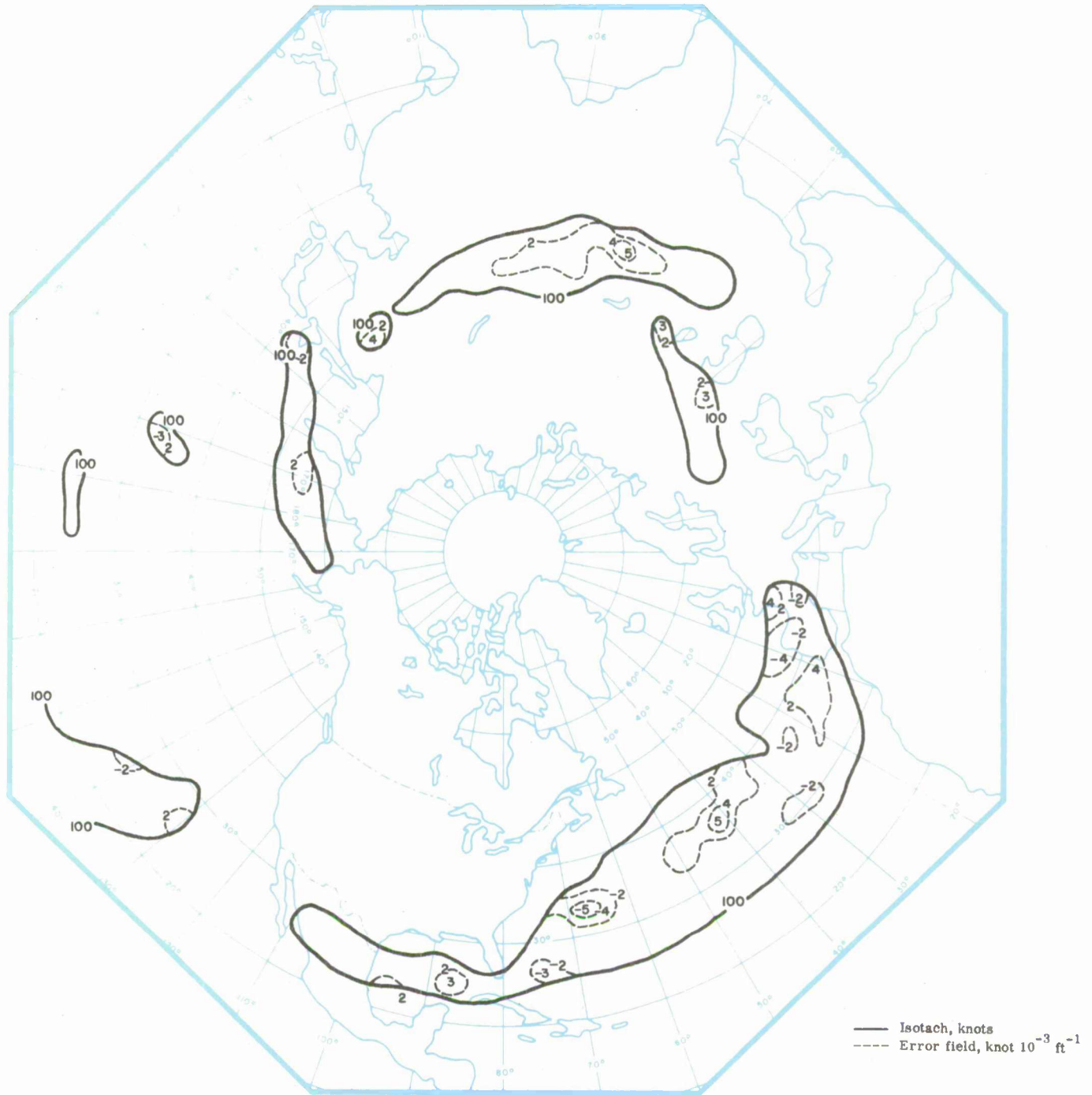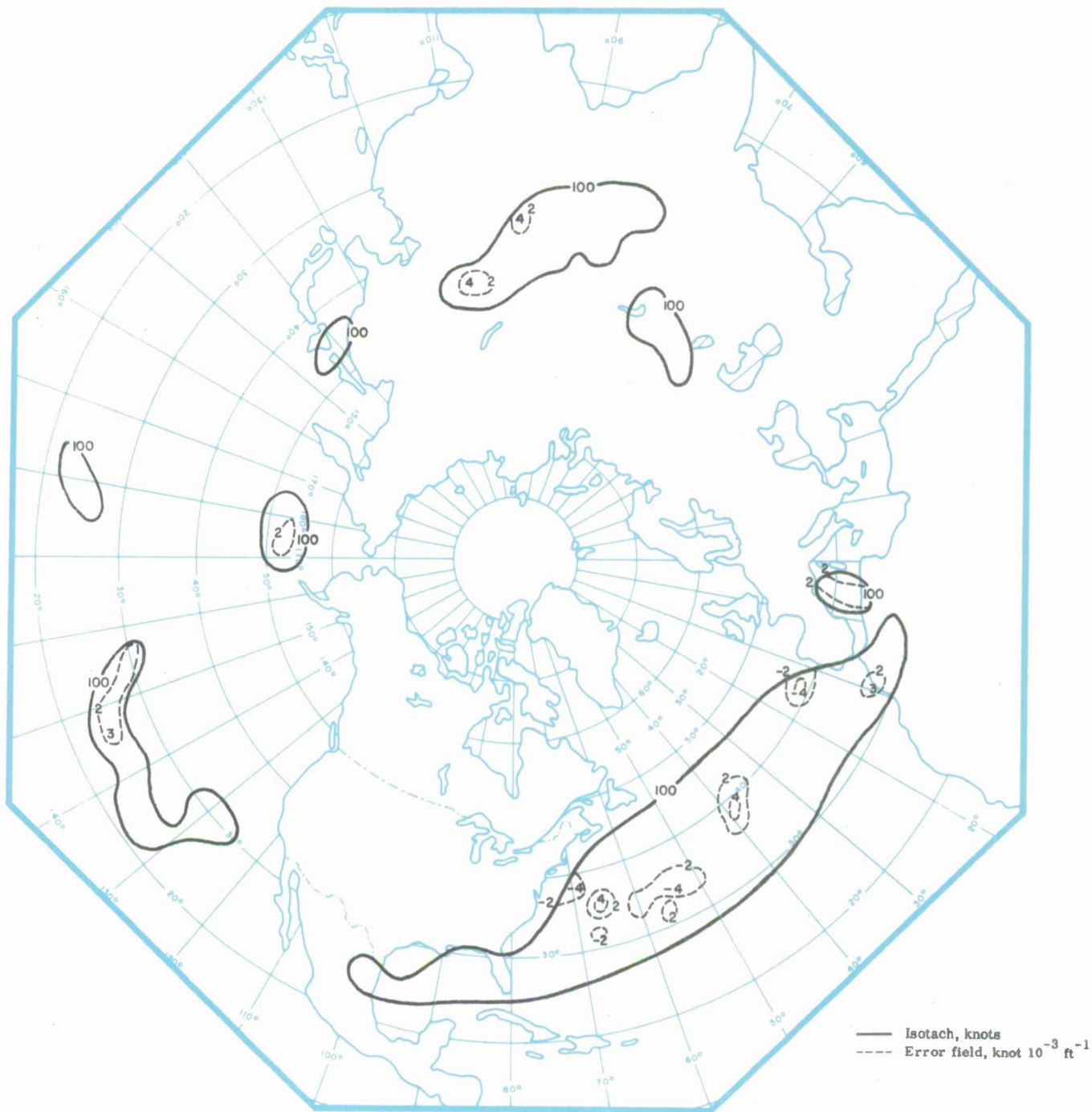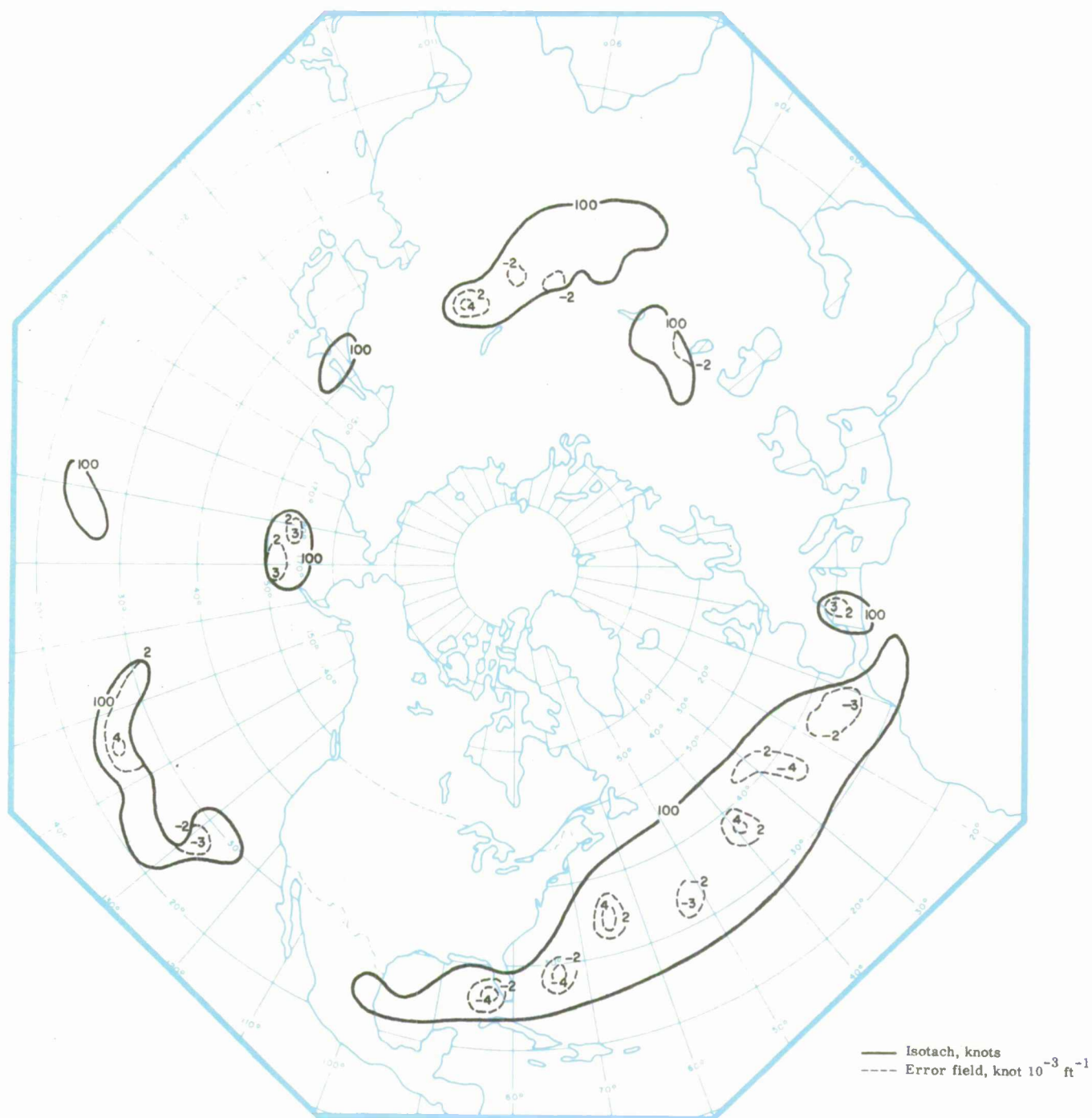[(forecast minus observed) over areas where $W_s(L)$ observed as > 100 knots)].
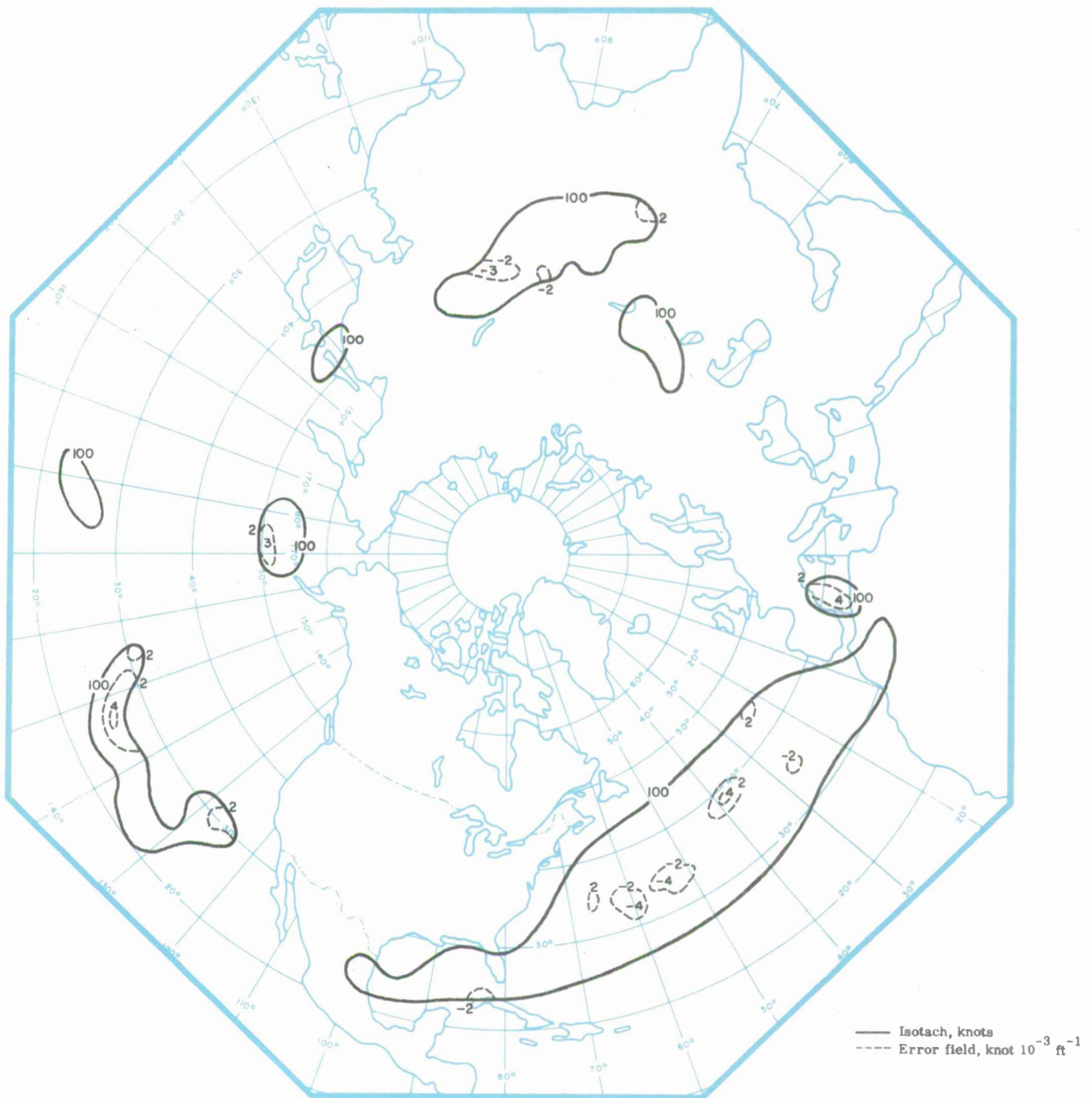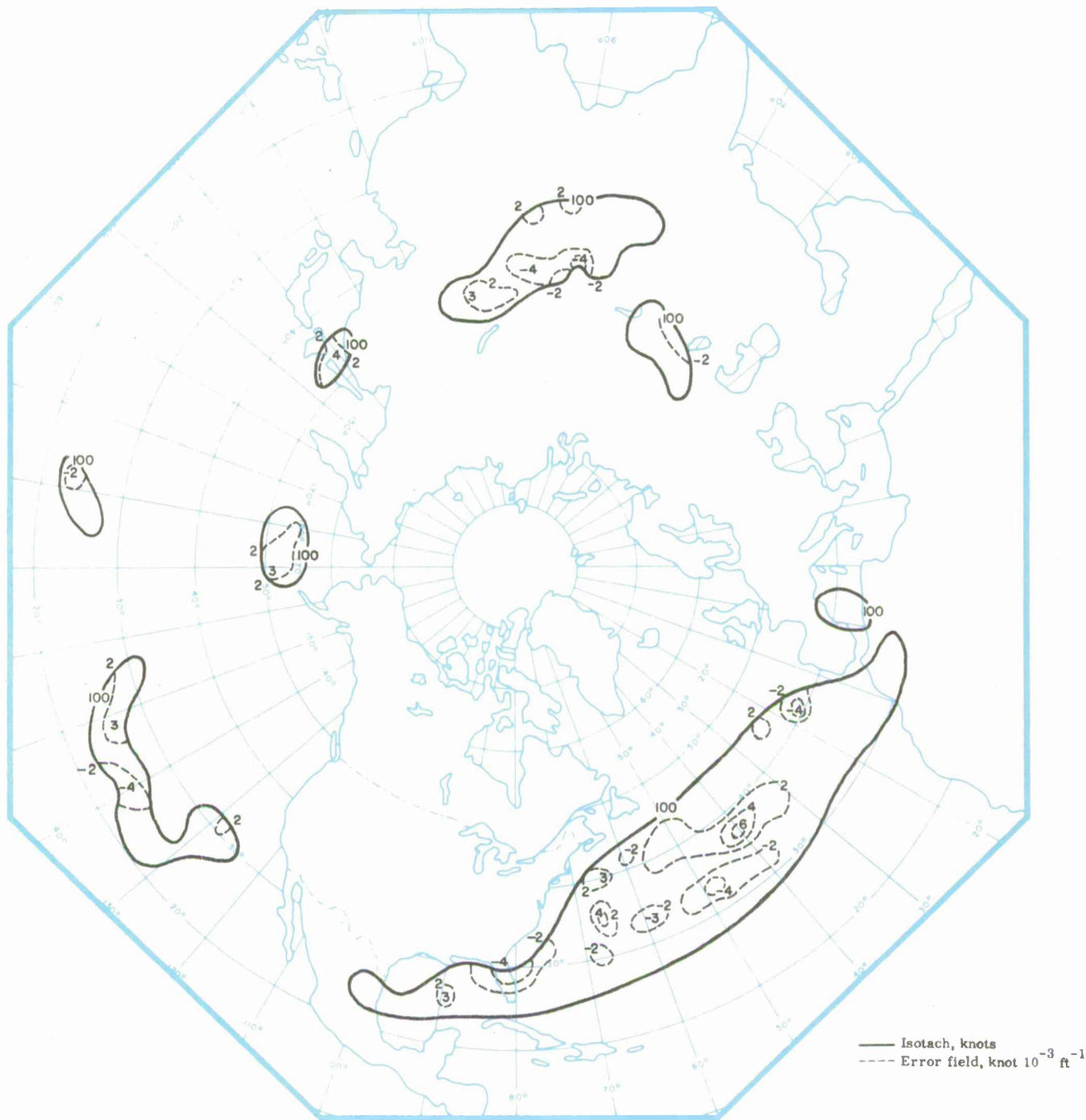
144

SECTION VI

CONCLUSIONS AND RECOMMENDATIONS

The feasibility study for the LMW Predictor Network Technique has demonstrated that prognoses of 12- and 24-hr LMW wind speed, height, shear above and shear below using a grid oriented according to the LMW wind direction are reasonable and much superior to persistence. The predictor fields comprising the initial-state and previous 12-hr changes of LMW wind speed, height, shear above and shear below, and the initial-state wind speed at constant pressure surfaces all provide useful prediction information. The categorization procedure used was, in general, successful. The separation into polar and subtropical systems and the classification, within each system, of grid points on or near the jet core, to the left of the core, and to the right of the core, proved worthwhile. The attempt, however, to further categorize grid points <u>along</u> the core by their location relative to wind speed maxima was judged to be unnecessary. This result is perhaps surprising but it must be remembered that the horizontal variations of the predictands <u>along</u> the jet core are usually smaller than the changes experienced to the left and right of the core.

While the feasibility study yielded promising results, additional effort would be required to develop an operationally-useful prediction technique. An expanded effort should be characterized by the following:

(a) larger data sample; a sample containing at least twice as many observation times as that used in the feasibility study should be used to insure the derivation of stable relationships for the subtropical jet stream,

(b) revision of grid-point categorization procedure; the three categories along the jet core should be combined into a single category, and a new category containing grid points further downstream from the initial-state position of the jet-stream wind-speed maximum should be added,

(c) use of prognostic data; operational prognoses of constant-pressure-surface height and wind speed should be included in further screening-regression experiments.

Evaluation of the prognoses of LMW parameters generated by using the <u>diagnostic</u> LMW equations (originally developed for generating initial-guess fields for the LMW

145

analyses) with numerical prognoses from the six-level dynamic model in operation at Offutt AFB, indicated that the 12- and 24-hr prognoses were, in general, a good representation of the observed fields. The 36- and 48-hr prognoses deteriorated, but were still considered at least fair and, occasionally, good over some areas of the Northern Hemisphere.

It is concluded that the quality of the LMW prognoses generated with the diagnostic LMW equations applied to constant-pressure-surface prognoses is largely a function of the quality of the constant-pressure-surface prognoses. Any improvement in the numerical prognoses will be reflected by an improvement in the LMW prognoses.

APPENDIX

EQUATIONS for POLAR and
SUBTROPICAL JET-STREAM CATEGORIES

Polar Jet-stream Categories

1. <u>Category 1A</u>

$$\hat{W}_s(L)_{12} = 17.095 + 0.4877[W_s(2)(3,3)] + 0.4487[W_s(L)(4,2)] - 3.2824[\Delta S_b(7,1)]$$

$$\Delta\hat{Z}(L)_{12} = 1546.5 - 0.4406[Z(L)(5,3)] - 0.2616[\Delta Z(L)(5,3)]$$

$$\Delta\hat{S}_{b\,12} = 1.1948 - 0.9698[S_b(5,3)] + 0.0214[W_s(L)(4,2)]$$

$$\Delta\hat{S}_{a\,12} = -1.0189 - 0.8770[S_a(5,3)] - 0.0216[W_s(L)(2,2)]$$

$$\hat{W}_s(L)_{24} = 18.290 + 0.6189[W_s(L)(3,3)] + 0.3682[W_s(2)(3,1)] - 4.2949[S_b(3,3)]$$

$$\Delta\hat{Z}(L)_{24} = 1907.7 - 0.9647[Z(L)(5,3)] + 0.3170[Z(L)(1,3)] + 6.4861[W_s(1)(5,3)]$$

$$\Delta\hat{S}_{b\,24} = 1.4101 - 1.0273[S_b(5,3)] + 0.0266[W_s(2)(3,1)]$$

$$\Delta\hat{S}_{a\,24} = -1.4198 - 0.9419[S_a(5,3)] - 0.0230[W_s(2)(3,1)]$$

2. <u>Category 1B</u>

$$\hat{W}_s(L)_{12} = -4.8861 + 0.3005[W_s(L)(3,3)] + 0.4266[W_s(5)(5,3)] + 0.3240[W_s(L)(6,2)]$$
$$+ 0.2960[W_s(1)(5,3)]$$

$$\Delta\hat{Z}(L)_{12} = 2059.5 - 0.9412[Z(L)(5,3)] + 0.2901[Z(L)(3,3)] + 4.0053[W_s(2)(3,1)]$$
$$- 4.7071[W_s(5)(5,3)] + 3.0909[W_s(L)(5,5)]$$

$$\Delta\hat{S}_{b\,12} = 1.1185 - 1.0498[S_b(5,3)] + 0.0259[W_s(L)(6,2)]$$

$$\Delta\hat{S}_{a\,12} = -0.7059 - 0.9096[S_a(5,3)] - 0.0170[W_s(3)(3,3)] - 0.0194[W_s(5)(5,3)]$$

$$\hat{W}_s(L)_{24} = -5.5470 + 0.3207[W_s(L)(3,3)] + 0.4771[W_s(L)(6,2)] + 0.3189[W_s(2)(3,5)]$$

$$\Delta\hat{Z}(L)_{24} = 2362.2 - 0.9523[Z(L)(5,3)] + 0.2539[Z(L)(3,1)] - 0.1629[\Delta Z(L)(7,3)]$$

$$\Delta\hat{S}_{b\,24} = 0.9473 - 1.0868[S_b(5,3)] + 0.0177[W_s(L)(6,2)] + 0.0177[W_s(1)(3,1)]$$

$$\Delta\hat{S}_{a\,24} = 0.6210 - 1.0106[S_a(5,3)] - 0.0284[W_s(2)(3,3)] - 0.2396[S_b(7,1)]$$
$$+ 0.0235[W_s(1)(3,3)] - 0.0006[Z(L)(3,1)]$$

3. Category 1C

$$\hat{W}_s(L)_{12} = 10.612 + 0.4848[W_s(L)(5,3)] + 0.2680[W_s(L)(3,3)] + 3.2712[S_a(5,3)]$$
$$+ 0.1915[W_s(L)(4,2)]$$

$$\Delta\hat{Z}(L)_{12} = 1142.2 - 0.8010[Z(L)(5,3)] + 0.2271[Z(L)(3,3)] + 0.1788[Z(L)(7,3)]$$
$$+ 2.6849[W_s(L)(5,1)]$$

$$\Delta\hat{S}_{b\,12} = 0.6738 - 0.8300[S_b(5,3)] + 0.0203[W_s(L)(4,2)]$$

$$\Delta\hat{S}_{a\,12} = -1.3579 - 0.8892[S_a(5,3)] - 0.0182[W_s(3)(3,3)]$$

$$\hat{W}_s(L)_{24} = 0.6702 + 0.3772[W_s(1)(5,3)] + 0.1464[W_s(3)(1,3)] + 0.2183[W_s(L)(6,4)]$$
$$+ 0.2100[W_s(3)(3,3)] + 0.2625[W_s(5)(3,5)] + 0.1562[W_s(2)(3,1)]$$

$$\Delta\hat{Z}(L)_{24} = 1576.1 - 0.9675[Z(L)(5,3)] + 0.2901[Z(L)(7,3)] + 0.2366[Z(L)(3,3)]$$

$$\Delta\hat{S}_{b\,24} = 0.8773 - 1.0092[S_b(5,3)] + 0.0158[W_s(L)(6,4)] + 0.0115[W_s(3)(1,3)]$$

$$\Delta\hat{S}_{a\,24} = -1.2374 - 0.9389[S_a(5,3)] - 0.0187[W_s(L)(2,4)] + 0.0096[\Delta W_s(L)(3,5)]$$

4. Category 1D

$$\hat{W}_s(L)_{12} = 2.2198 + 0.4372[W_s(2)(5,3)] + 0.3545[W_s(L)(4,2)] + 0.2724[\Delta W_s(L)(3,3)]$$
$$+ 0.3065[W_s(L)(6,4)]$$

$$\Delta\hat{Z}(L)_{12} = 1761.2 - 0.7108[Z(L)(5,3)] + 0.2557[Z(L)(3,3)] - 4.0631[W_s(3)(7,3)]$$

$$\Delta\hat{S}_{b\,12} = 0.8290 - 1.0071[S_b(5,3)] + 0.0133[W_s(L)(4,2)] + 0.0130[\Delta W_s(L)(3,3)]$$
$$+ 0.0160[W_s(2)(5,3)]$$

$$\Delta\hat{S}_{a\,12} = -0.6257 - 0.9887[S_a(5,3)] - 0.0120[W_s(L)(4,2)] - 0.0154[\Delta W_s(L)(3,3)]$$
$$- 0.0216[W_s(3)(5,3)]$$

$$\hat{W}_s(L)_{24} = 21.646 + 0.3392[W_s(2)(3,3)] + 0.1752[W_s(L)(5,1)] + 0.2602[\Delta W_s(L)(3,3)]$$
$$+ 0.3257[W_s(2)(5,3)]$$

$$\Delta\hat{Z}(L)_{24} = 1897.2 - 0.6691[Z(L)(5,3)] + 8.1958[W_s(1)(3,3)] - 0.2088[\Delta Z(L)(5,3)]$$

$$\Delta \hat{S}_{b\,24} = 1.7910 - 1.0590[S_b(5,3)] - 0.0186[\Delta W_s(L)(7,5)] + 0.0135[W_s(L)(4,2)]$$

$$\Delta \hat{S}_{a\,24} = -1.5516 - 0.8312[S_a(5,3)] - 0.0180[W_s(2)(3,3)]$$

5.   Category 1E

$$\hat{W}_s(L)_{12} = 3.9027 + 0.3656[W_s(L)(5,3)] + 0.2151[W_s(L)(4,2)] + 0.2195[W_s(L)(7,5)]$$
$$+ 0.1894[W_s(3)(3,3)]$$

$$\Delta \hat{Z}(L)_{12} = 743.78 - 0.5463[Z(L)(5,3)] + 0.3422[Z(L)(3,3)] - 0.1827[\Delta Z(L)(5,3)]$$

$$\Delta \hat{S}_{b\,12} = 1.3318 - 0.8551[S_b(5,3)] + 0.0108[W_s(L)(3,3)]$$

$$\Delta \hat{S}_{a\,12} = -0.5632 - 0.7209[S_a(5,3)] + 0.1977[S_a(7,5)] - 0.0121[W_s(3)(3,3)]$$

$$\hat{W}_s(L)_{24} = 1.4805 + 0.3101[W_s(L)(5,3)] + 0.2819[W_s(L)(2,4)] + 0.3125[W_s(L)(6,2)]$$
$$- 3.3884[S_a(7,5)]$$

$$\Delta \hat{Z}(L)_{24} = 1521.4 - 0.8865[Z(L)(5,3)] + 0.4084[Z(L)(3,3)] + 5.3421[W_s(1)(7,3)]$$

$$\Delta \hat{S}_{b\,24} = 1.6615 - 0.7991[S_b(5,3)] - 0.1966[S_a(7,5)]$$

$$\Delta \hat{S}_{a\,24} = -0.5484 - 0.7733[S_a(5,3)] + 0.2505[S_a(7,5)] - 0.0137[W_s(L)(1,1)]$$

Subtropical Jet-stream Categories

6. Category 2A

$$\hat{W}_s(L)_{12} = -1.5142 + 0.5737[W_s(L)(5,3)] + 0.3287[W_s(3)(5,3)]$$

$$\Delta\hat{Z}(L)_{12} = 3805.6 - 0.8121[Z(L)(5,3)] - 12.520[W_s(5)(3,3)] + 6.9727[W_s(1)(1,3)]$$
$$- 4.4566[W_s(L)(7,3)] + 0.2311[\Delta Z(L)(1,3)] + 3.7162[\Delta W_s(L)(7,1)]$$

$$\Delta\hat{S}_{b\,12} = 2.8210 - 0.8550[S_b(5,3)]$$

$$\Delta\hat{S}_{a\,12} = 0.1014 - 0.8701[S_a(5,3)] - 0.0330[W_s(3)(5,3)] - 0.1896[\Delta S_b(5,3)]$$

$$\hat{W}_s(L)_{24} = 29.650 + 0.7894[W_s(L)(6,2)]$$

$$\Delta\hat{Z}(L)_{24} = 3887.3 - 0.9214[Z(L)(5,3)] - 6.3240[W_s(3)(3,3)] - 50.623[S_a(7,3)]$$

$$\Delta\hat{S}_{b\,24} = 3.5424 - 0.8072[S_b(5,3)] - 0.0332[\Delta W_s(L)(5,3)]$$

$$\Delta\hat{S}_{a\,24} = -2.8107 - 0.8164[S_a(5,3)]$$

7. Category 2B

$$\hat{W}_s(L)_{12} = -0.8421 + 0.5364[W_s(L)(5,3)] + 0.4871[W_s(L)(4,2)]$$

$$\Delta\hat{Z}(L)_{12} = 3093.4 - 0.6087[Z(L)(5,3)] - 7.8424[W_s(L)(2,2)]$$

$$\Delta\hat{S}_{b\,12} = -0.9554 - 0.3656[\Delta S_b(5,3)] + 0.0301[\Delta W_s(L)(1,3)] - 0.0216[\Delta W_s(L)(7,5)]$$
$$- 0.3157[S_b(5,3)] + 0.0182[W_s(L)(4,2)]$$

$$\Delta\hat{S}_{a\,12} = 1.2432 - 0.5327[S_a(5,3)] - 0.0308[W_s(2)(5,3)]$$

$$\hat{W}_s(L)_{24} = 20.087 + 0.3186[W_s(L)(4,2)] + 0.3224[W_s(L)(5,3)] + 4.7280[\Delta S_b(3,1)]$$
$$- 3.9829[S_a(3,3)]$$

$$\Delta\hat{Z}(L)_{24} = 2785.5 - 0.7130[Z(L)(5,3)] - 73.241[\Delta S_b(7,5)] - 68.015[\Delta S_b(3,1)]$$
$$- 60.323[S_a(7,3)] + 48.199[S_a(5,3)]$$

$$\Delta\hat{S}_{b\,24} = 0.7058 - 0.7571[S_b(5,3)] - 0.4444[S_a(3,1)]$$

$$\Delta\hat{S}_{a\,24} = 0.6807 - 0.5762[S_a(5,3)] - 0.0263[W_s(L)(4,2)]$$

8.   Category 2C

$$\hat{W}_s(L)_{12} = 12.144 + 0.4928[W_s(L)(5,3)] + 0.4321[W_s(L)(5,1)]$$

$$\Delta\hat{Z}(L)_{12} = 2177.2 - 0.2932[\Delta Z(L)(5,3)] - 11.112[W_s(5)(3,3)] - 0.4261[Z(L)(5,3)]$$
$$- 3.4979[\Delta W_s(L)(3,5)]$$

$$\Delta\hat{S}_{b\,12} = 1.8988 - 0.6107[S_b(5,3)] + 0.4323[\Delta S_a(7,3)]$$

$$\Delta\hat{S}_{a\,12} = -1.4245 - 0.7990[S_a(5,3)] + 0.4787[S_a(5,1)]$$

$$\hat{W}_s(L)_{24} = -3.7601 + 0.3850[W_s(2)(5,3)] + 0.7078[W_s(L)(5,1)] + 0.2830[W_s(L)(3,5)]$$
$$- 6.4601[S_b(5,1)]$$

$$\Delta\hat{Z}(L)_{24} = 2240.5 - 0.5834[Z(L)(5,3)]$$

$$\Delta\hat{S}_{b\,24} = -0.2932 - 1.0465[S_b(5,3)] + 0.0231[W_s(2)(5,3)] - 0.3866[\Delta S_a(1,3)]$$
$$+ 0.0017[\Delta Z(L)(3,3)] + 0.5484[\Delta S_a(1,1)] + 0.0315[W_s(3)(3,1)]$$

$$\Delta\hat{S}_{a\,24} = -2.7770 - 0.8112[S_a(5,3)]$$

9.   Category 2D

$$\hat{W}_s(L)_{12} = 12.141 + 0.4560[W_s(L)(5,3)] + 0.3706[W_s(2)(3,3)] + 0.2835[W_s(5)(5,3)]$$

$$\Delta\hat{Z}(L)_{12} = 506.6 - 0.5185[Z(L)(5,3)] + 0.3897[Z(L)(3,3)]$$

$$\Delta\hat{S}_{b\,12} = 1.1400 - 0.6452[S_b(5,3)] + 0.3062[S_b(3,3)]$$

$$\Delta\hat{S}_{a\,12} = -0.4872 - 0.8305[S_a(5,3)] - 0.0252[W_s(L)(3,3)]$$

$$\hat{W}_s(L)_{24} = 3.8416 + 0.6138[W_s(L)(4,2)] + 0.3972[W_s(2)(3,3)]$$

$$\Delta\hat{Z}(L)_{24} = 3033.6 - 0.7333[Z(L)(5,3)] - 7.000[W_s(5)(1,3)]$$

$$\Delta\hat{S}_{b\,24} = 0.2924 - 0.9657[S_b(5,3)] + 0.0281[W_s(L)(4,2)]$$

$$\Delta\hat{S}_{a\,24} = -0.6528 - 0.9875[S_a(5,3)] - 0.0265[W_s(L)(4,2)]$$

10.   Category 2E

$$\hat{W}_s(L)_{12} = 15.975 + 0.4418[W_s(3)(5,3)] + 0.4946[W_s(1)(7,3)] + 0.3421[W_s(5)(3,3)]$$

$$\Delta\hat{Z}(L)_{12} = 3582.2 - 1.0579[Z(L)(5,3)] - 6.5998[W_s(3)(5,3)] + 0.2748[Z(L)(3,3)]$$
$$- 7.5708[W_s(5)(5,3)] + 4.5680[W_s(L)(3,3)]$$

$$\Delta\hat{S}_{b\,12} = 1.9054 - 0.7954[S_b(5,3)]$$

$$\Delta\hat{S}_{a\,12} = -1.2837 - 1.1193[S_a(5,3)] - 0.0500[W_s(5)(7,3)]$$

$$\hat{W}_s(L)_{24} = 16.673 + 0.5346[W_s(3)(5,3)] + 0.3307[W_s(L)(6,4)] - 0.0123[\Delta Z(L)(3,3)]$$

$$\Delta\hat{Z}(L)_{24} = 3724.2 - 0.8996[Z(L)(5,3)]$$

$$\Delta\hat{S}_{b\,24} = 2.0674 - 0.8722[S_b(5,3)] + 0.5770[\Delta S_a(3,3)] + 0.0344[\Delta W_s(L)(3,3)]$$

$$\Delta\hat{S}_{a\,24} = -1.0445 - 0.3837[S_a(5,3)] - 0.3386[\Delta S_a(5,3)]$$

REFERENCES

1. Endlich, R. M. and G. S. McLean, 1957: "The Structure of the Jet Stream Core," J. Meteorol., vol. 14, pp. 543—552.

2. Miller, R. G., 1958: "A Computer Program for the Screening Procedure," Studies in Statistical Weather Prediction. Final Rpt., Contract AF19(604)-1590, The Travelers Weather Research Center, pp. 96—136.

3. Ostby, F. P., Jr., K. W. Veigas and B. J. Erickson, 1965: Prediction in the Stratosphere, Tech. Rpt. 7463-170, The Travelers Research Center, Inc.

DOCUMENT CONTROL DATA - R&D

(Security classification of title, body of abstract and indexing annotation must be entered when the overall report is classified)

1. ORIGINATING ACTIVITY *(Corporate author)*	2a. REPORT SECURITY CLASSIFICATION
The Travelers Research Center, Inc. 250 Constitution Plaza Hartford, Connecticut 06103	Unclassified 2b. GROUP

3. REPORT TITLE

TECHNIQUES FOR OBJECTIVE HEMISPHERIC ANALYSIS AND
PREDICTION OF THE JET STREAM

4. DESCRIPTIVE NOTES *(Type of report and inclusive dates)*

Final Report   1 October, 1964—31 July, 1965

5. AUTHOR(S) *(Last name, first name, initial)*

Spiegler, David B.; Ball, John T.; Ball, Robert J.; Erickson, Bernard J.

6. REPORT DATE	7a. TOTAL NO. OF PAGES	7b. NO. OF REFS
September 1965	157	3

8a. CONTRACT OR GRANT NO. AF19(628)-3437 (15107)	9a. ORIGINATOR'S REPORT NUMBER(S)
b. PROJECT NO. 2.0	7463-176
c. Task no. 2.3	9b. OTHER REPORT NO(S) *(Any other numbers that may be assigned this report)*
d. Milestone 2.3.5	ESD-TR-65-13

10. AVAILABILITY/LIMITATION NOTICES

Availability Notice (1) and Legal Notice (1)

11. SUPPLEMENTARY NOTES	12. SPONSORING MILITARY ACTIVITY
	Electronic Systems Division Air Force Systems Command

13. ABSTRACT

This report comprises two parts: Part I documents an objective <u>analysis</u> technique for level of maximum wind (LMW) parameters, and Part II presents two LMW <u>prediction</u> techniques.

The objective hemispheric <u>analysis</u> technique incorporates information from data areas into LMW analyses for no-data areas. This is done in a quantitative, objective, and consistent manner by using LMW regression equations that specify the initial-guess fields for the analysis. The analysis technique locates jet cores between grid points, and generates observations along these cores by using horizontal jet profiles. This technique produces high-quality analyses that compare favorably with subjective analyses, and that are generally consistent with one another.

The first <u>prediction</u> technique is based on a procedure wherein potential predictors are obtained from a network grid oriented with respect to the LMW wind direction at the predictand point. Prediction equations are obtained by applying the screening regression technique to predictors selected from initial-state LMW parameters (and their 12-hr change) and wind speed values at constant pressure surfaces. Tests on independent data showed that these equations produce prognoses that are better than persistence for all polar and subtropical jet-stream categories.

The second <u>prediction</u> technique applies diagnostic LMW regression equations (originally derived to produce the initial-guess fields in the LMW analysis) to constant-pressure-surface numerical prognoses. A five-day data sample of numerical prognoses was used to test the technique. Evaluation of the resulting LMW prognoses indicated that the 12- and 24-hr prognoses were generally good representations of the observed LMW fields, and that the 36- and 48-hr prognoses were occasionally good over some areas of the hemisphere.

DD FORM **1473**
1 JAN 64

14. KEY WORDS	LINK A		LINK B		LINK C	
	ROLE	WT	ROLE	WT	ROLE	WT
Level of maximum wind						
Jet-stream modeling						

INSTRUCTIONS

1. ORIGINATING ACTIVITY: Enter the name and address of the contractor, subcontractor, grantee, Department of Defense activity or other organization *(corporate author)* issuing the report.

2a. REPORT SECURITY CLASSIFICATION: Enter the overall security classification of the report. Indicate whether "Restricted Data" is included. Marking is to be in accordance with appropriate security regulations.

2b. GROUP: Automatic downgrading is specified in DoD Directive 5200.10 and Armed Forces Industrial Manual. Enter the group number. Also, when applicable, show that optional markings have been used for Group 3 and Group 4 as authorized.

3. REPORT TITLE: Enter the complete report title in all capital letters. Titles in all cases should be unclassified. If a meaningful title cannot be selected without classification, show title classification in all capitals in parenthesis immediately following the title.

4. DESCRIPTIVE NOTES: If appropriate, enter the type of report, e.g., interim, progress, summary, annual, or final. Give the inclusive dates when a specific reporting period is covered.

5. AUTHOR(S): Enter the name(s) of author(s) as shown on or in the report. Enter last name, first name, middle initial. If military, show rank and branch of service. The name of the principal author is an absolute minimum requirement.

6. REPORT DATE: Enter the date of the report as day, month, year; or month, year. If more than one date appears on the report, use date of publication.

7a. TOTAL NUMBER OF PAGES: The total page count should follow normal pagination procedures, i.e., enter the number of pages containing information.

7b. NUMBER OF REFERENCES: Enter the total number of references cited in the report.

8a. CONTRACT OR GRANT NUMBER: If appropriate, enter the applicable number of the contract or grant under which the report was written.

8b, 8c, & 8d. PROJECT NUMBER: Enter the appropriate military department identification, such as project number, subproject number, system numbers, task number, etc.

9a. ORIGINATOR'S REPORT NUMBER(S): Enter the official report number by which the document will be identified and controlled by the originating activity. This number must be unique to this report.

9b. OTHER REPORT NUMBER(S): If the report has been assigned any other report numbers *(either by the originator or by the sponsor)*, also enter this number(s).

10. AVAILABILITY/LIMITATION NOTICES: Enter any limitations on further dissemination of the report, other than those imposed by security classification, using standard statements such as:

(1) "Qualified requesters may obtain copies of this report from DDC."

(2) "Foreign announcement and dissemination of this report by DDC is not authorized."

(3) "U. S. Government agencies may obtain copies of this report directly from DDC. Other qualified DDC users shall request through

_____ ."

(4) "U. S. military agencies may obtain copies of this report directly from DDC. Other qualified users shall request through

_____ ."

(5) "All distribution of this report is controlled. Qualified DDC users shall request through

_____ ."

If the report has been furnished to the Office of Technical Services, Department of Commerce, for sale to the public, indicate this fact and enter the price, if known.

11. SUPPLEMENTARY NOTES: Use for additional explanatory notes.

12. SPONSORING MILITARY ACTIVITY: Enter the name of the departmental project office or laboratory sponsoring *(paying for)* the research and development. Include address.

13. ABSTRACT: Enter an abstract giving a brief and factual summary of the document indicative of the report, even though it may also appear elsewhere in the body of the technical report. If additional space is required, a continuation sheet shall be attached.

It is highly desirable that the abstract of classified reports be unclassified. Each paragraph of the abstract shall end with an indication of the military security classification of the information in the paragraph, represented as *(TS), (S), (C), or (U)*.

There is no limitation on the length of the abstract. However, the suggested length is from 150 to 225 words.

14. KEY WORDS: Key words are technically meaningful terms or short phrases that characterize a report and may be used as index entries for cataloging the report. Key words must be selected so that no security classification is required. Identifiers, such as equipment model designation, trade name, military project code name, geographic location, may be used as key words but will be followed by an indication of technical context. The assignment of links, roles, and weights is optional.